BELLCOMM, INC.
955 L'ENFANT PLAZA NORTH, S.W.   WASHINGTON, D. C. 20024

B69 09103

ABSTRACT

An alternative to the usual method of orbit determination is the approach of fitting functions to the osculating orbital elements. Programs based on this concept have been used at Bellcomm and elsewhere.

An investigation was conducted to find functional forms suitable to represent a variety of lunar orbits. Three Apollo-type orbits were artificially generated and used as data. Both classical and Hubbard elements were used.

The functional forms which were found were evaluated and compared with the original data. Plots of the UVW component residuals are presented. Two-revolution fits had much better propagation characteristics than one-revolution fits. It is felt that Hubbard elements are more useful than classical elements.

MEMORANDUM FOR FILE

INTRODUCTION

An alternative approach to orbit determination
consists of representing the osculating orbital elements by
appropriate functions. In such a method the concern is with
the solutions of the equations of motion rather than with the
equations themselves. A significant consequence is that this
formulation does not involve a description of the forcing
function -- the gravitational field. The concept was described
by Veis. [1]

A computer program, OLEP, which uses this approach
has been developed at Bellcomm. [2] A potential advantage
of this program is that, as mentioned above, precise knowledge
of all the minutiae of the lunar gravitational field (size
and location of mascons, for example) is not required -- indeed,
is irrelevant -- if suitable functional representations of
the osculating elements are used. In support of this program
a study was undertaken, using artificially generated data,
to find functional forms for the elements which would adequately
represent a variety of lunar orbits.

DISCUSSION OF PROCEDURE

Artificial data representing three different Apollo-
type lunar orbits, described by osculating elements vs. time,
were generated for use in this study. There were about four
complete revolutions of each. The gravitational field model
used in the data generation was the NASA (LRC) 7/28 B model.
The coefficients of this model, obtained from Reference 3,
are listed in Table 1. Of the several competing lunar gravi-
tational models at the time this work was undertaken the 7/28 B
model was one of the "roughest". [4] It was therefore felt
to be a more strenuous test of the method than a simpler model.

One of the three orbits had a very low eccentricity
(<.003). For small eccentricity the classical orbital elements
become indeterminate. To treat this orbit the set of elements
described by Hubbard [5] and Kovalevsky [6] was introduced.

These elements, called Hubbard elements in this memorandum, are a, e_c = e cos ω, e_s = e sin ω, i, Ω, m = ω + M. This set circumvents the lack of definition of argument of perigee and mean anomaly. The low eccentricity orbit was expressed in terms of the Hubbard set, and the other two in both classical and Hubbard elements, making five sets of data in all. The five sets of data are described more fully in Table 2. They are depicted in Figures 1a - 1f, 2a - 2f, 3a - 3f, 4a - 4f, and 5a - 5f.

Two sets of functional forms were determined: one for classical elements and one for Hubbard elements. In each case the basic procedure was to use one set of data to determine a possible analytical model for the orbital elements, and then to check the suitability of these functional forms by assessing how well they described the other sets. There were two criteria for evaluating the results:

1. The functional forms determined should be valid for more than one specific orbit. This was the reason for using three different orbits.

2. The fits should have good propagation characteristics. That is, the error should not increase rapidly beyond the region over which the fits are performed.

As mentioned previously, one set of data (for each type of elements) was used to determine a set of functional forms. In order to obtain good propagation characteristics, the analytic forms were determined by examining fits made to all four revolutions. Then fits of the "best" functions were performed over two different intervals, corresponding to one complete revolution (not just the portion which would be visible from the earth) and two partial revolutions with a gap in between. (This latter case does simulate the gap in tracking data caused by occultation of the satellite by the moon.) In both cases the fits were then evaluated for the four complete revolutions and compared with the original data, in order to study the propagation characteristics of the analytic representations. Finally, one and two-revolution fits of the same functional forms were made to the other sets of data; these fits were also evaluated for all four revolutions and compared with the original data.

Three computer programs were used in the regression analysis. One was an orthogonal-polynomial-fitting program which contained a statistical significance test (F test) implemented so as to reject terms of degree higher than necessary. Another was a spectral analysis program with the special

capabilities, among others, of evaluating the spectrum at points
other than the "Fourier frequencies", and of improving the
estimates of spectral peaks by simultaneously solving for the
exact frequencies and coefficients of one or more dominant spectral
terms.   Another important feature of this program is its ability
to Fourier analyze unequally spaced data, which made it possible
to process the data with the gap in the middle. The third
program was a general linearized least-squares differential
correction program, capable of fitting any given function.

Using the three computer programs, several sets of
functions were tried, including various combinations of poly-
nomials and trigonometric functions. The search for functional
representations of the osculating orbital elements was restricted
to such simple functions for ease of application in a program
such as OLEP. Also, as is discussed below, the fits obtained
with simple functions were deemed acceptable.

A difficulty was experienced in using trigonometric
functions with frequency as one of the fit parameters. Unless
the initial estimate of the frequency is close to the correct
value the solution "runs away" -- the regression process does
not converge. In addition, there is correlation between
sinusoidal and polynomial terms, making the convergence pro-
blem more acute.

An initial estimate of zero for frequency leads auto-
matically to a singular normal matrix. It was felt that the
only reasonable frequency estimate available to a user of OLEP
might be the orbital frequency. Inclination was the only one
of the orbital elements for which no polynomial term reduced
the variance about the mean very much, and for which a sinusoidal
fit, with the orbital frequency as an estimate for frequency,
both converged and produced a significant improvement in
variance.

A possibility which was not investigated was _fixing_
the frequency of a sinusoidal term at the orbital frequency
and solving for the coefficients. Implementation of such a
scheme in an orbit determination program would require in-
putting the orbital frequency, or obtaining it in an iterative
fashion from the solution process, possibly materially adding
to the complexity of the program.

RESULTS

The functional forms chosen for the orbital elements,
classical and Hubbard, are listed in Tables 3 and 4. Plots
of the elements, and of the fit residuals in UVW coordinates
for the several cases considered, are shown in Figures 1a - 5ℓ.
The UVW coordinate system is an instantaneous frame of reference

with the U axis in the direction of the radius vector from
the center of the moon to the satellite, the V axis along
the component of the velocity vector perpendicular to U,
and the W axis pointing in the direction of the angular
momentum vector of the satellite. The orign was chosen to
be at the instantaneous position of the satellite.

In addition to making fits to both one and two
consecutive orbits, comparisons of the fits with the original
data were made using both the fitted value of semimajor axis
and the value obtained from $a = (\mu/n^2)^{1/3}$, where n is the
coefficient of the linear term in mean anomaly (or modified
anomaly $m = \omega + M$ for Hubbard elements). The plots for the
latter comparisons are labeled "semimajor axis implied".
Thus there are four groups of position and velocity residuals
for each of the five sets of data.

Table 5 is a table of contents for the figures.
Figures 1a - 2ℓ are for Hubbard elements. The fit region for the
one-revolution   case is shown in Figures 1a - 1f, 1k, and 1ℓ;
the fit zones for the two-revolution fits are marked "data".
(The difference between the longest and shortest orbital
periods is only about 9%, so the same fit regions were used
for all five sets of data.)

Some results of the fitting are summarized in Table 6.
The most striking comparison is between one- and two-revolution
fits. In the fit zone the two-revolution fits gave rise to
somewhat larger errors than the one-revolution fits, on the
average, but in the propagation zone the two-revolution fits
gave markedly smaller errors in every case. The maximum
position errors were smaller using the fitted value of semi-
major axis, but the maximum velocity errors were mainly smaller
using the implied value for a.

For a given orbit, the UVW residual plots for
classical and Hubbard elements look virtually identical. From
the standpoint of this analysis apparently nothing is lost by
using Hubbard elements, and their use makes it possible to
treat orbits with very low eccentricity. Therefore, Hubbard
elements would appear to be a better choice than classical
elements for use in an orbit determination program like that
described in Reference 2.

CONCLUSIONS

A study was undertaken to find an appropriate set
of functional forms for the osculating orbital elements
representing three Apollo-type lunar orbits. Two sets (one
for classical elements, one for Hubbard elements) of simple
functions were found which gave reasonably good fits. Results
are presented in the form of residual plots in UVW coordinates.

Fits made to two consecutive revolutions had much better propagation characteristics than one-revolution fits, without serious loss of accuracy in the fit region. On the whole, fits using semimajor axis implied from mean motion by $a = (\mu/n^2)^{1/3}$ had larger maximum position errors (primarily caused by a bias in U) but smaller maximum velocity errors than those using a fit to a.

Hubbard elements are determinate when classical elements lose their definition because of very small eccentricity. In addition, it was found that even when classical elements are a valid representation of the data, Hubbard elements gave equally good results in this study.

ACKNOWLEDGEMENT

M. Lybanon

R. M. Scott

2014-$\frac{ML}{RMS}$-bsb

Attachments

BELLCOMM, INC.

REFERENCES

1. Veis, George, "A Differential Orbit Improvement Program for Lunar Orbits", in Scientific Horizons from Satellite Tracking, Smithsonian Astrophysical Observatory Special Report 235, December 30, 1966.

2. Bullock, M. V., and Ferrari, A. J., "An Analysis of Lunar Orbiter III Tracking Data Utilizing Osculating Orbital Elements", Bellcomm Technical Memorandum TM-69-2014-2, March 26, 1969.

3. Ferrari, A. J., and Scott, R. M., "Lunar Gravitational Potential Functions - Case 310", Bellcomm Memorandum for File, April 25, 1968.

4. Ferrari, A. J., "Analysis of Equipotential Surfaces Generated from Lunar Gravitational Potential Models - Case 310", Bellcomm Memorandum for File, May 3, 1968.

5. Hubbard, E. C., "Orbit Elements Determinate at Zero Eccentricity", U.S. Naval Weapons Naval Laboratory Technical Memorandum Number K-26/63, October 1963.

6. Kovalevsky, J., Introduction to Celestial Mechanics, Springer - Verlag New York Inc., 1967.

TABLE 1

NASA (LRC) 7/28 B LUNAR GRAVITATIONAL MODEL

n,m	$10^4 C_{n,m}$	$10^4 S_{n,m}$
2,0	-2.092	- - -
2,1	-.001571	-.05515
2,2	.1766	-.01667
3,0	.1738	- - -
3,1	.2272	-.1355
3,2	.07405	.02090
3,3	.03755	.003523
4,0	.3793	- - -
4,1	-.03263	.06798
4,2	.0009158	-.007879
4,3	-.004107	-.009379
4,4	-.0004731	.0001580
5,0	-.3176	- - -
5,1	-.07216	-.006547
5,2	.04039	.01951
5,3	-.002503	.009193
5,4	.001076	.0009155
5,5	-.0004162	.0004836
6,0	0	- - -
6,1	.05216	.02231
6,2	-.01715	.005328
6,3	-.005840	-.001616
6,4	.0009962	-.001047
6,5	-.00003961	-.0002166
6,6	.00004314	-.00006016
7,0	0	- - -
7,1	.1305	.03413
7,2	-.02053	-.009328
7,3	.001342	-.002469
7,4	.0005499	-.0001402
7,5	-.00006878	.000006343
7,6	-.000001945	.000005396
7,7	-.000002571	.000003969

TABLE 2

DATA USED IN STUDY

NAME	a	e	i	ELEMENTS
e = .04 data	6.459×10^6 ft	.0437	21.3°	classical and Hubbard
Arc 305 data	6.459×10^6 ft	.0527	21.3°	classical and Hubbard
Low eccentricity data	6.067×10^6 ft	.0014	173.1°	Hubbard

There were approximately four revolutions of each orbit.
Values given for a, e, and i are averages over the entire
span of data.

TABLE 3

FUNCTIONAL FORMS FOR CLASSICAL ELEMENTS

Orbital Element	Functional Form
a	Constant
e	Straight line
i	Constant + Sinusoid
Ω	Straight line
ω	Straight line
M	Straight line

TABLE 4

FUNCTIONAL FORMS FOR HUBBARD ELEMENTS

Orbital Element	Functional Form
a	Constant
e_c	Straight line
e_s	Straight line
i	Constant + Sinusoid
Ω	Straight line
m	Straight line

TABLE 5

CONTENTS OF FIGURES

Data	Element Set	Orbital Elements	Residuals 1 Rev. Fits	Residuals 2 Rev. Fits
e = .04	Classical	Fig. 1a-1f	Fig. 1g-1j	Fig. 1k-1ℓ
Arc 305	Classical	Fig. 2a-2f	Fig. 2g-2j	Fig. 2k-2ℓ
Low eccentricity	Hubbard	Fig. 3a-3f	Fig. 3g-3j	Fig. 3k-3n
e = .04	Hubbard	Fig. 4a-4f	Fig. 4g-4j	Fig. 4k-4ℓ
Arc 305	Hubbard	Fig. 5a-5f	Fig. 5g-5j	Fig. 5k-5ℓ

TABLE 6

MAXIMUM UVW RESIDUAL COMPONENTS

Data	Comp.	1 Rev. Fits		2 Rev. Fits	
		Fit Zone	Prop. Zone	Fit Zone	Prop. Zone
e = .04 data Classical elements	U	1500/3000	7500/7500	2000/4500	4500/5500
	V	2000/2000	12,000/12,000	1000/1000	7000/7000
	W	1500/1500	8500/8500	2000/2000	2000/2000
	$\dot{U}$	1.5/ 1.5	5.5/ 5.5	1.5/ 1.5	4/4
	$\dot{V}$	1/ 1.5	6/5	1.5/2	3.5/3
	$\dot{W}$	1.5/ 1.5	5.5/ 5.5	1.5/1	1.5/ 1.5
Arc 305 data Classical elements	U	2000/3500	10,500/12,500	3000/1500	6500/4000
	V	4500/4500	18,500/18,500	2500/2500	7500/7500
	W	2000/2000	8,000/ 8,000	2500/2500	6500/6500
	$\dot{U}$	2/2	8.5/ 8.5	2/2	3.5/ 3.5
	$\dot{V}$	2/ 1.5	8/ 9.5	3/2	3.5/3
	$\dot{W}$	2/2	9/9	2/2	>4/>4
Low eccentricity data Hubbard elements	U	2500/4000	8500/5000	3000/4500	5500/6500
	V	1000/1500	>20,000/>20,000	4000/4000	11,500/9500
	W	500/500	5000/5000	1000/1000	3500/3500
	$\dot{U}$	3/3	>10/>10	4.5/4.5	8.5/8.5
	$\dot{V}$	2.5/2	7/8	3/2	5/4
	$\dot{W}$	1.5/ 1.5	3.5/ 3.5	2/2	3/3
e = .04 data Hubbard elements	U	1500/3000	7500/7500	2000/4500	4500/5500
	V	2000/2000	12,000/12,000	1000/1000	7000/7000
	W	1500/1500	8500/8500	2000/2000	2000/2000
	$\dot{U}$	1.5/ 1.5	5.5/ 5.5	1.5/ 1.5	4/4
	$\dot{V}$	1/ 1.5	6/5	1.5/2	3.5/3
	$\dot{W}$	1.5/ 1.5	5.5/ 5.5	1.5/1	1.5/ 1.5
Arc 305 data Hubbard elements	U	2000/3500	10,500/12,500	3000/1500	6500/4000
	V	4500/4500	18,500/18,500	2500/2500	7500/7500
	W	2000/2000	8000/8000	2500/2500	6500/6500
	$\dot{U}$	2/2	8.5/ 8.5	2/2	3.5/ 3.5
	$\dot{V}$	2/ 1.5	8/ 9.5	3/2	3.5/3
	$\dot{W}$	2/2	9/9	2/2	>4/>4

Position components are in feet, velocities in feet/second. The
first number of each pair is for a fitted, the second for a
implied by a = $(\mu/n^2)^{1/3}$.
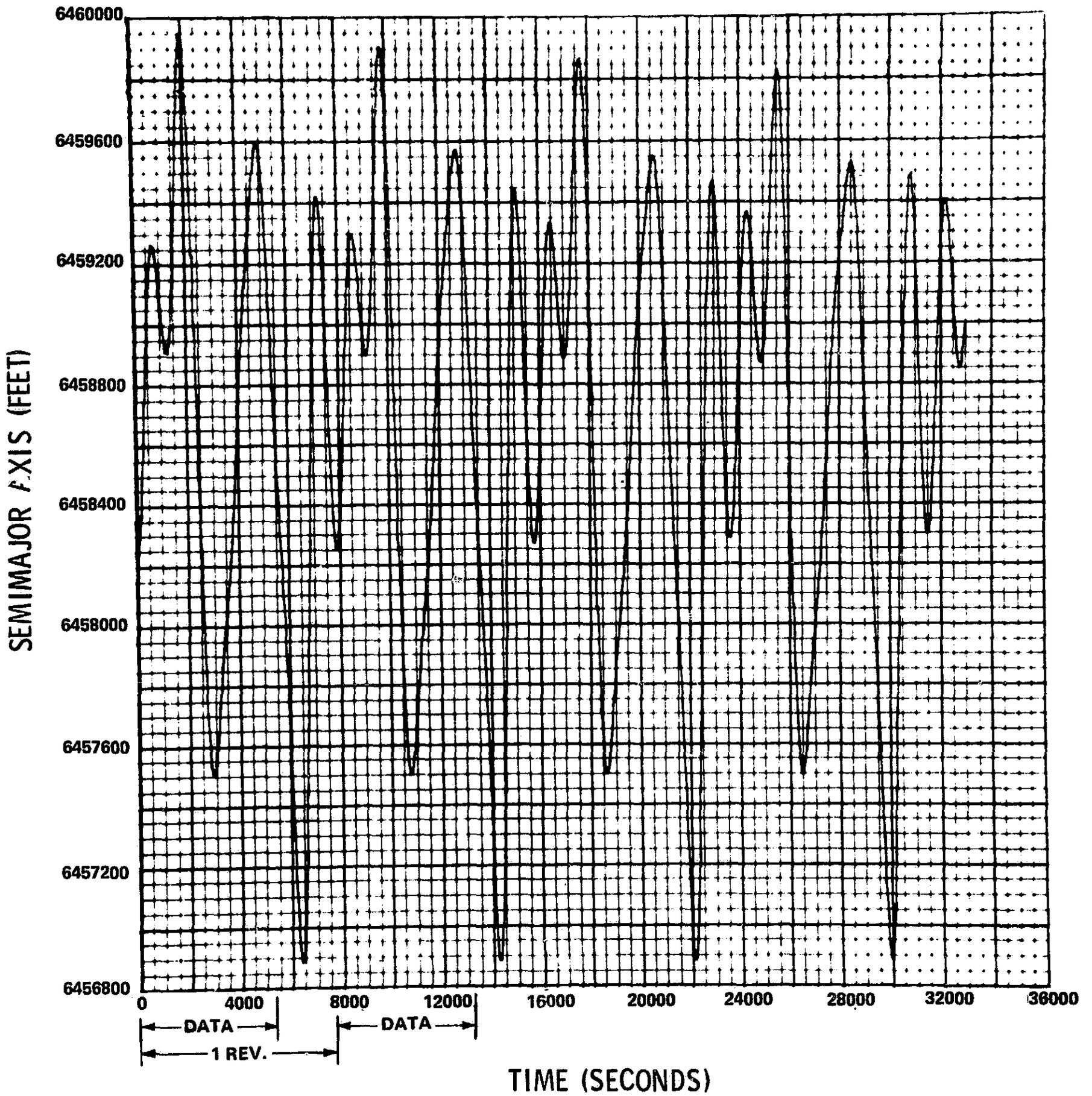
FIGURE 1a
e = .04 DATA

SEMIMAJOR AXIS TIME HISTORY
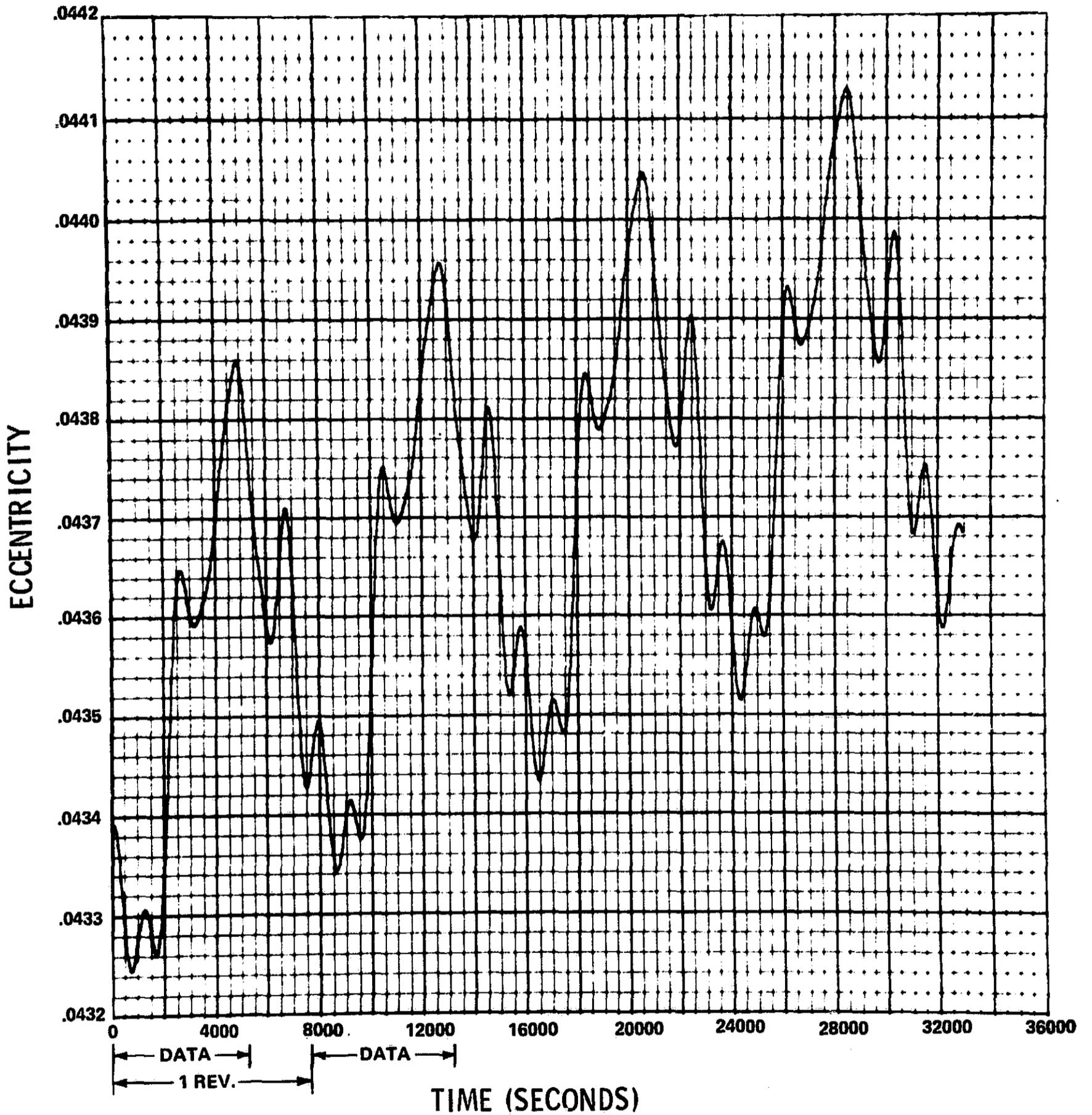
FIGURE 1b
e = .04 DATA

ECCENTRICITY TIME HISTORY
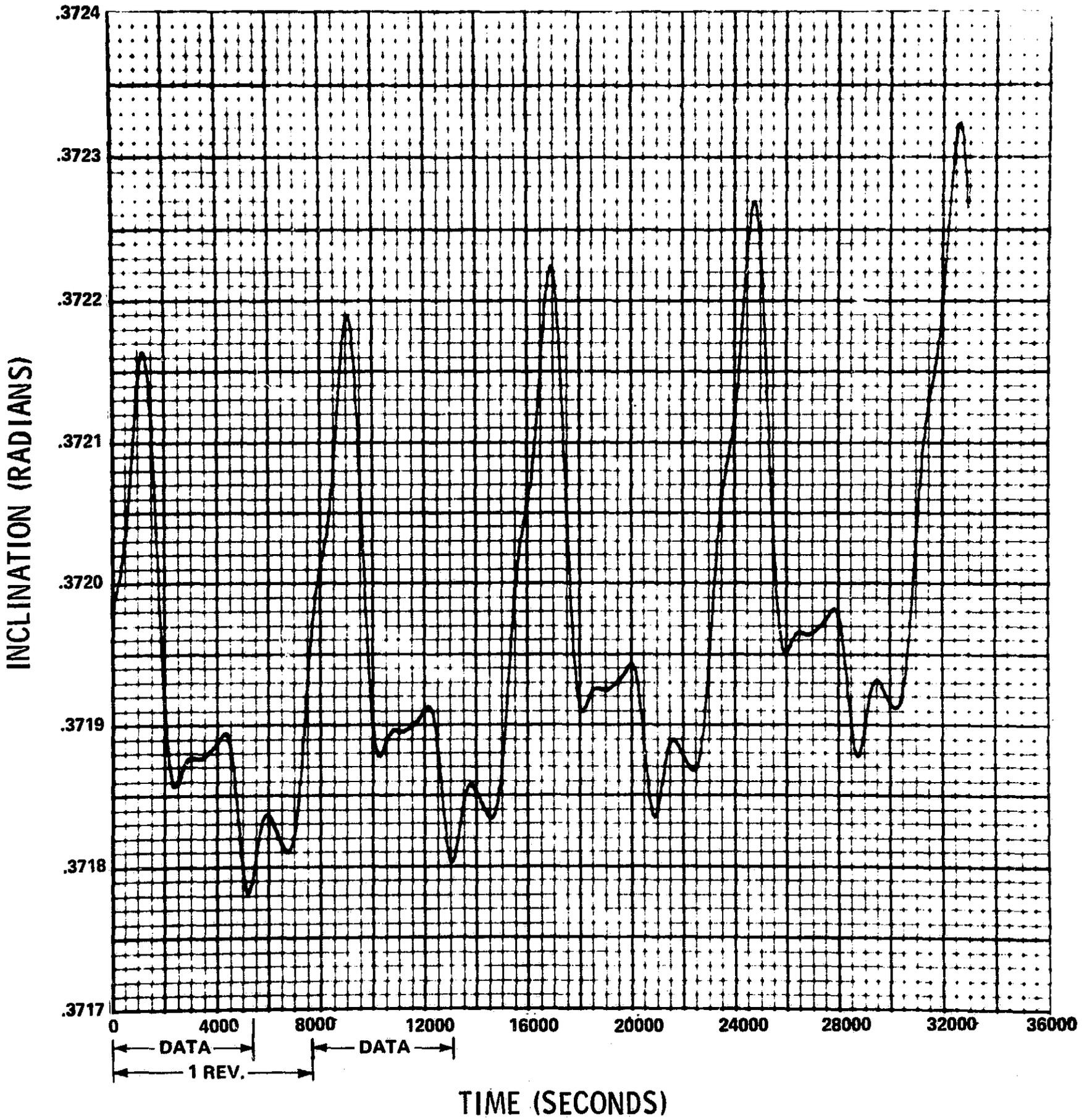
FIGURE 1c
e = .04 DATA

INCLINATION TIME HISTORY
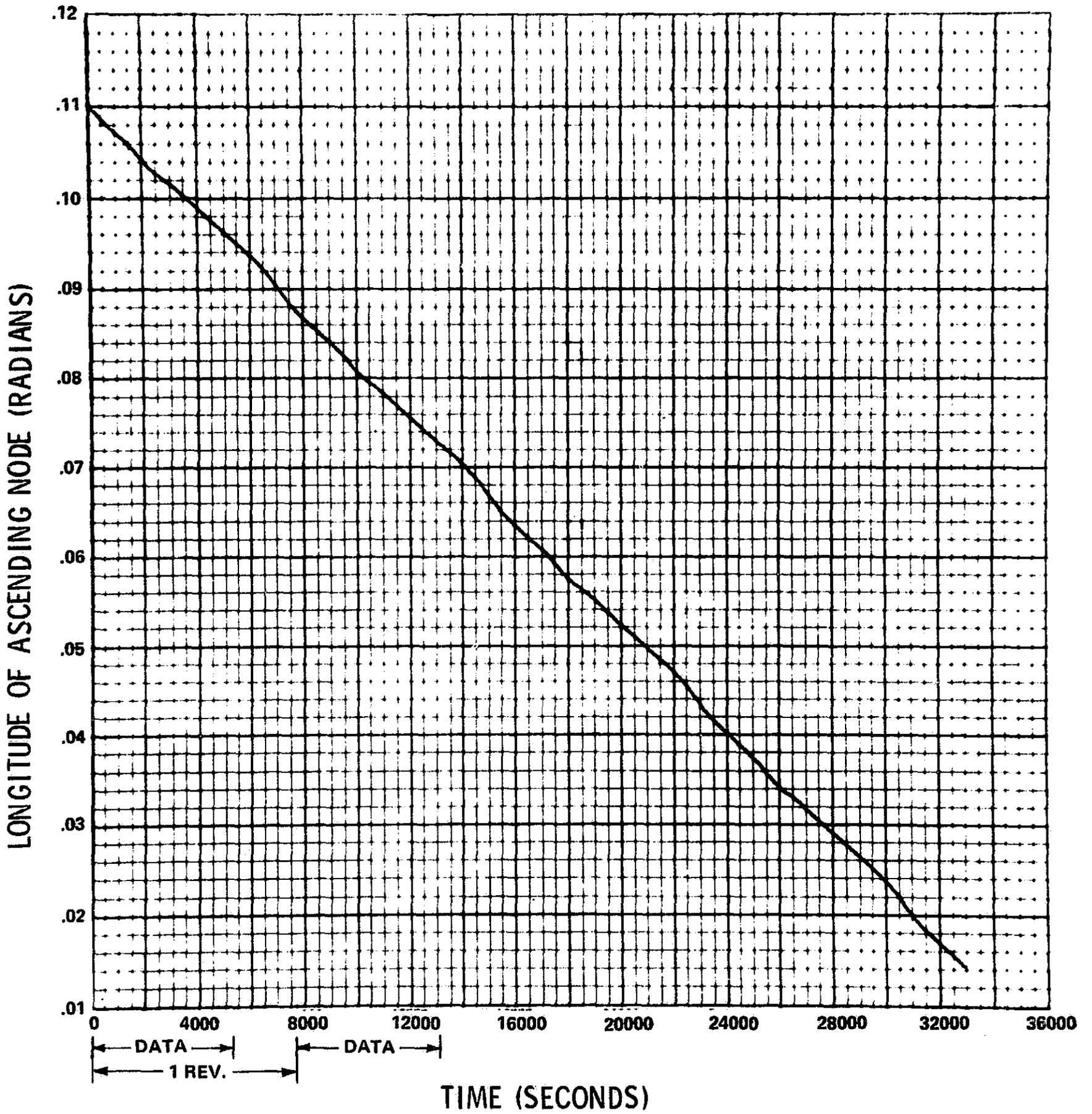
FIGURE 1d
e = .04 DATA

LONGITUDE OF ASCENDING NODE TIME HISTORY
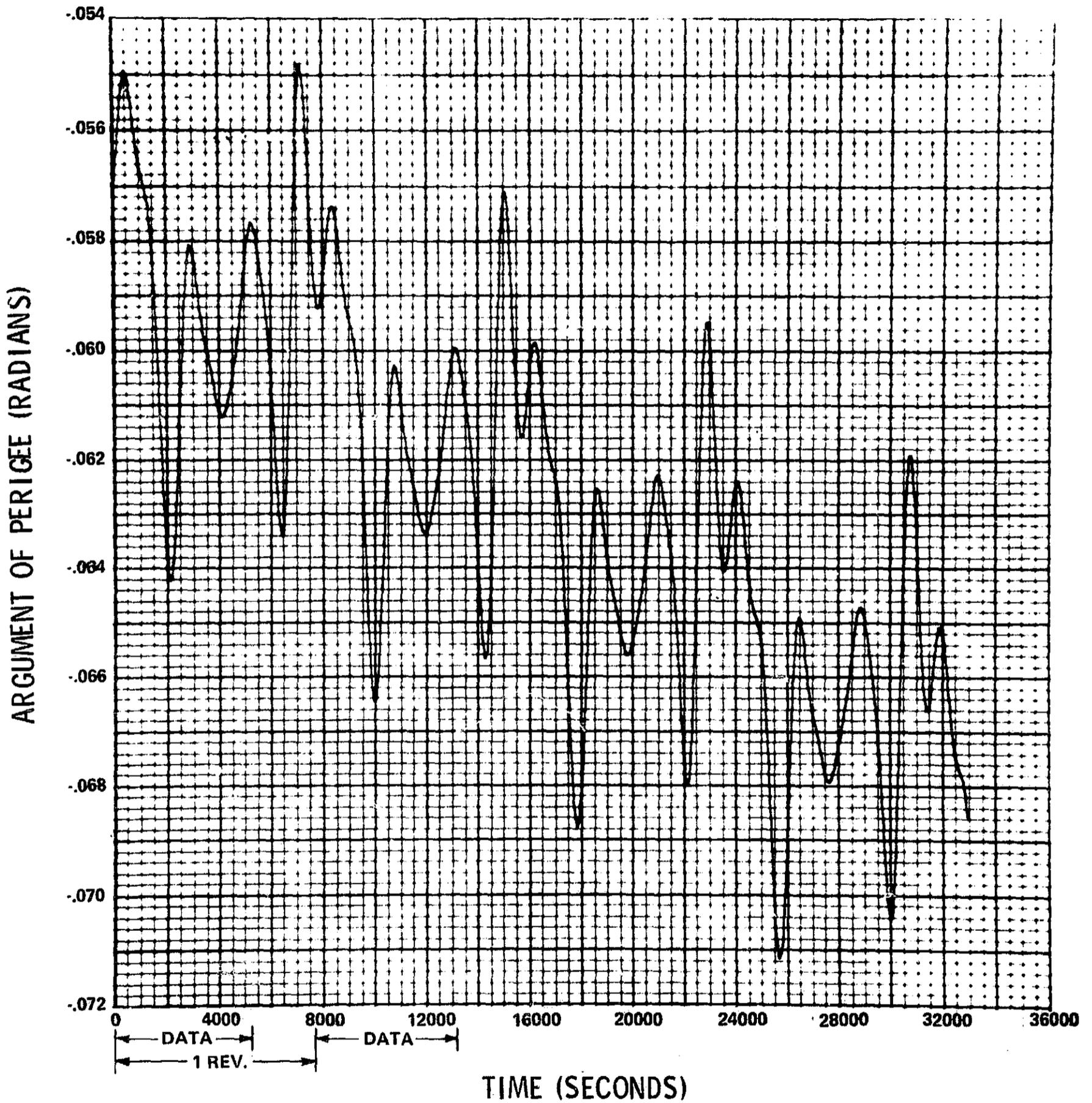
FIGURE 1e
e = .04 DATA

ARGUMENT OF PERIGEE TIME HISTORY
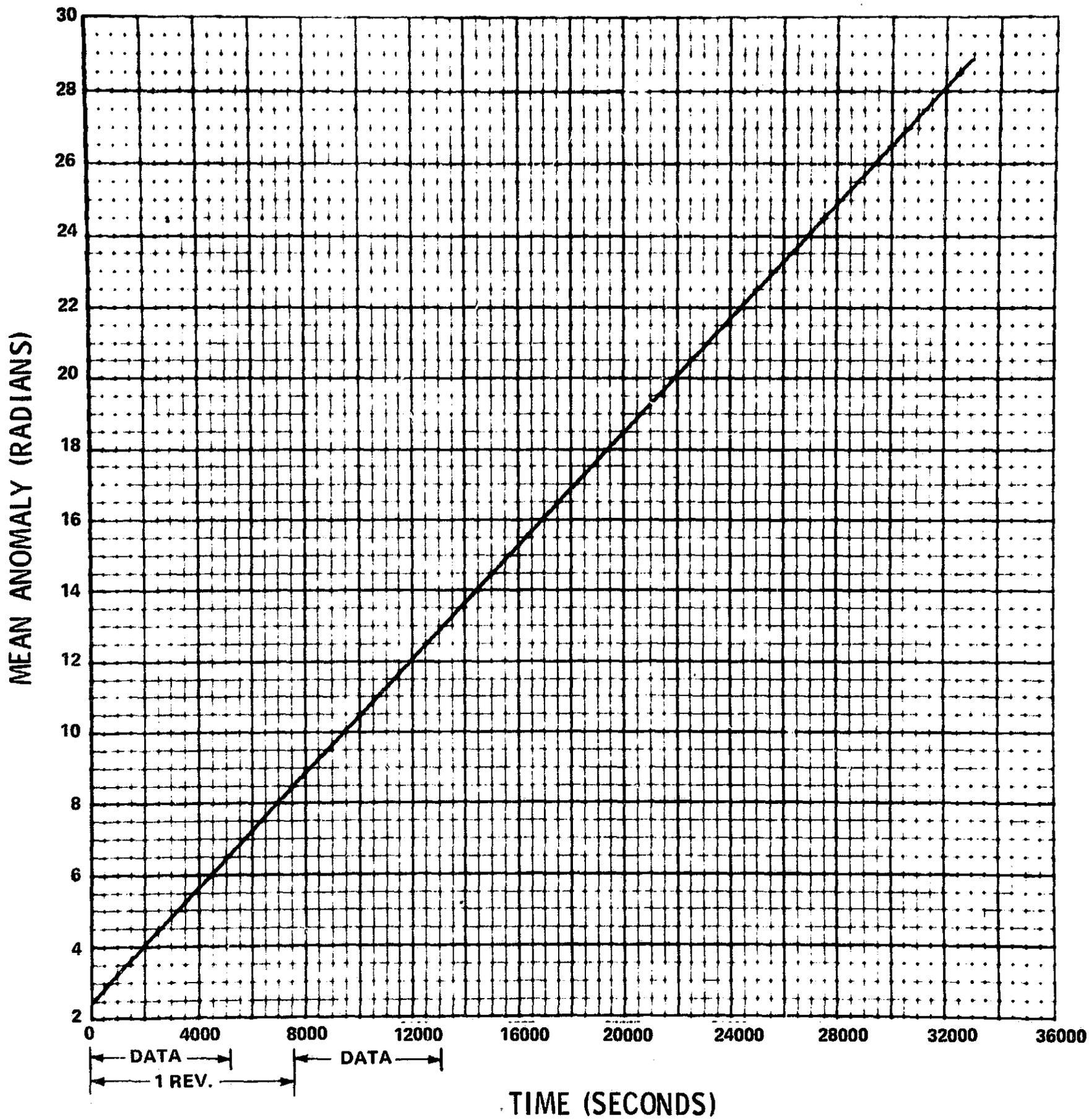
FIGURE 1f
e = .04 DATA

MEAN ANOMALY TIME HISTORY
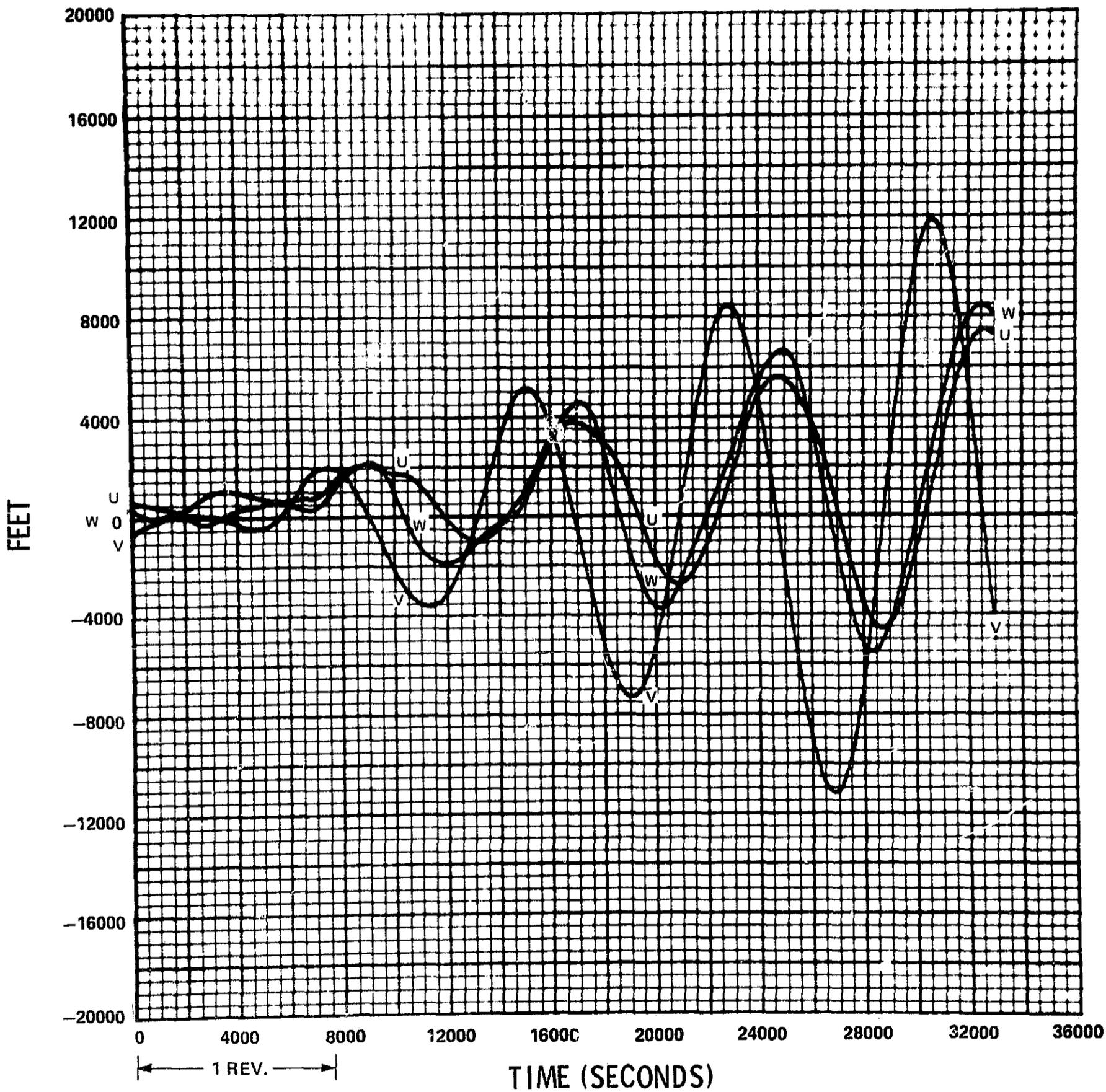
FIGURE 1g
e = .04 DATA, FITS TO 1 ORBIT
UVW POSITION COMPONENT RESIDUALS
ALL ELEMENTS FIT
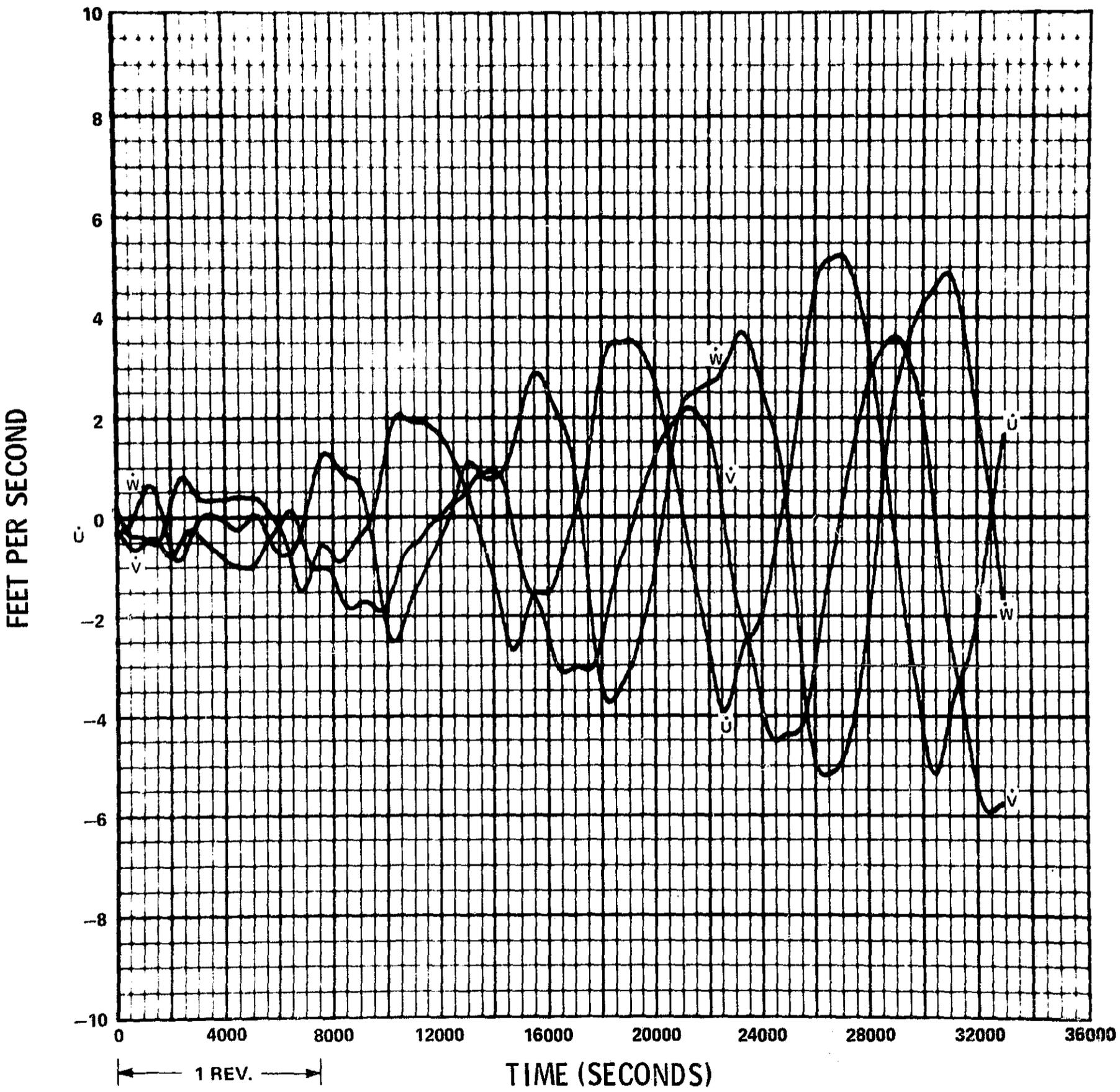
FIGURE 1h
e = .04 DATA, FITS TO 1 ORBIT
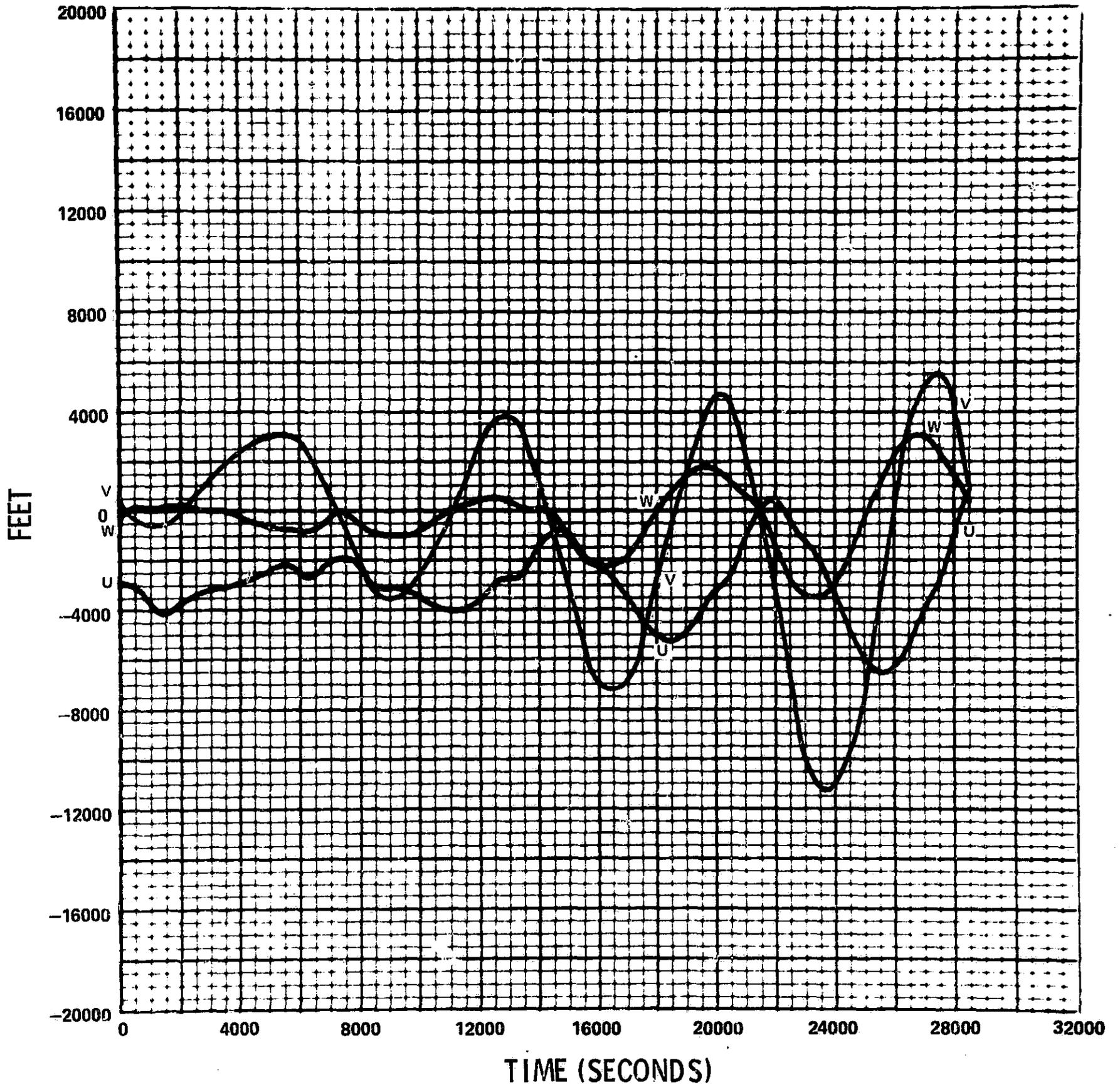UVW VELOCITY COMPONENT RESIDUALS
ALL ELEMENTS FIT
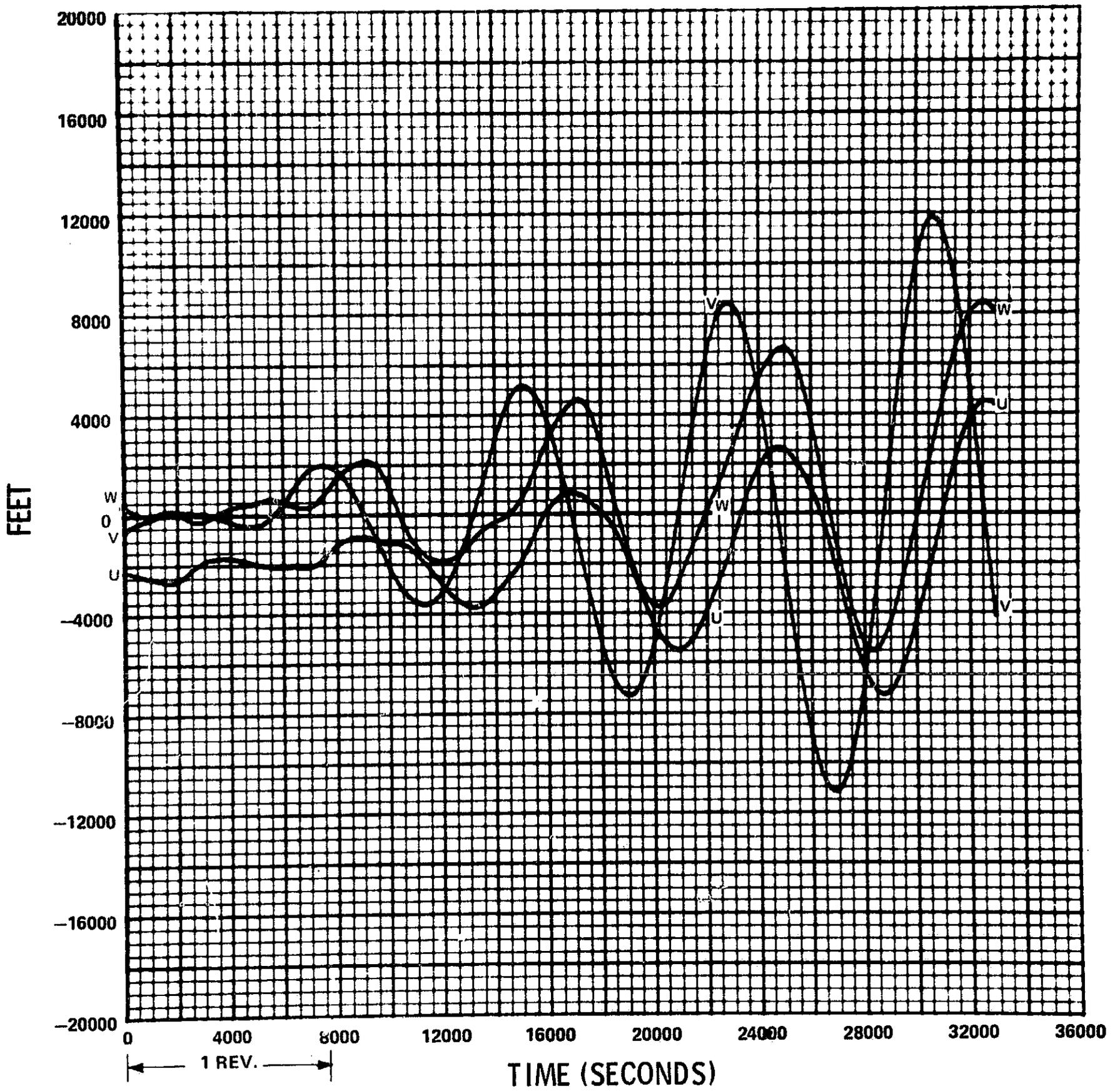
FIGURE 1i
e = .04 DATA, FITS TO 1 ORBIT
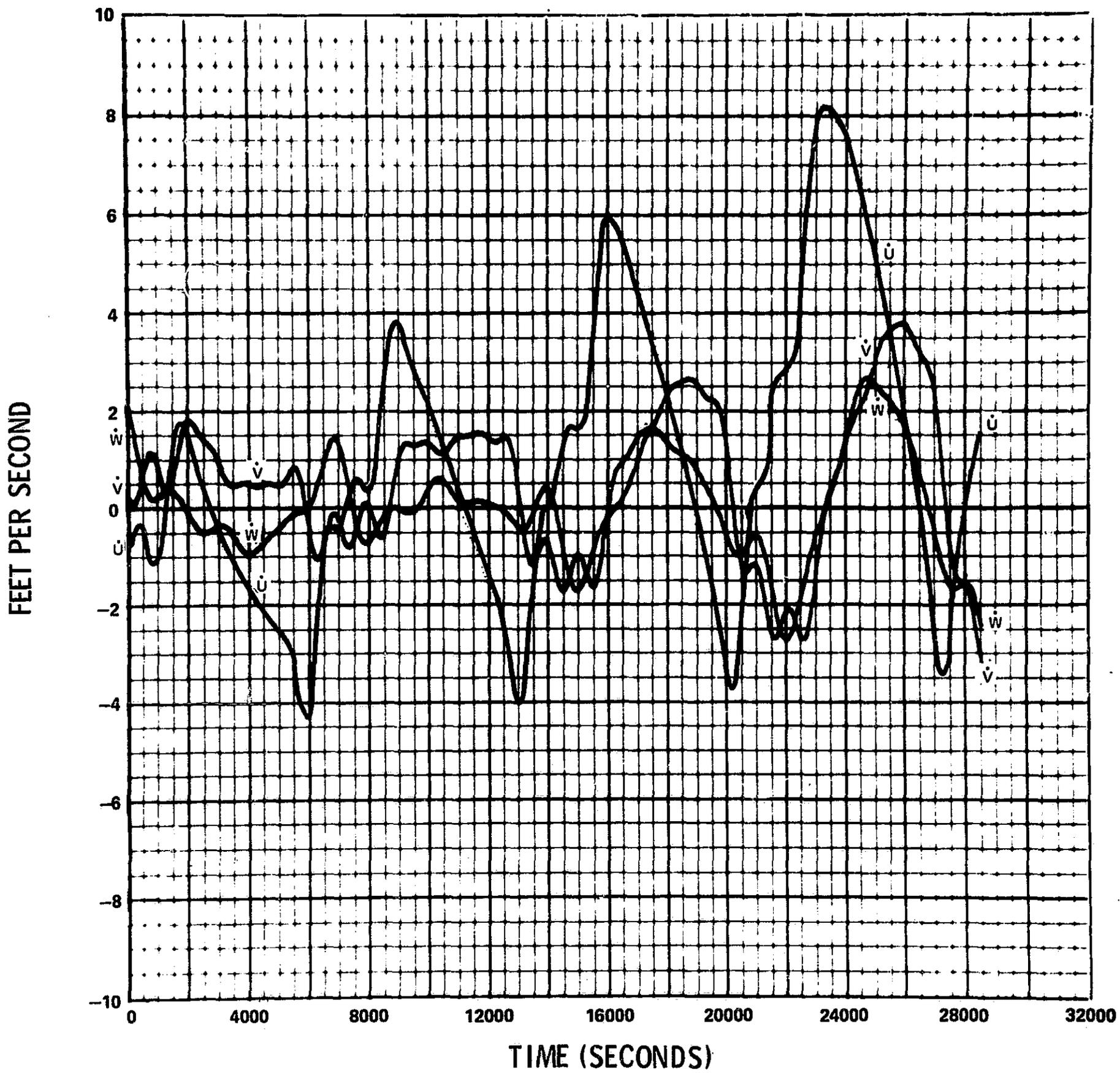UVW POSITION COMPONENT RESIDUALS
SEMIMAJOR AXIS IMPLIED
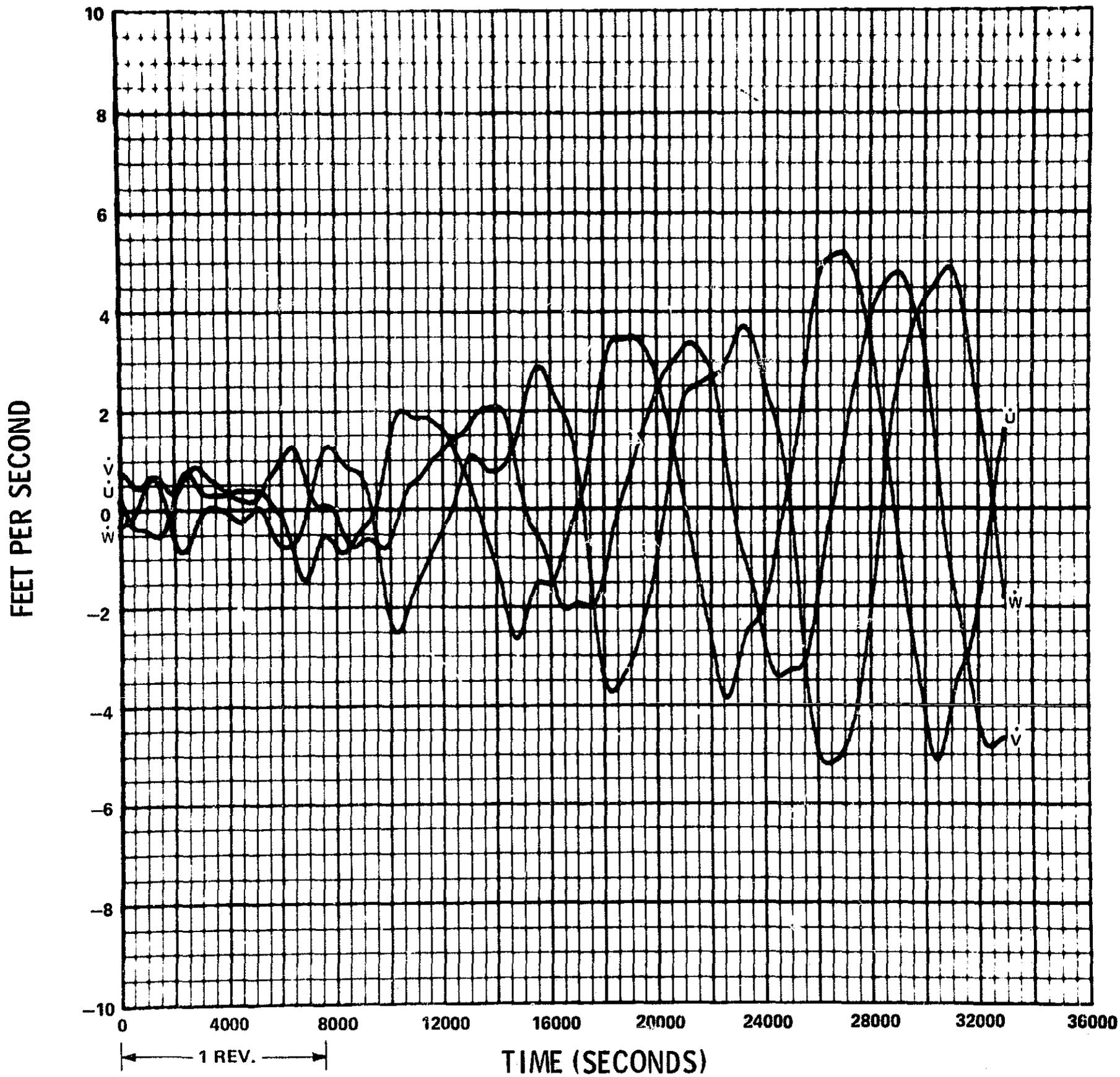
FIGURE 1j
e = .04 DATA, FITS TO 1 ORBIT
UVW VELOCITY COMPONENT RESIDUALS
SEMIMAJOR AXIS IMPLIED

POSITION RESIDUALS

VELOCITY RESIDUALS
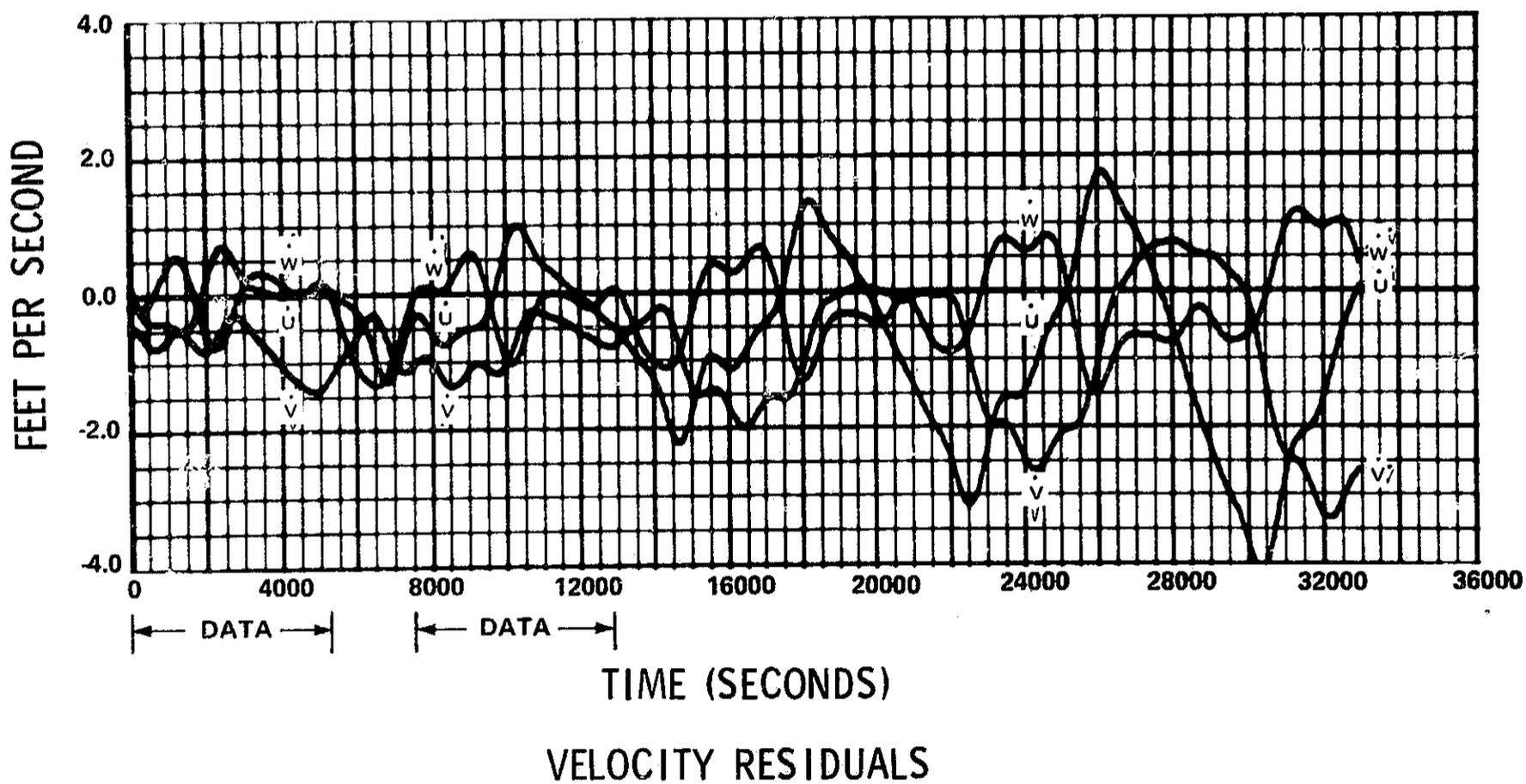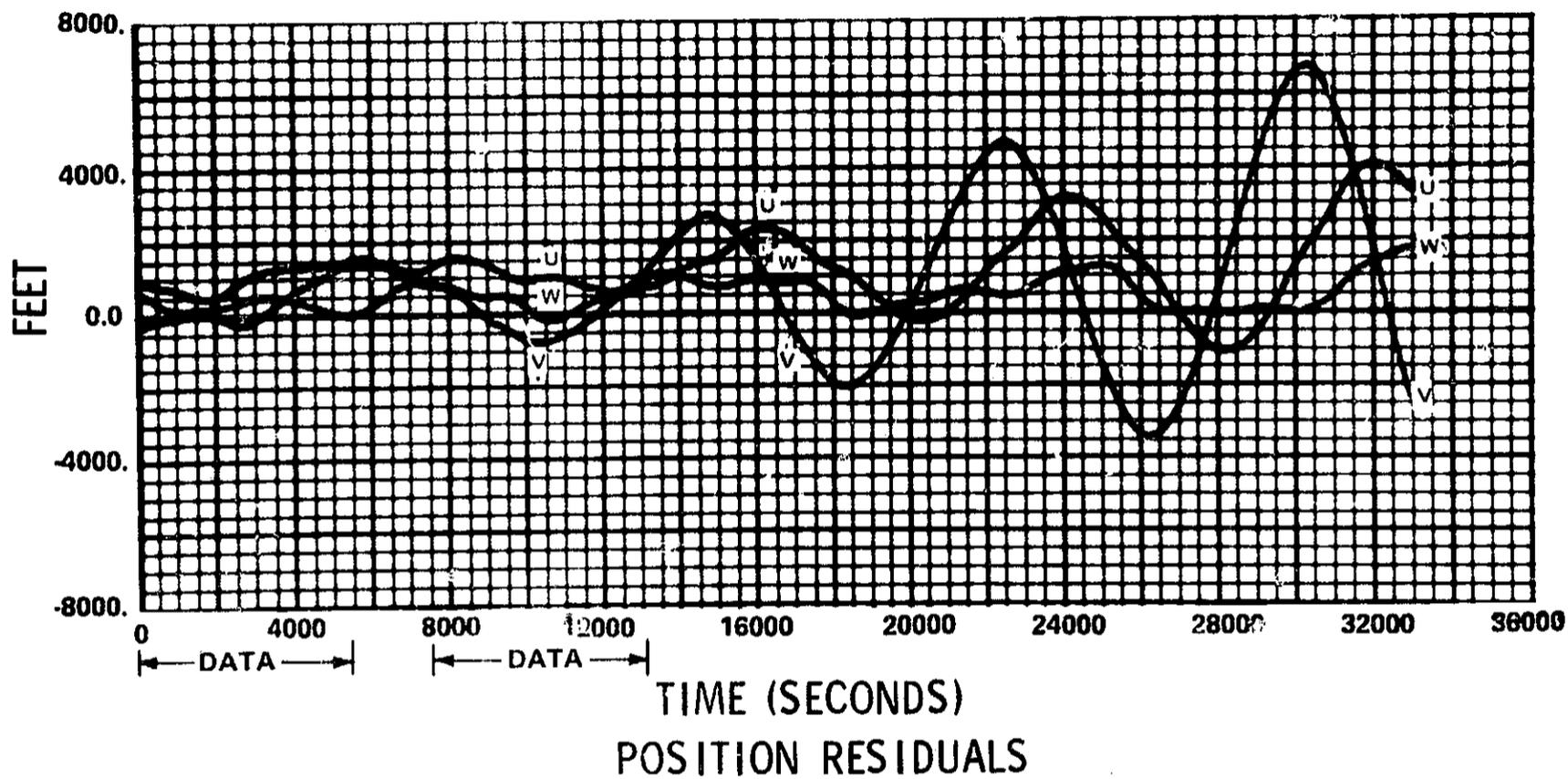
FIGURE 1k
e = .04 DATA, FITS TO 2 ORBITS
UVW COMPONENT RESIDUALS
ALL ELEMENTS FIT
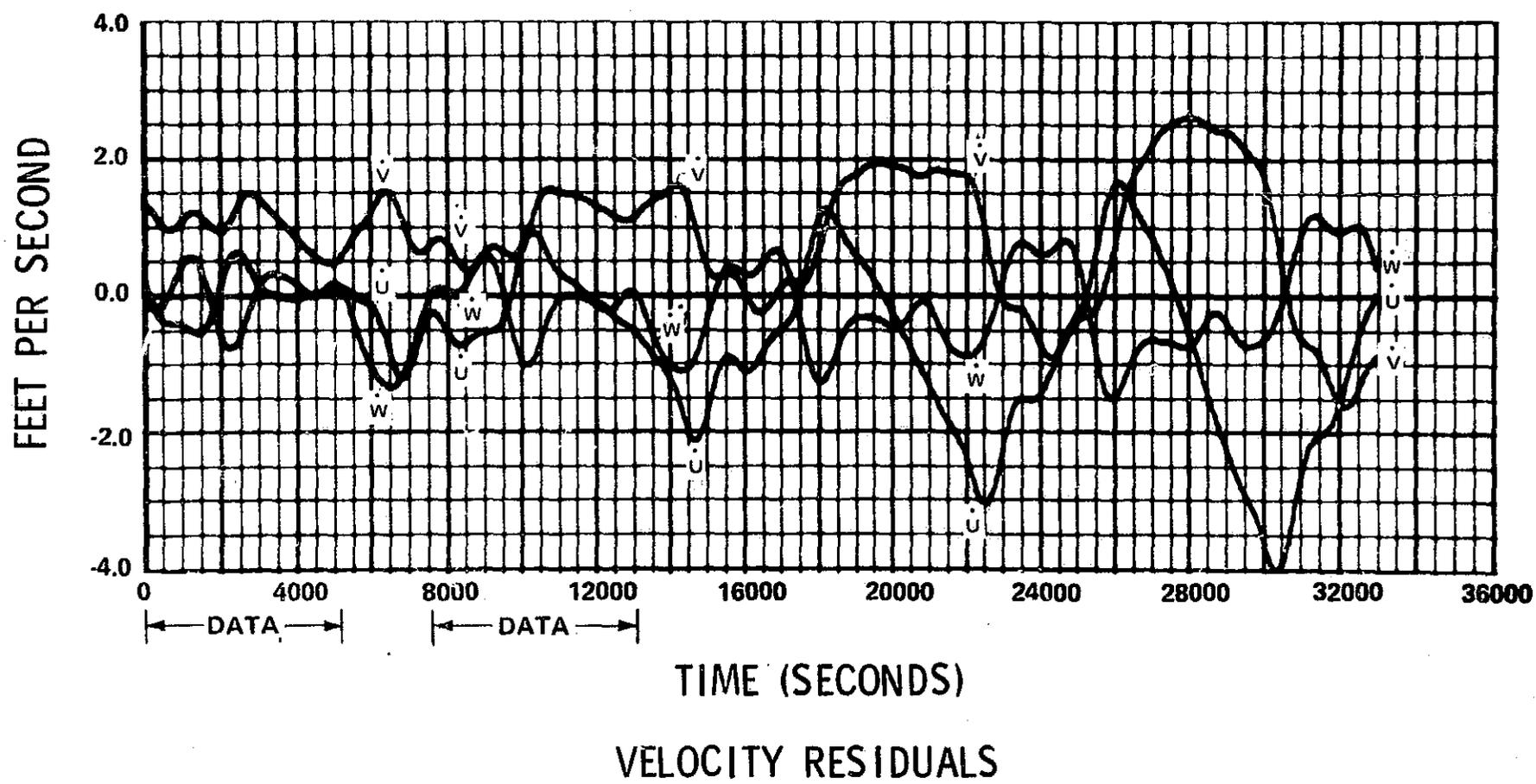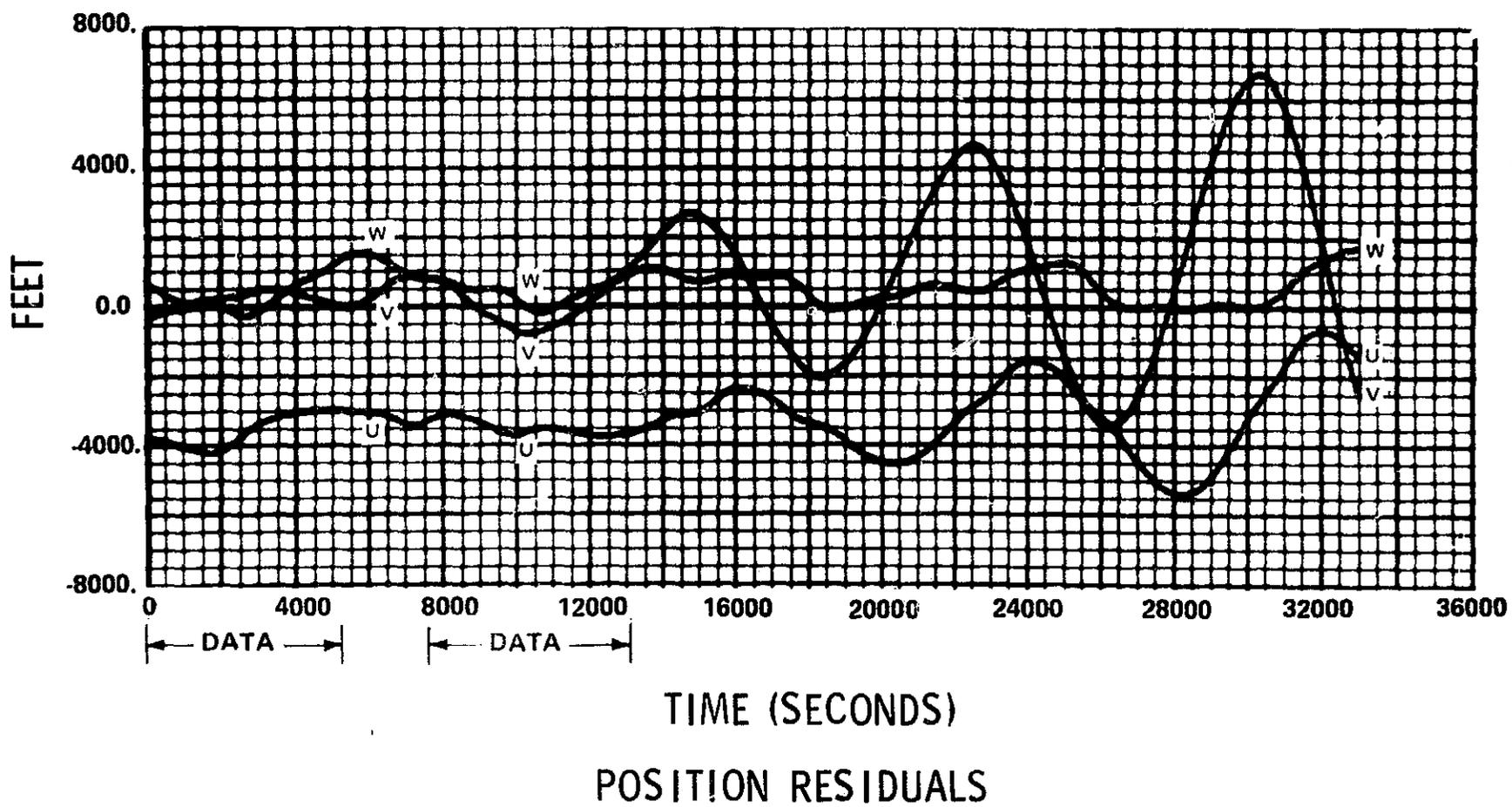
FIGURE 1ℓ
e = .04 DATA, FITS TO 2 ORBITS
UVW COMPONENT RESIDUALS
SEMIMAJOR AXIS IMPLIED
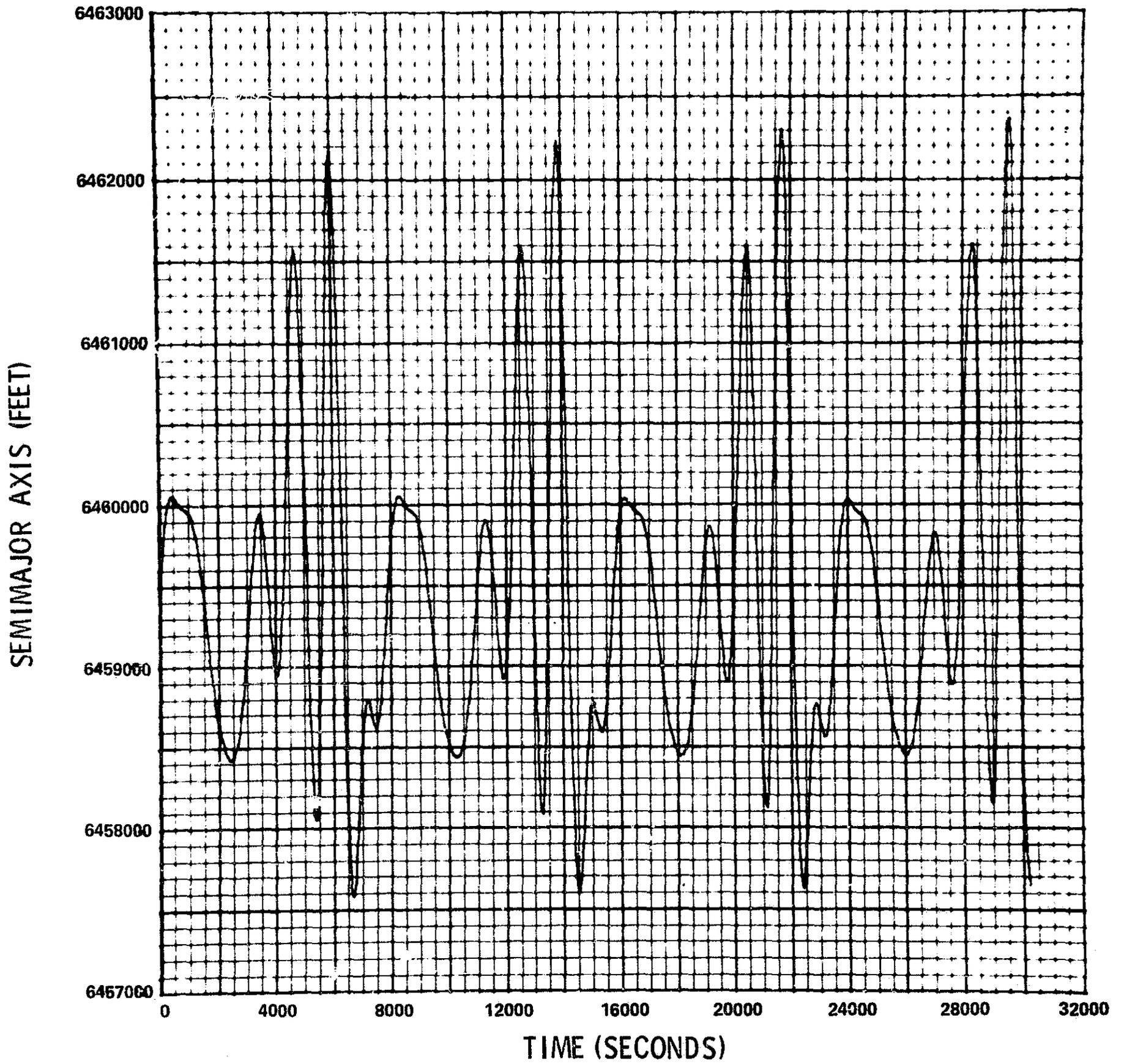
FIGURE 2a
ARC 305 DATA
SEMIMAJOR AXIS TIME HISTORY
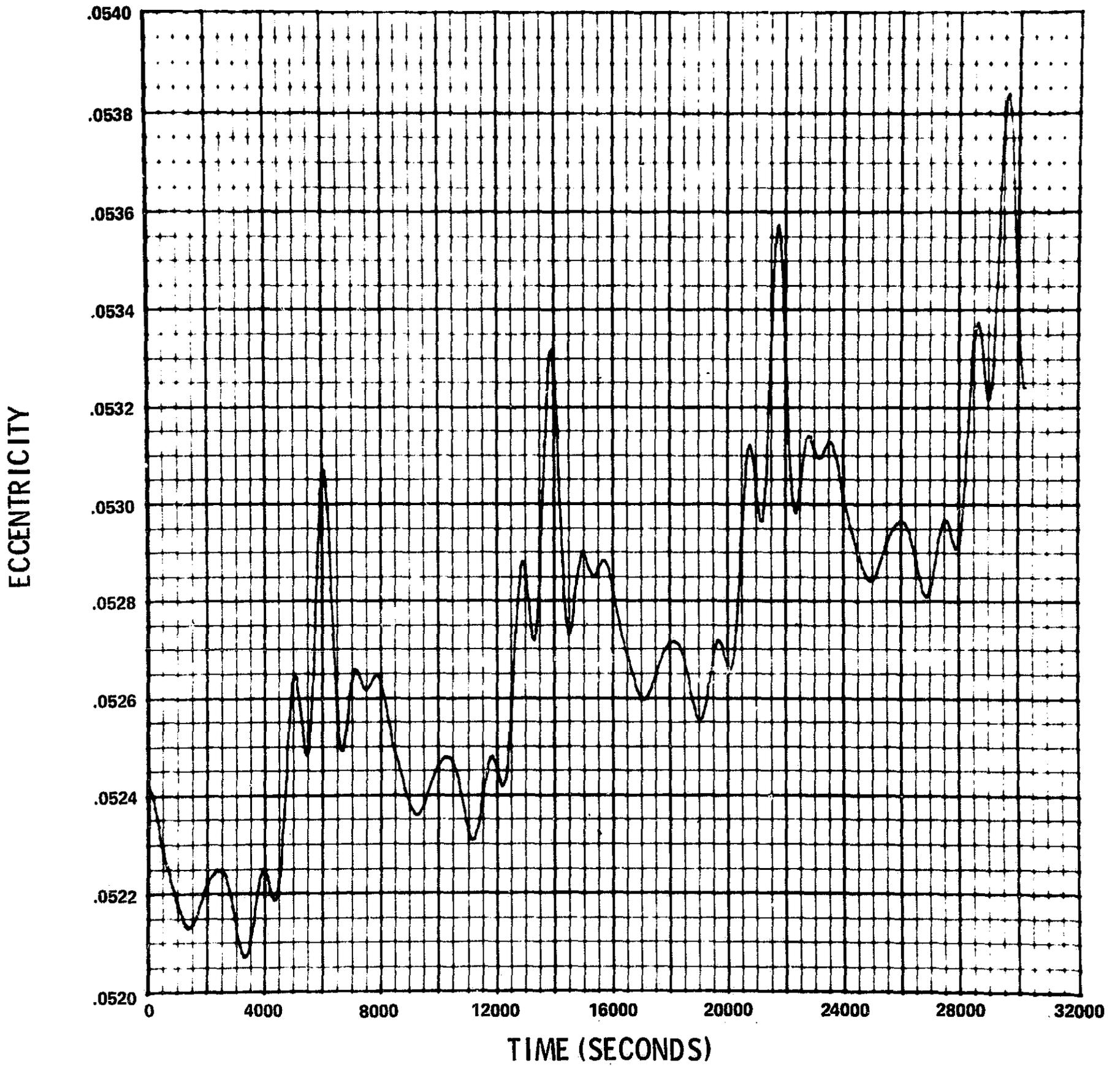
FIGURE 2b
ARC 305 DATA
ECCENTRICITY TIME HISTORY
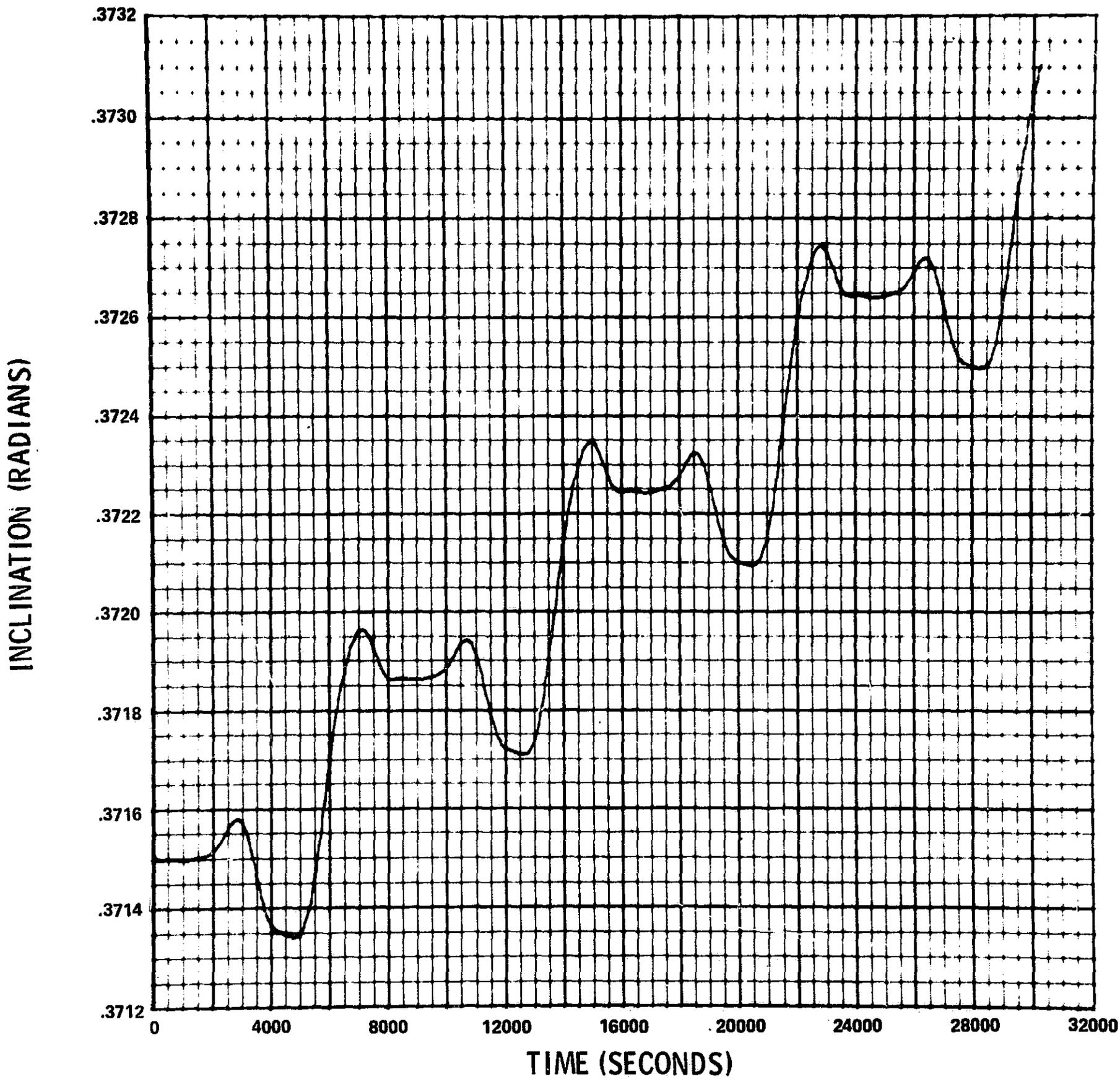
FIGURE 2c
ARC 305 DATA
INCLINATION TIME HISTORY
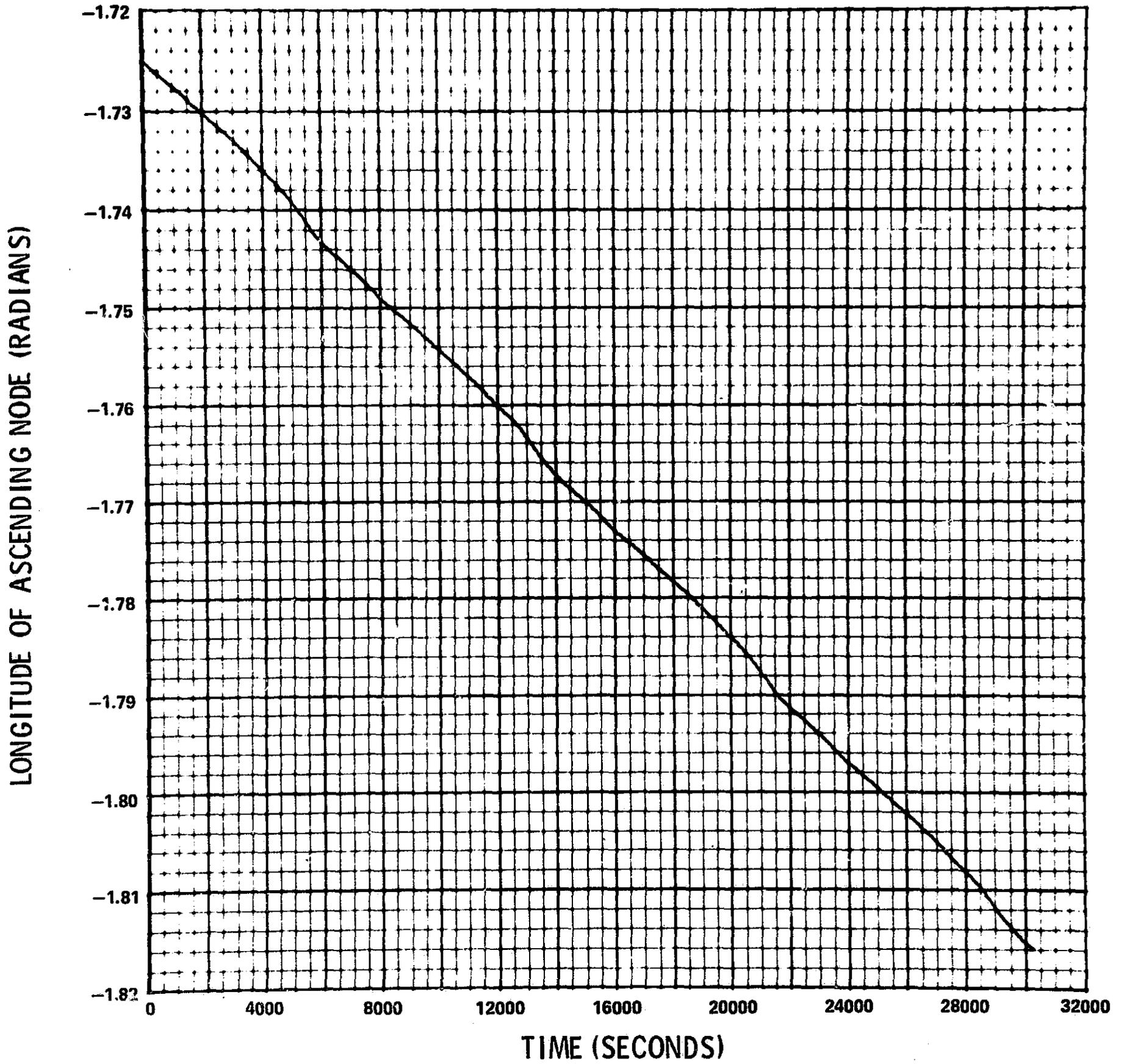
FIGURE 2d
ARC 305 DATA
LONGITUDE OF ASCENDING NODE TIME HISTORY
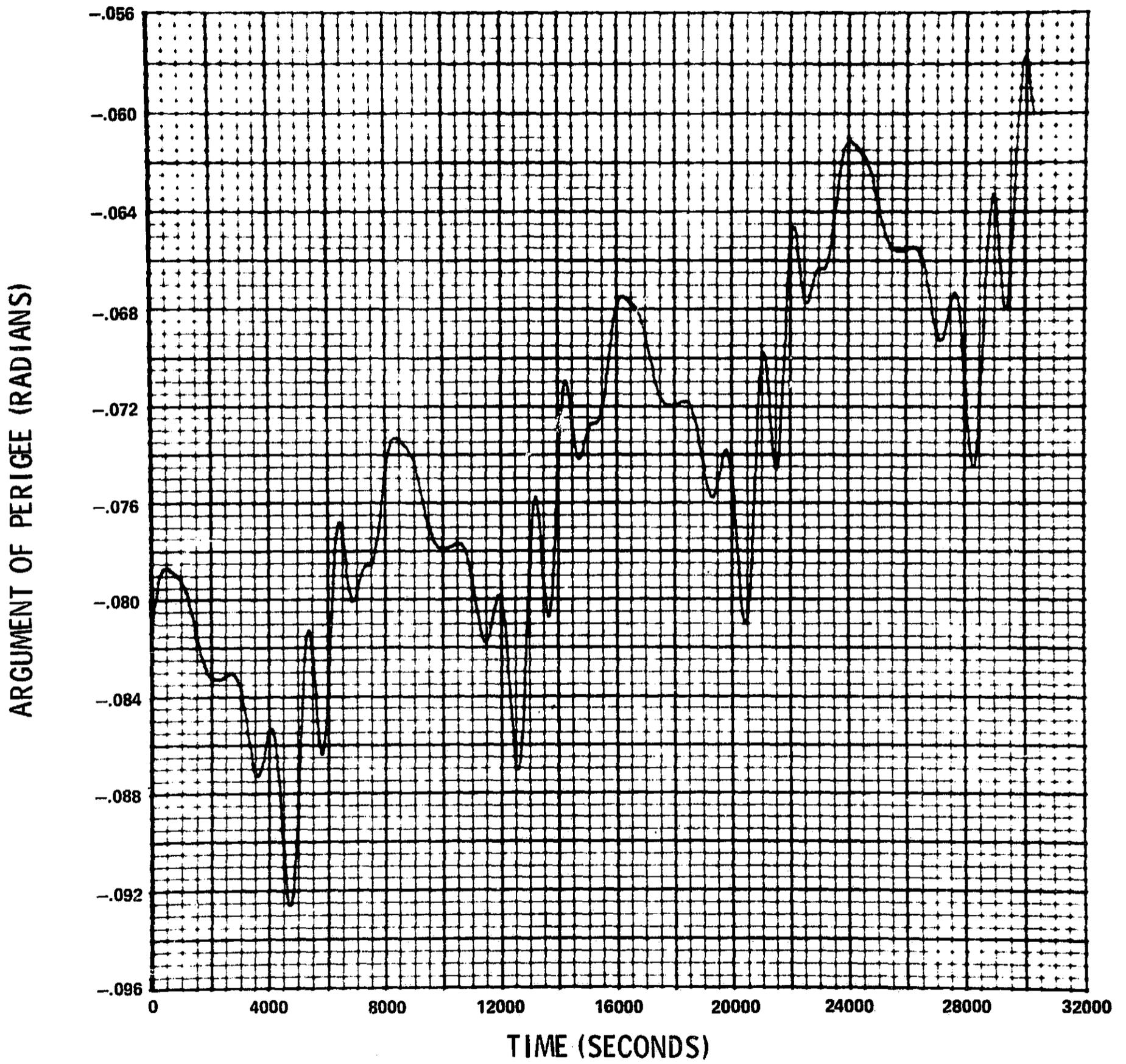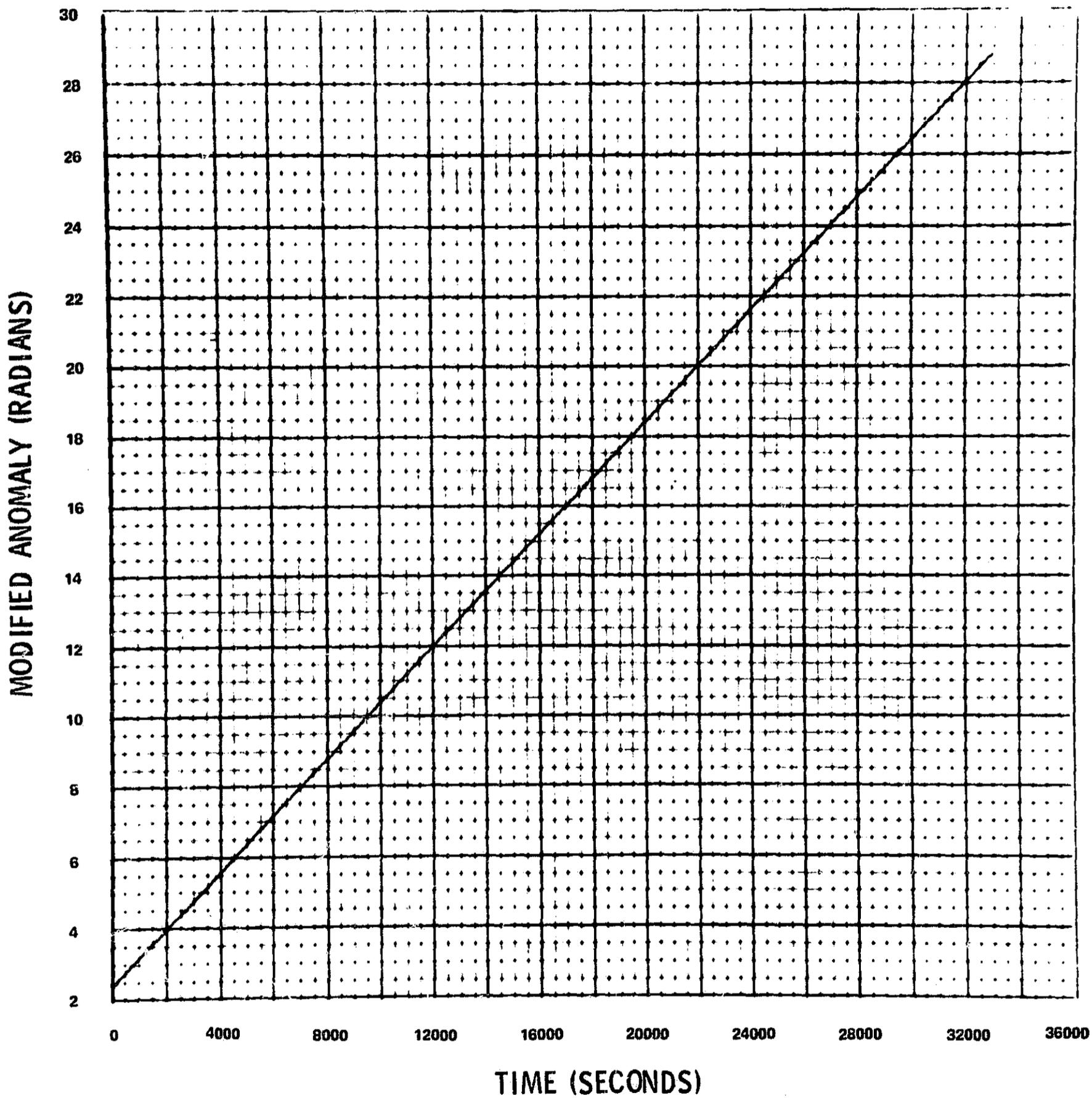
FIGURE 2e
ARC 305 DATA
ARGUMENT OF PERIGEE TIME HISTORY
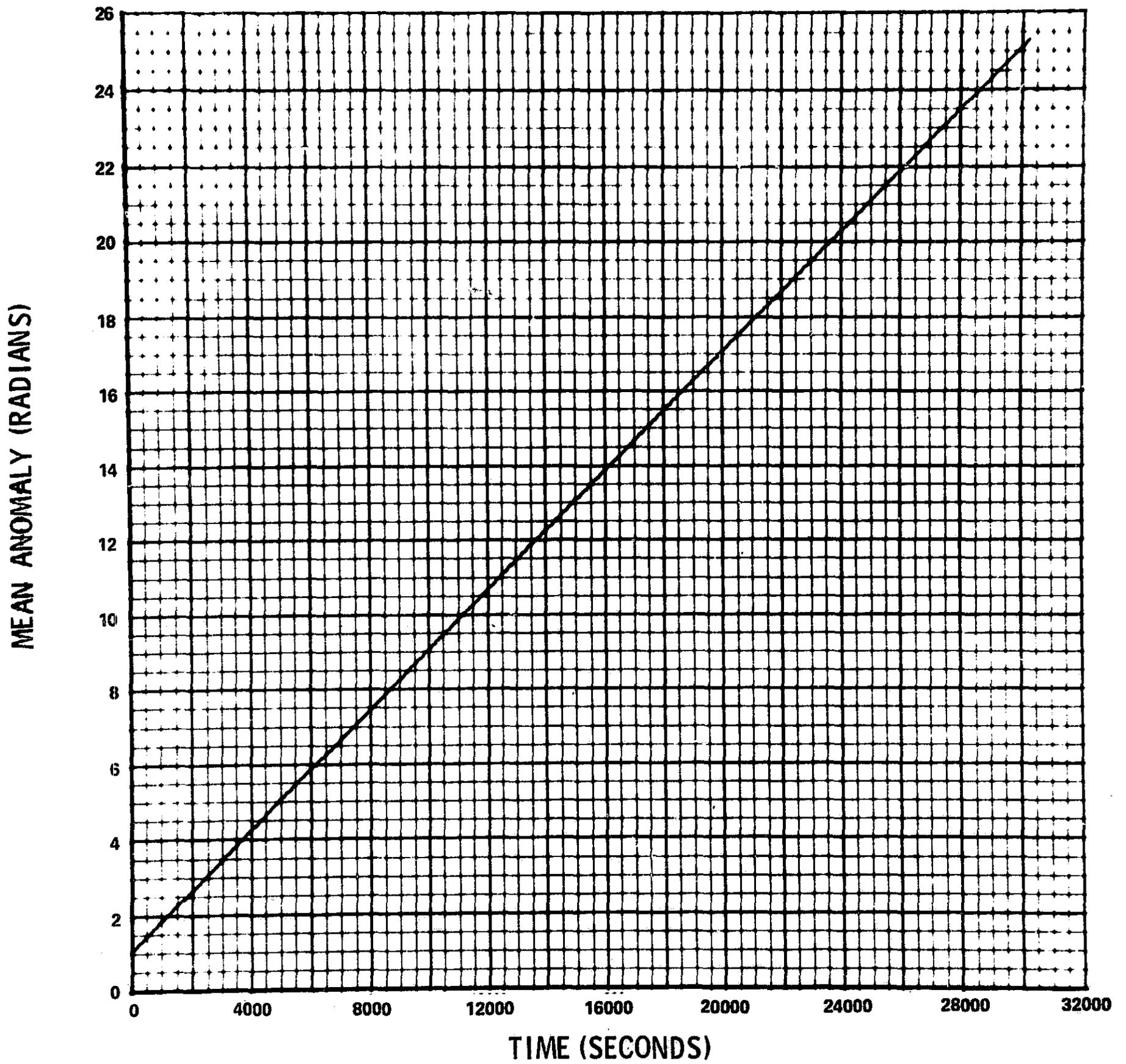
FIGURE 2f
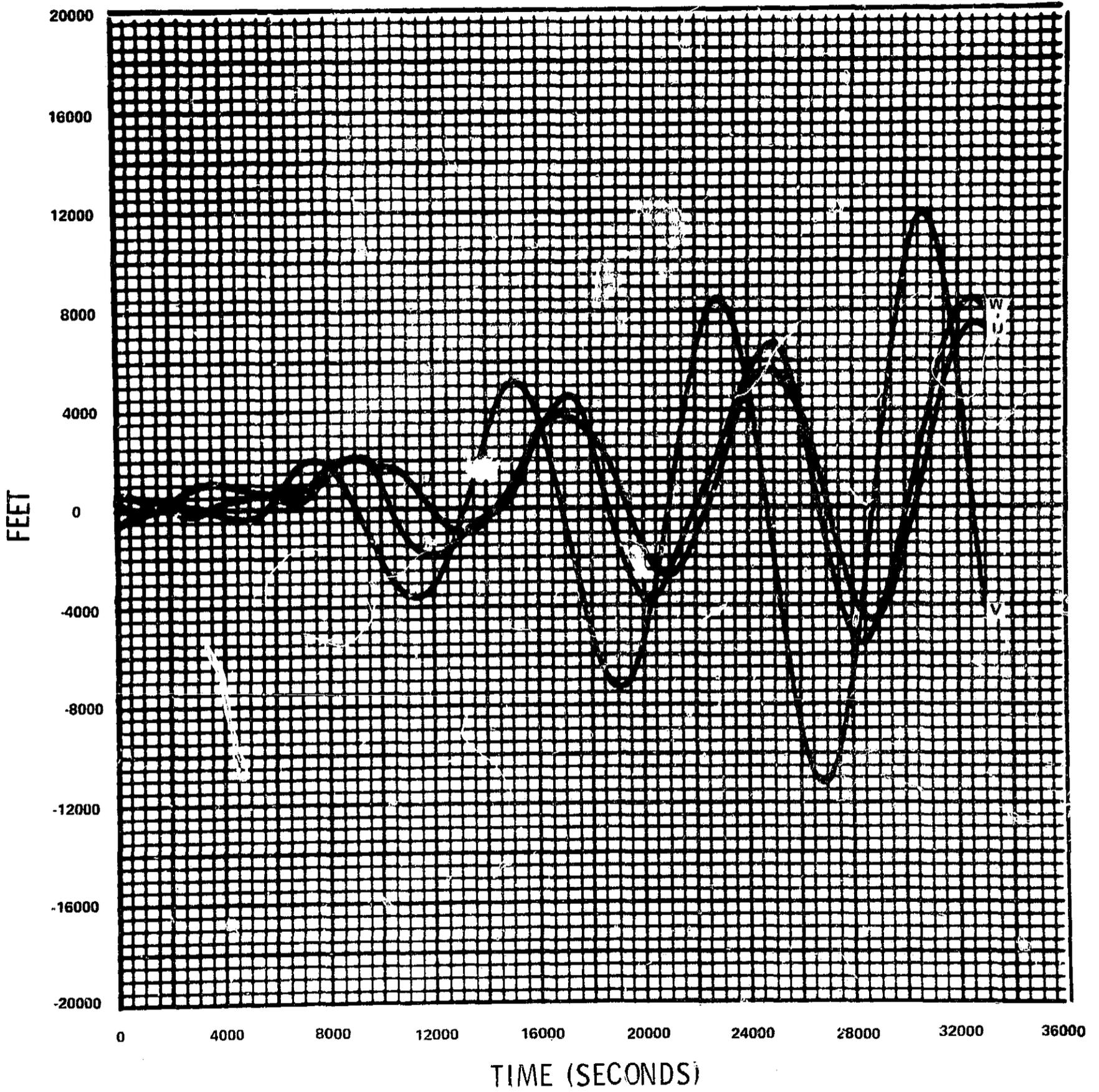ARC 305 DATA
MEAN ANOMALY TIME HISTORY
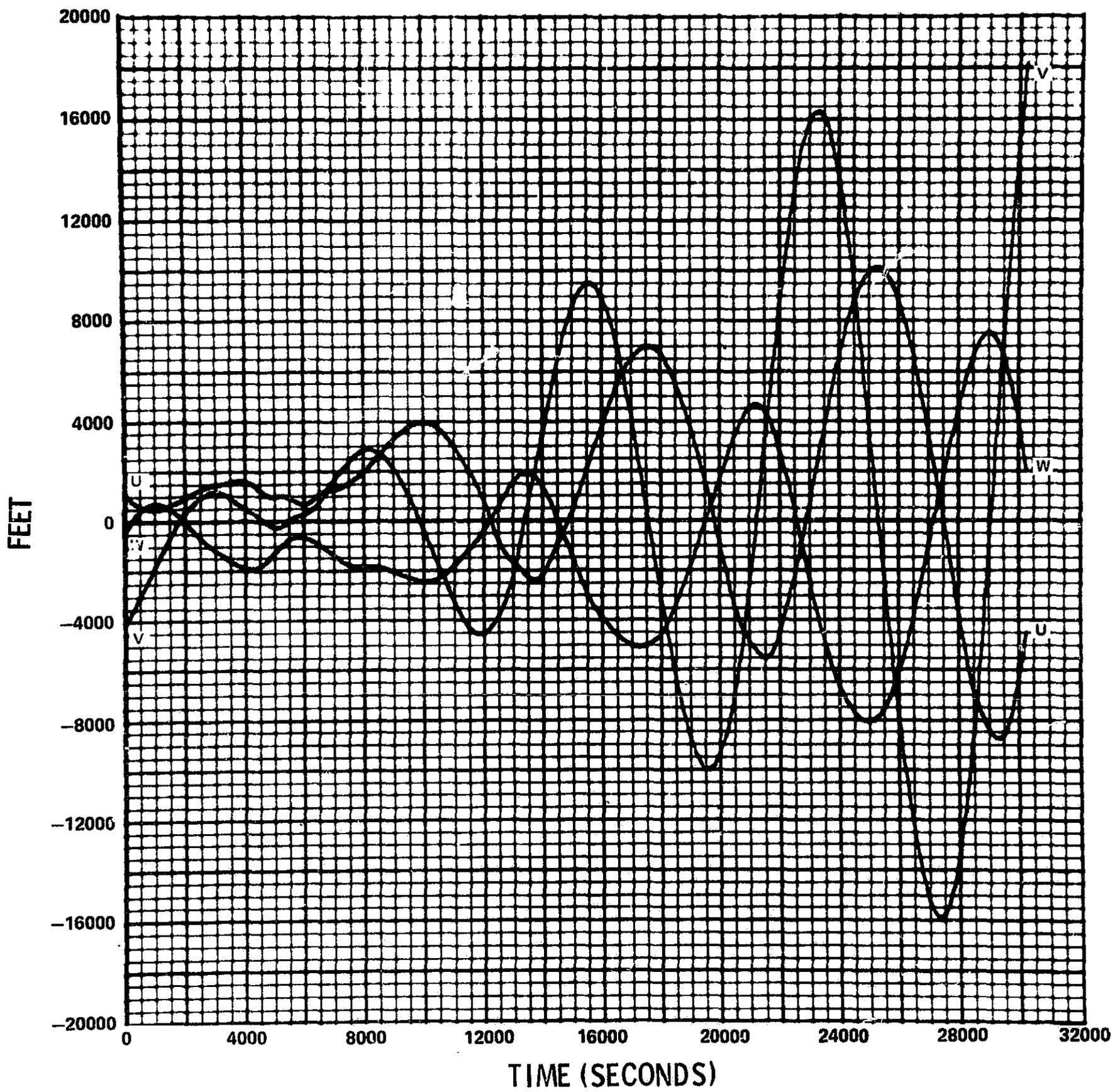
FIGURE 2g
ARC 305 DATA, FITS TO 1 ORBIT
UVW POSITION COMPONENT RESIDUALS
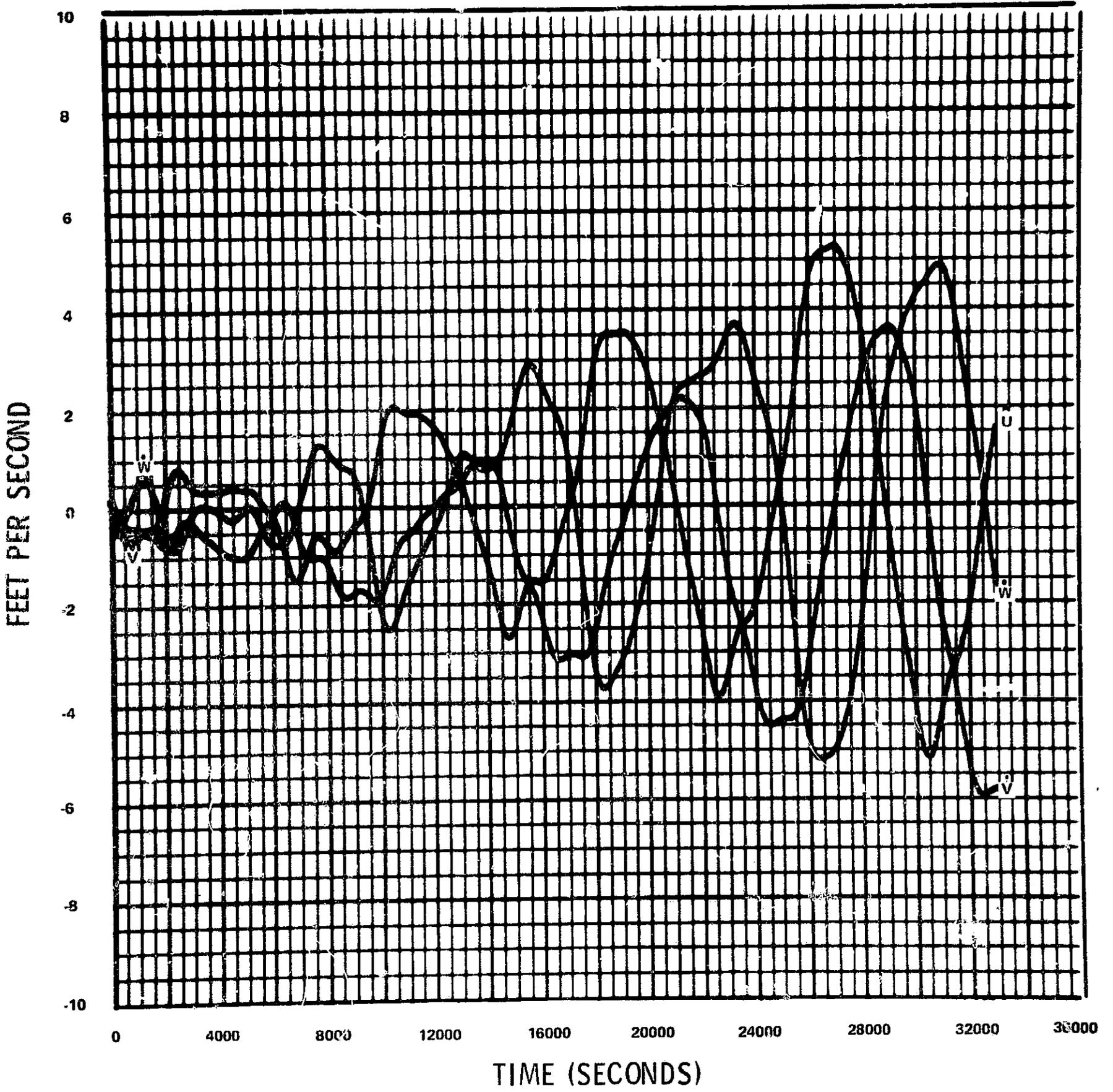ALL ELEMENTS FIT
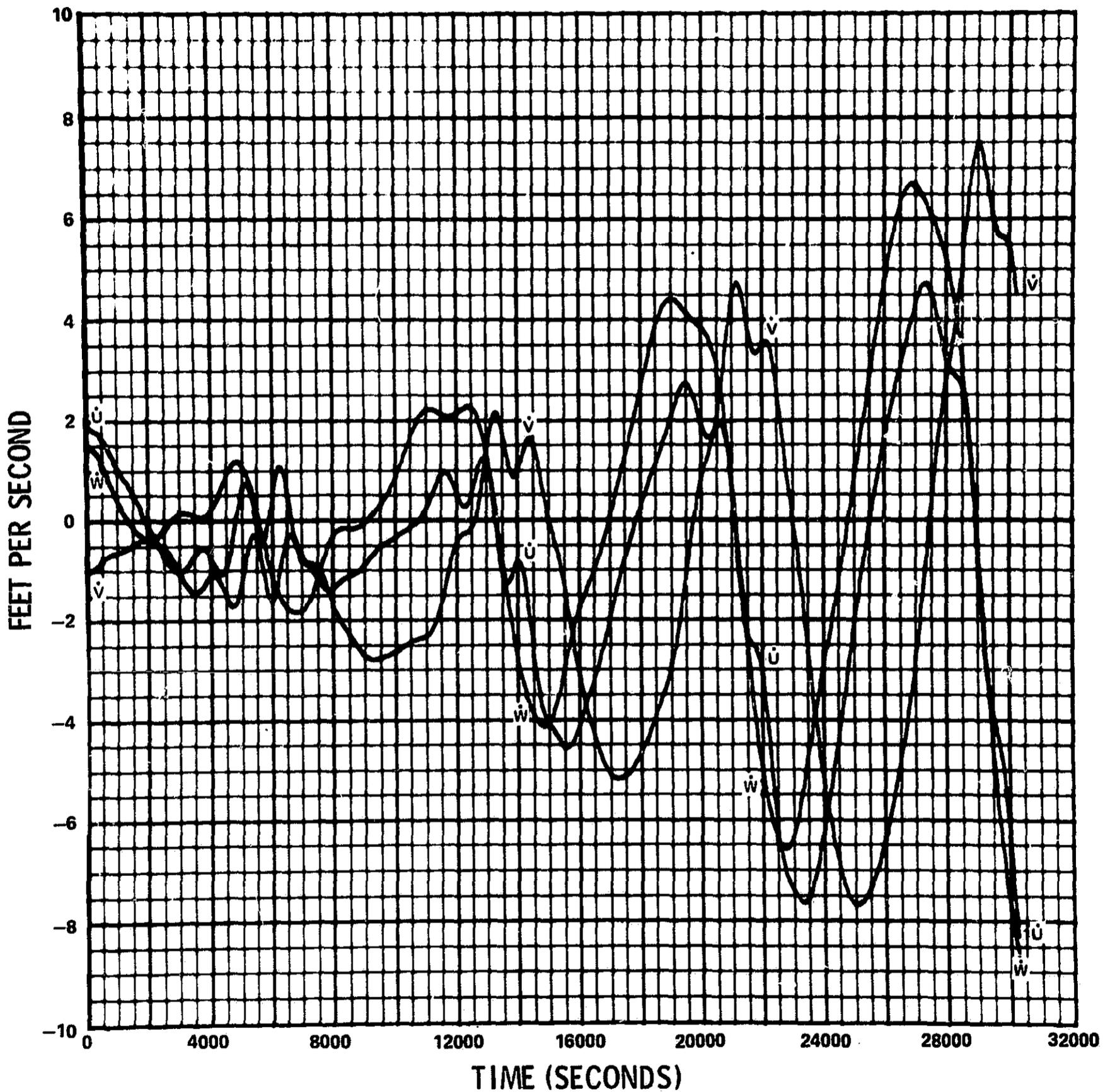
FIGURE 2h
ARC 305 DATA, FITS TO 1 ORBIT
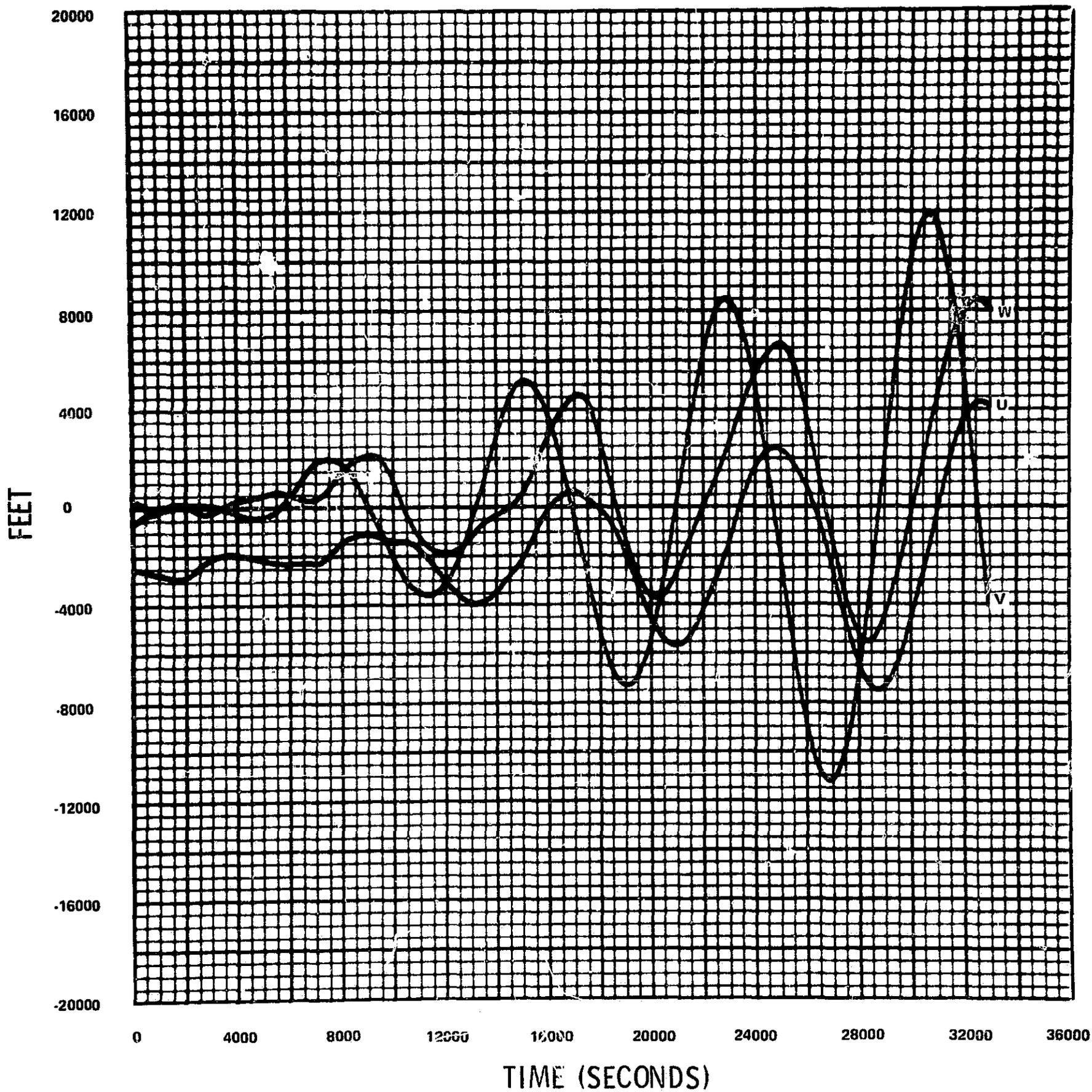UVW VELOCITY COMPONENT RESIDUALS
ALL ELEMENTS FIT
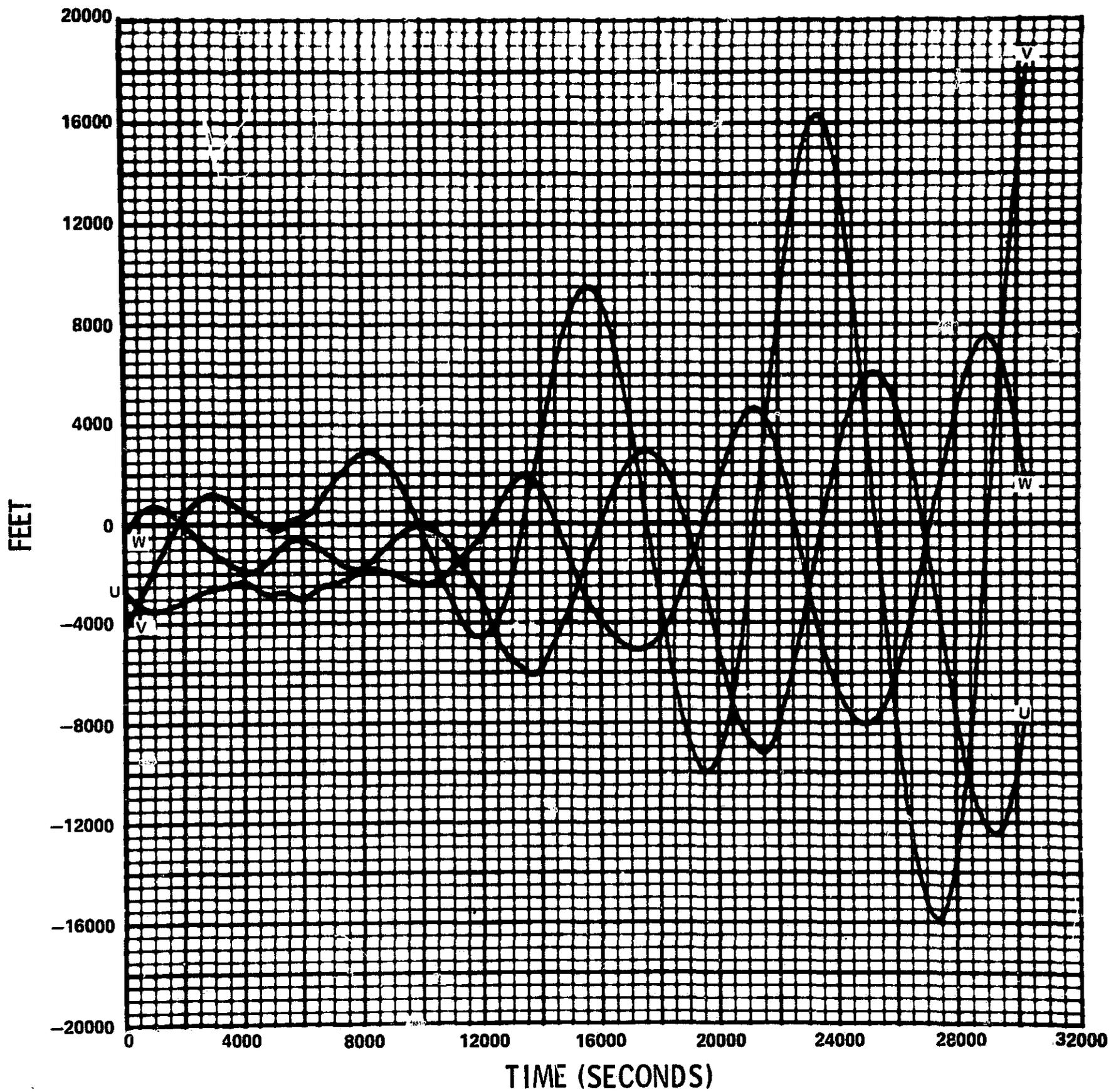
FIGURE 2i
ARC 305 DATA, FITS TO 1 ORBIT
UVW POSITION COMPONENT RESIDUALS
SEMIMAJOR AXIS IMPLIED
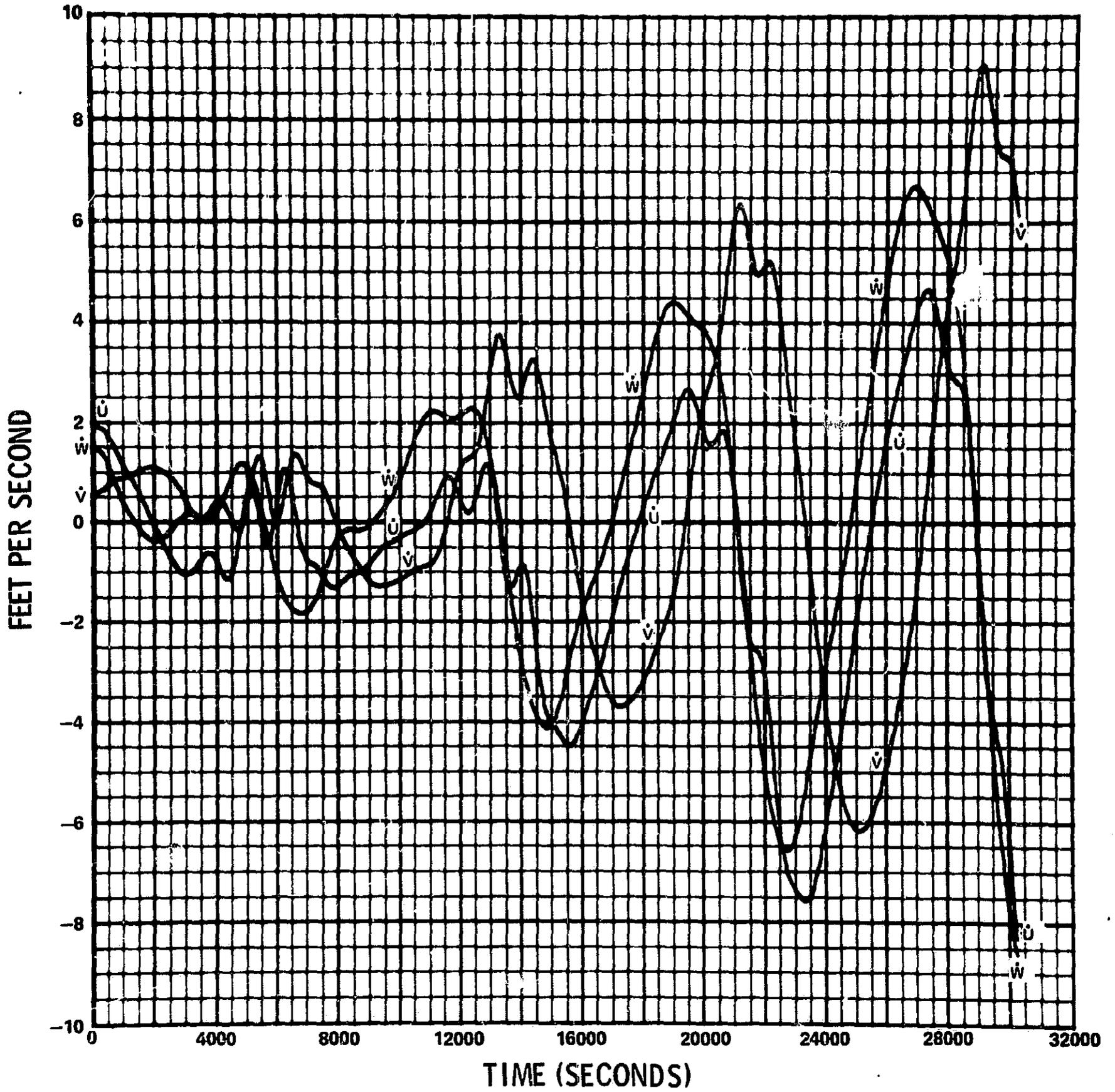
FIGURE 2j
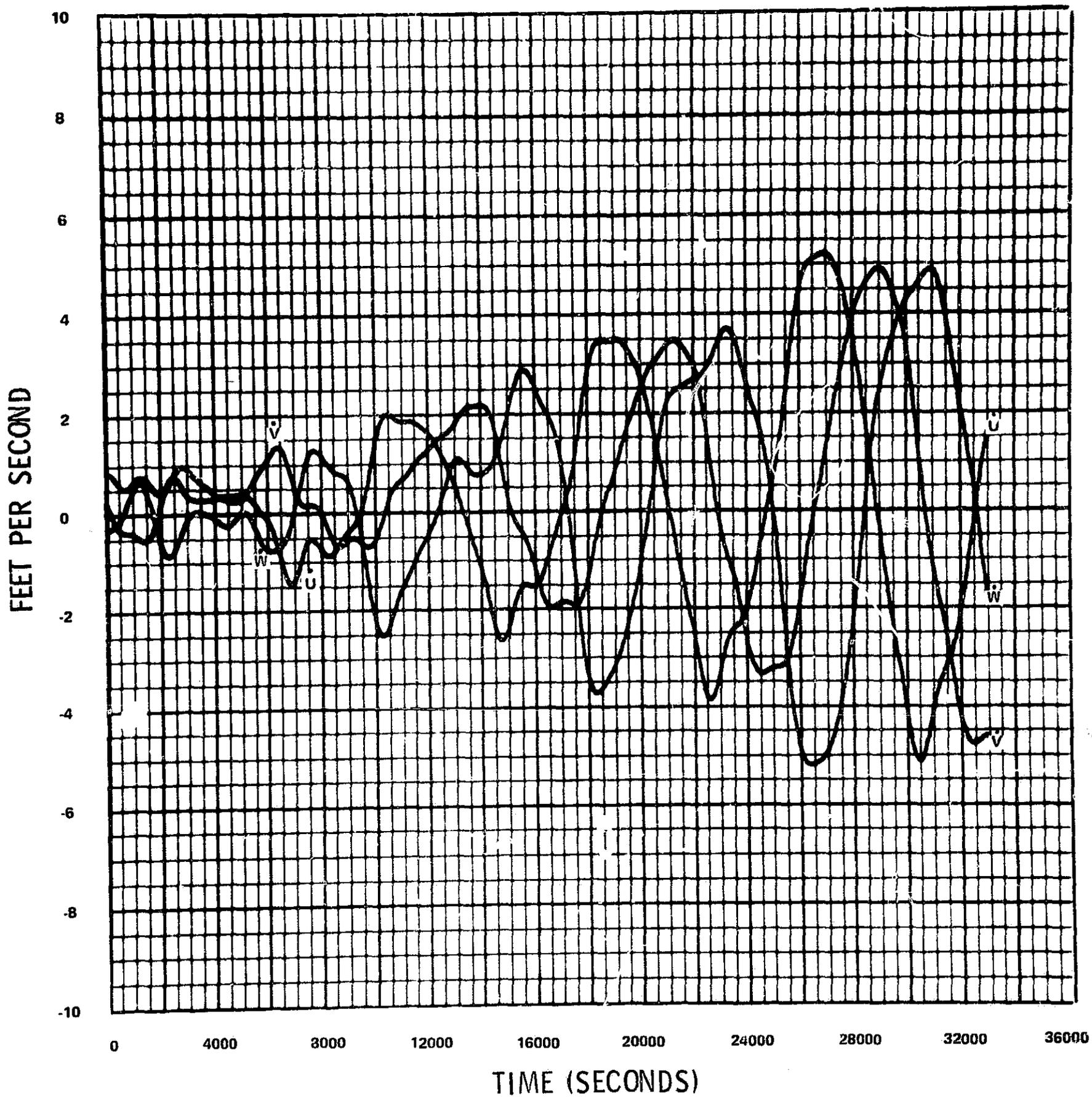ARC 305 DATA, FITS TO 1 ORBIT
UVW VELOCITY COMPONENT RESIDUALS
SEMIMAJOR AXIS IMPLIED

TIME (SECONDS)
POSITION RESIDUALS

TIME (SECONDS)
VELOCITY RESIDUALS
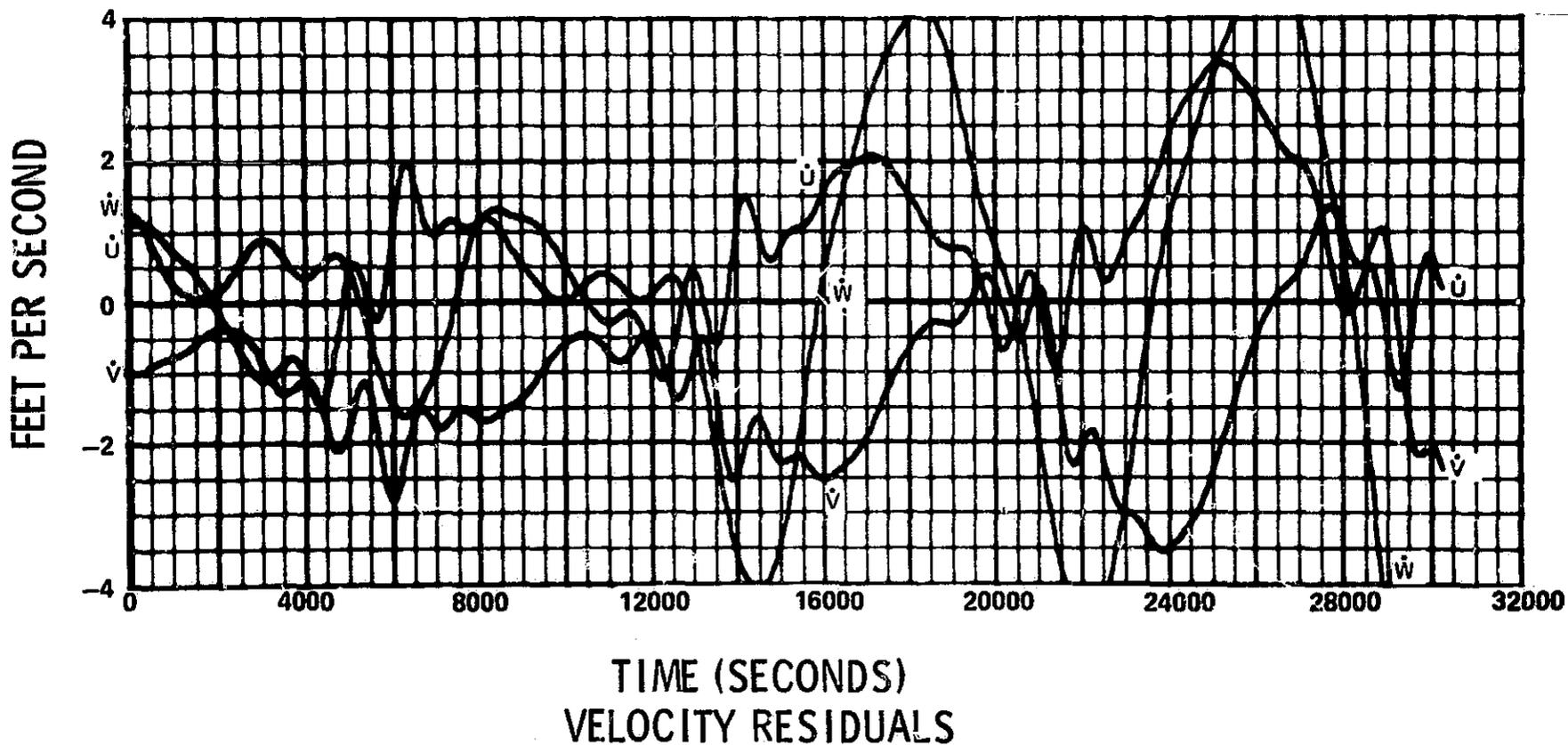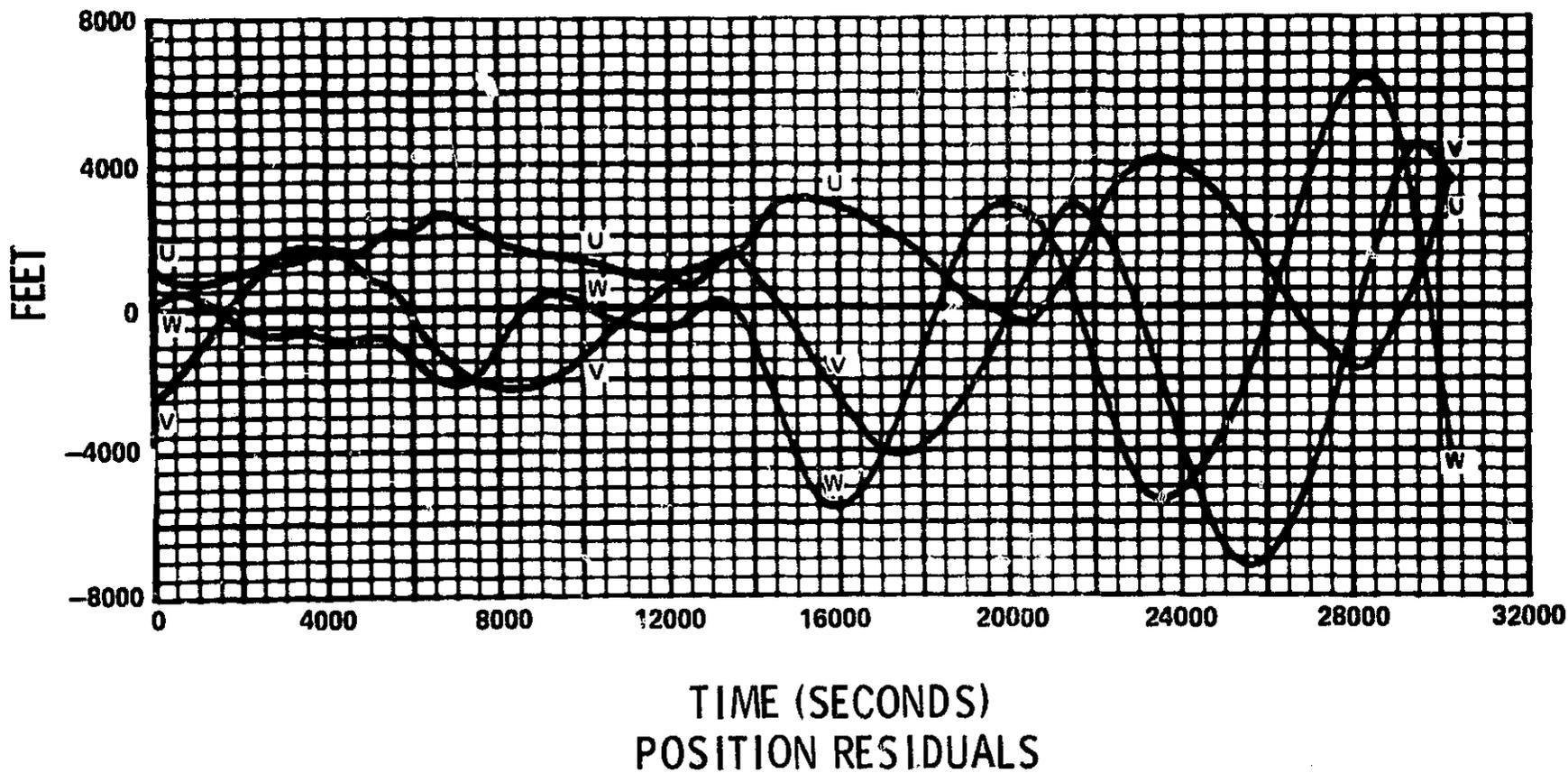
FIGURE 2k
ARC 305 DATA, FITS TO 2 ORBITS
UVW COMPONENT RESIDUALS
ALL ELEMENTS FIT
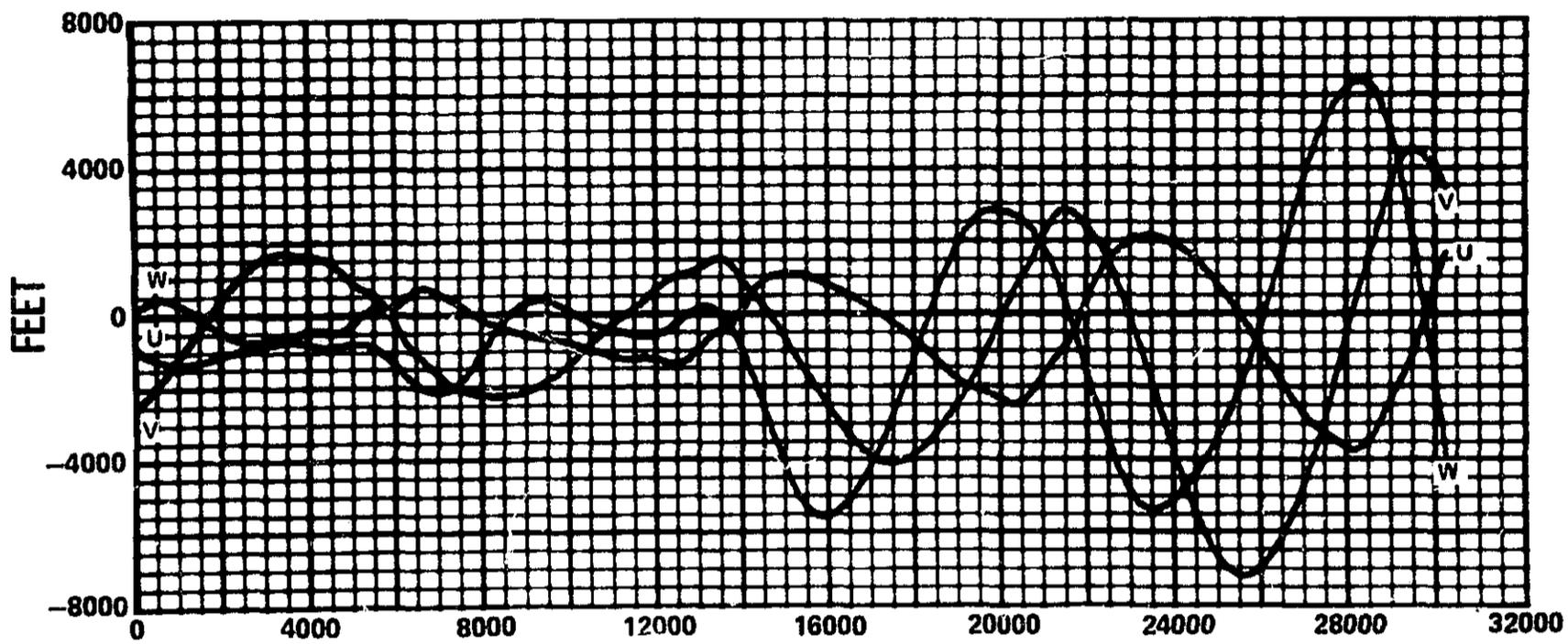
TIME (SECONDS)
POSITION RESIDUALS
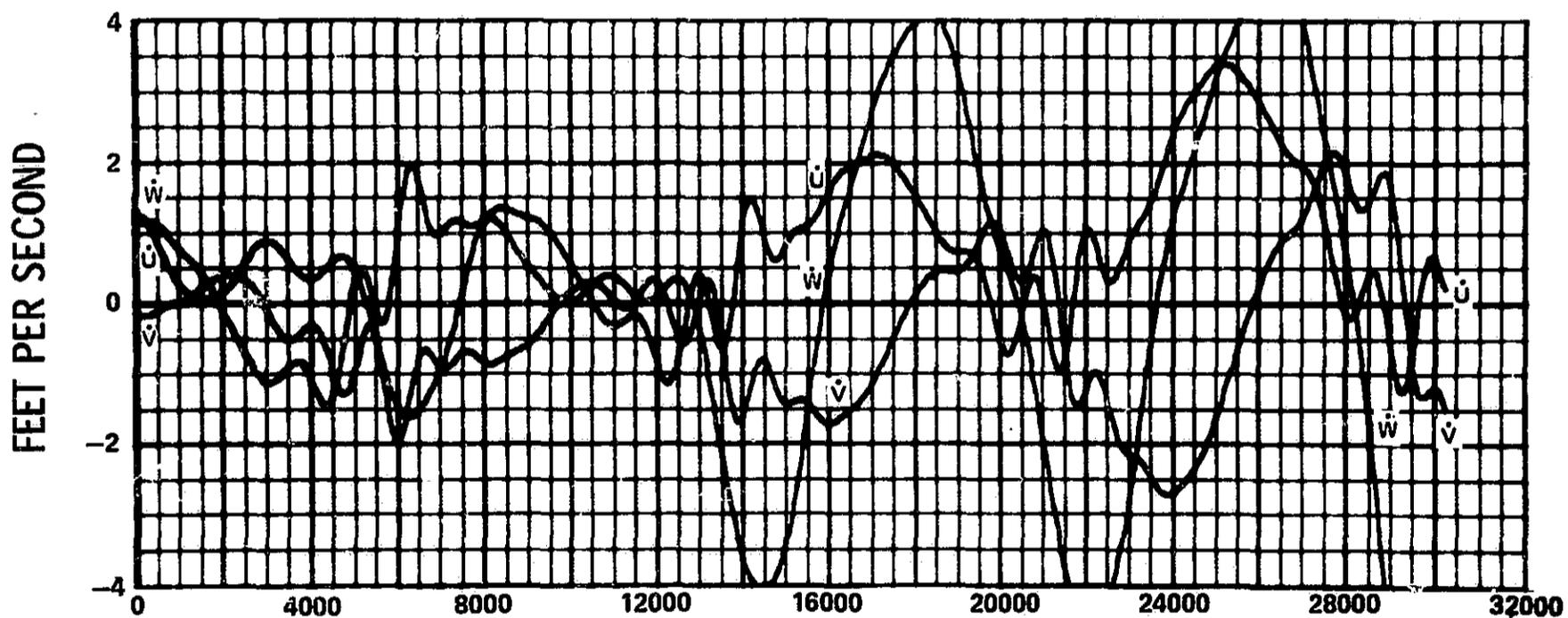
TIME (SECONDS)
VELOCITY RESIDUALS

FIGURE 2l
ARC 305 DATA, FITS TO 2 ORBITS
UVW COMPONENT RESIDUALS
SEMIMAJOR AXIS IMPLIED
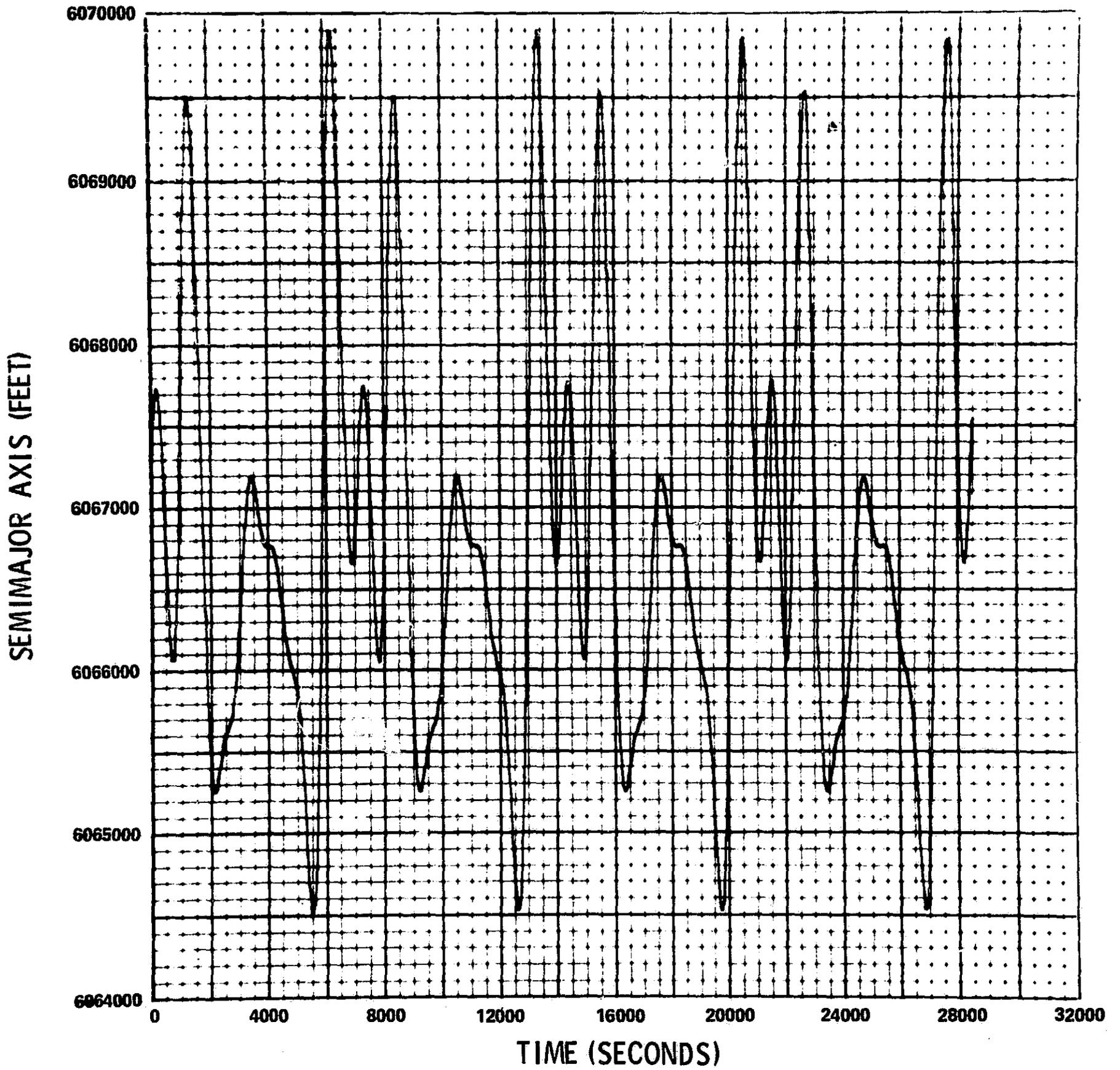
FIGURE 3a
LOW ECCENTRICITY DATA
SEMIMAJOR AXIS TIME HISTORY
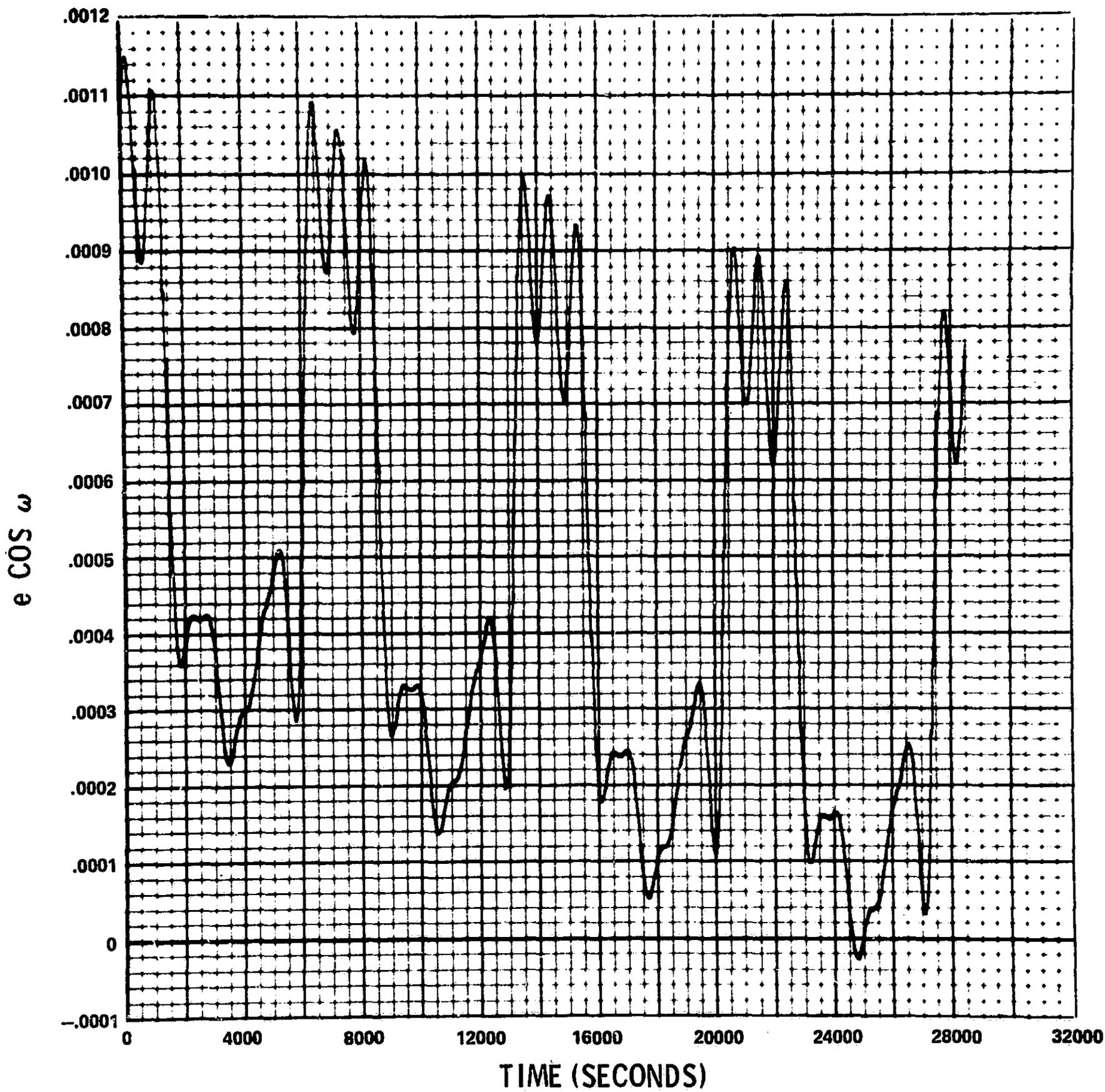
FIGURE 3b
LOW ECCENTRICITY DATA
e COS ω TIME HISTORY
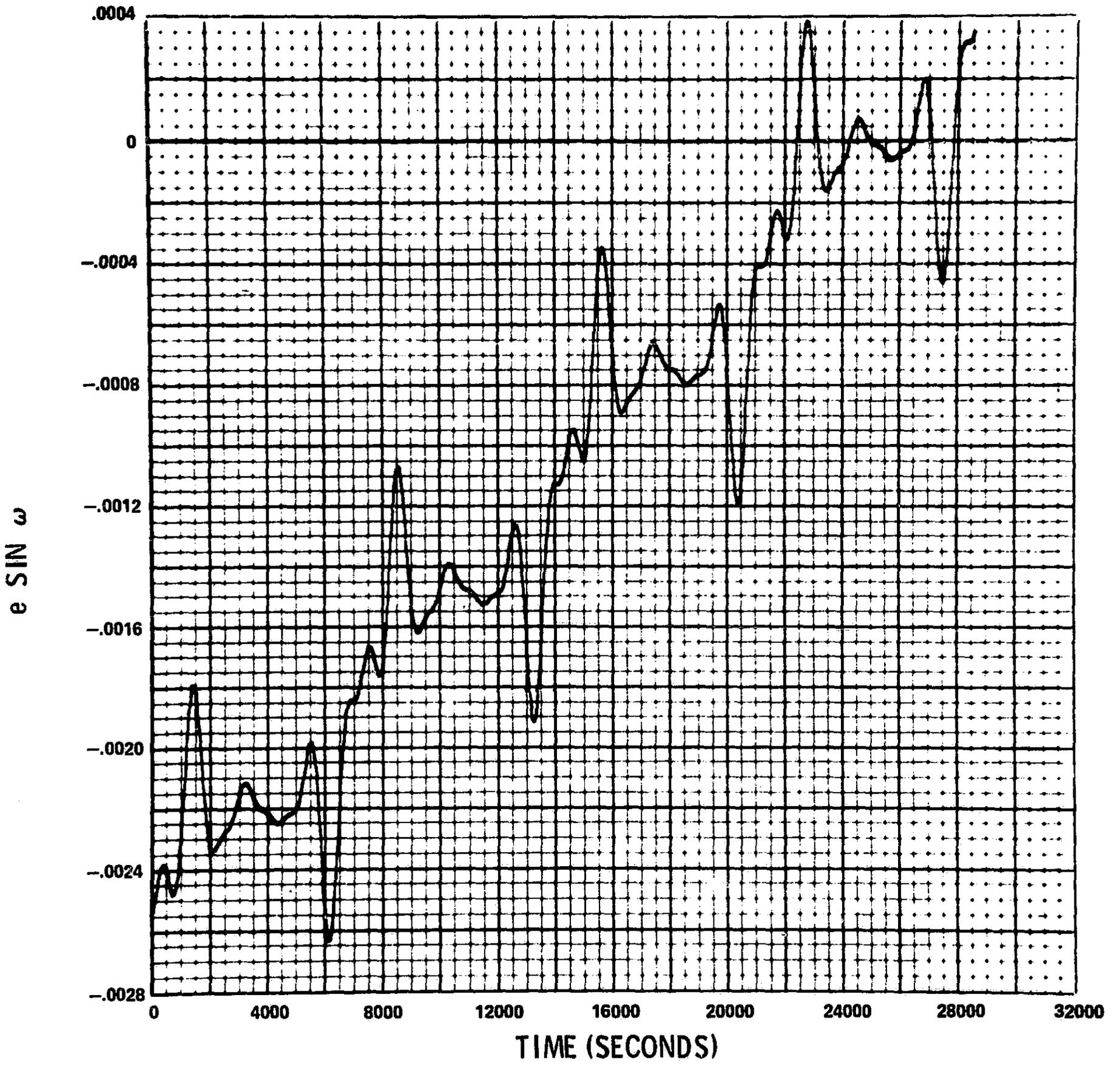
FIGURE 3c
LOW ECCENTRICITY DATA
e SIN ω TIME HISTORY
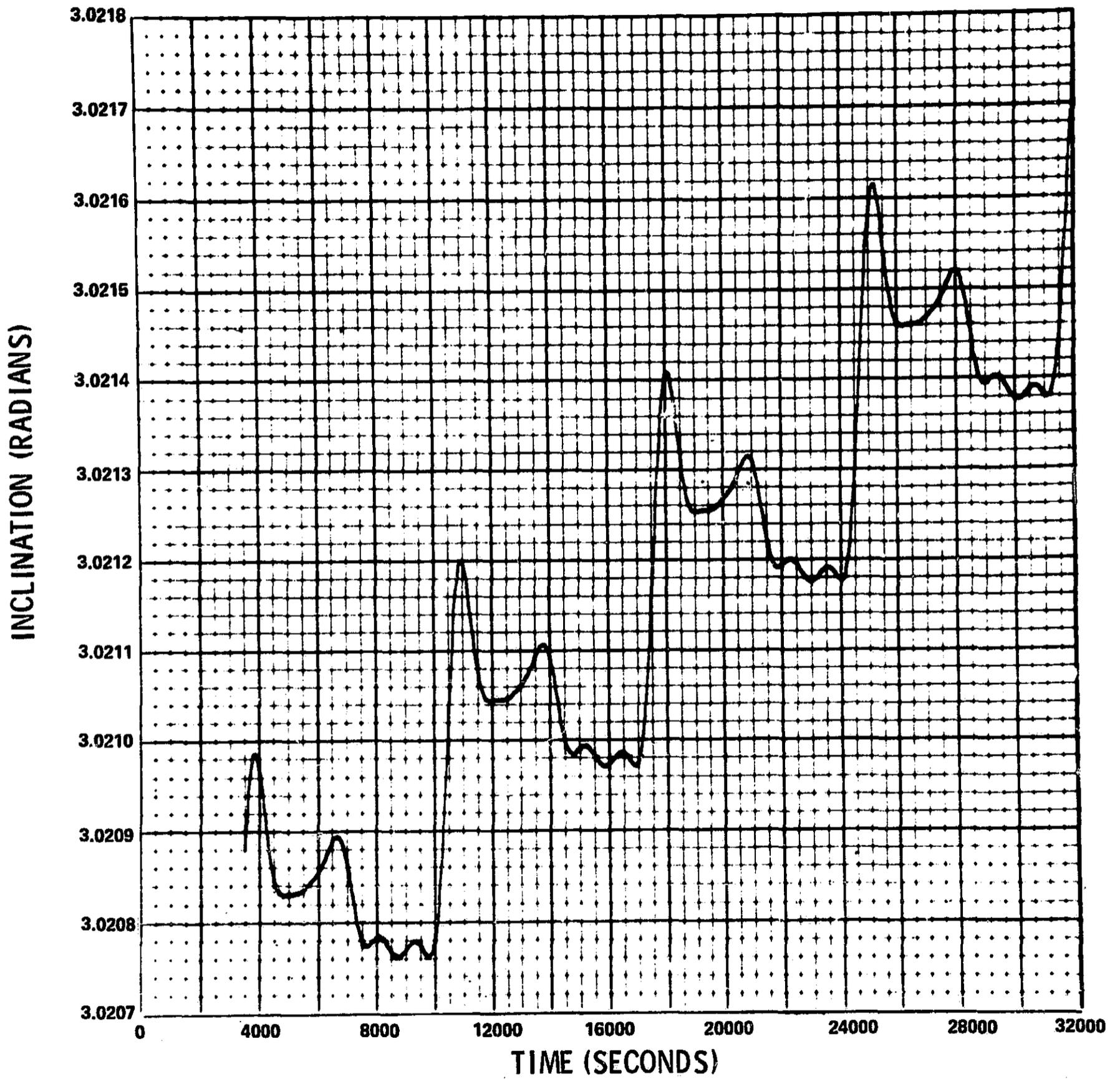
FIGURE 3d
LOW ECCENTRICITY DATA
INCLINATION TIME HISTORY
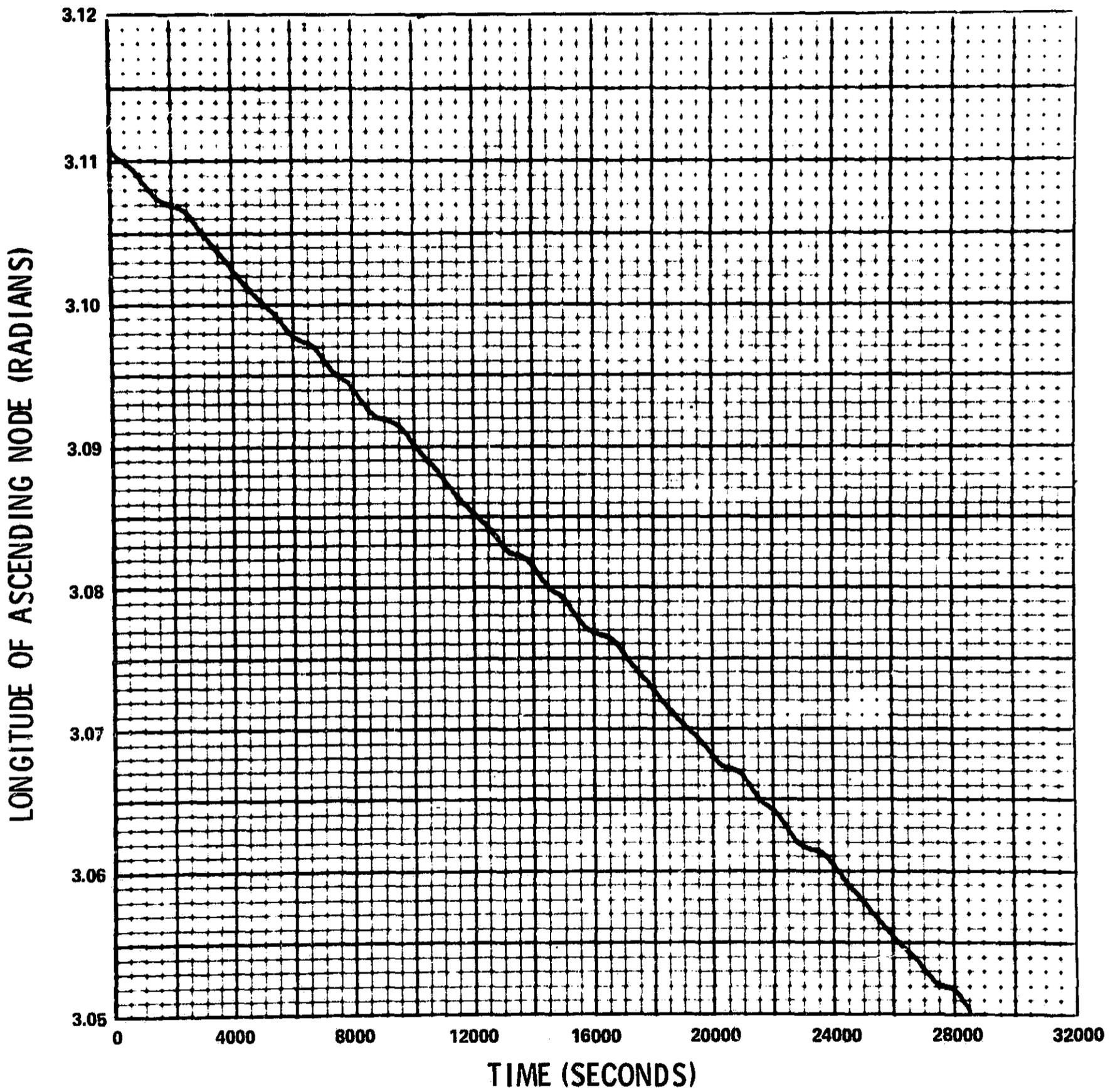
FIGURE 3e
LOW ECCENTRICITY DATA
LONGITUDE OF ASCENDING NODE TIME HISTORY
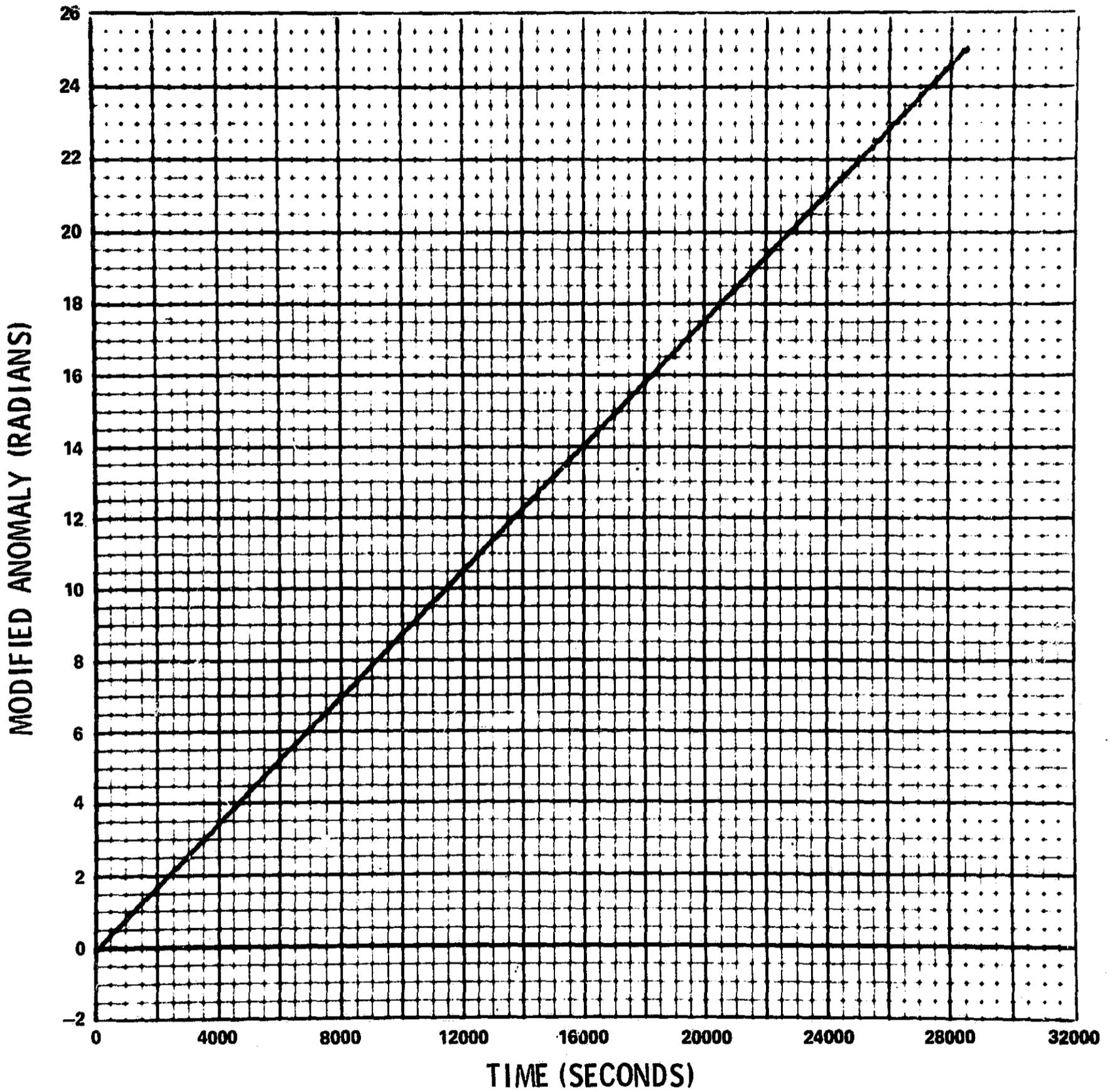
FIGURE 3f
LOW ECCENTRICITY DATA
MODIFIED ANOMALY TIME HISTORY
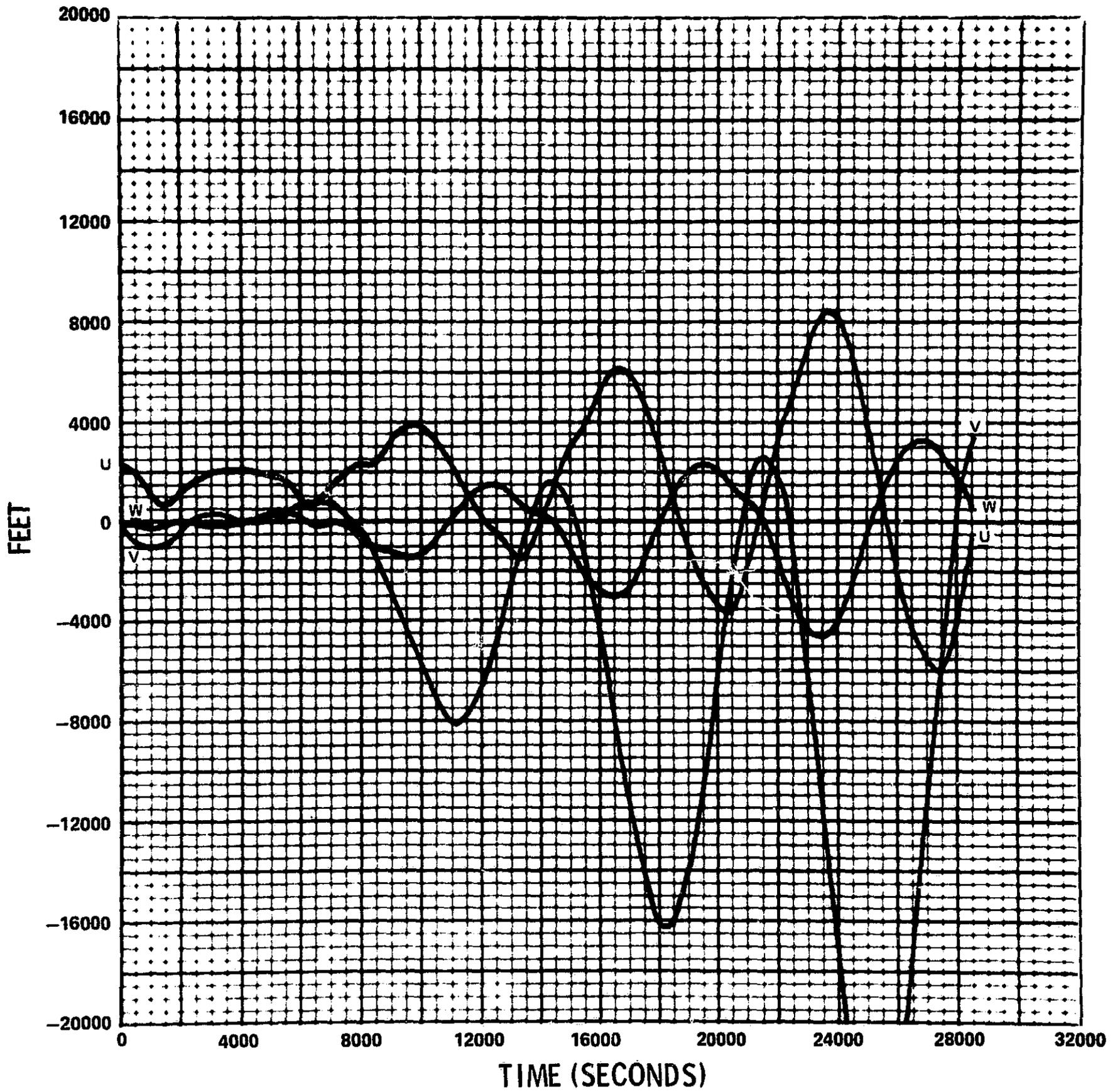
FIGURE 3g
LOW ECCENTRICITY DATA, FITS TO 1 ORBIT
UVW POSITION COMPONENT RESIDUALS
ALL ELEMENTS FIT
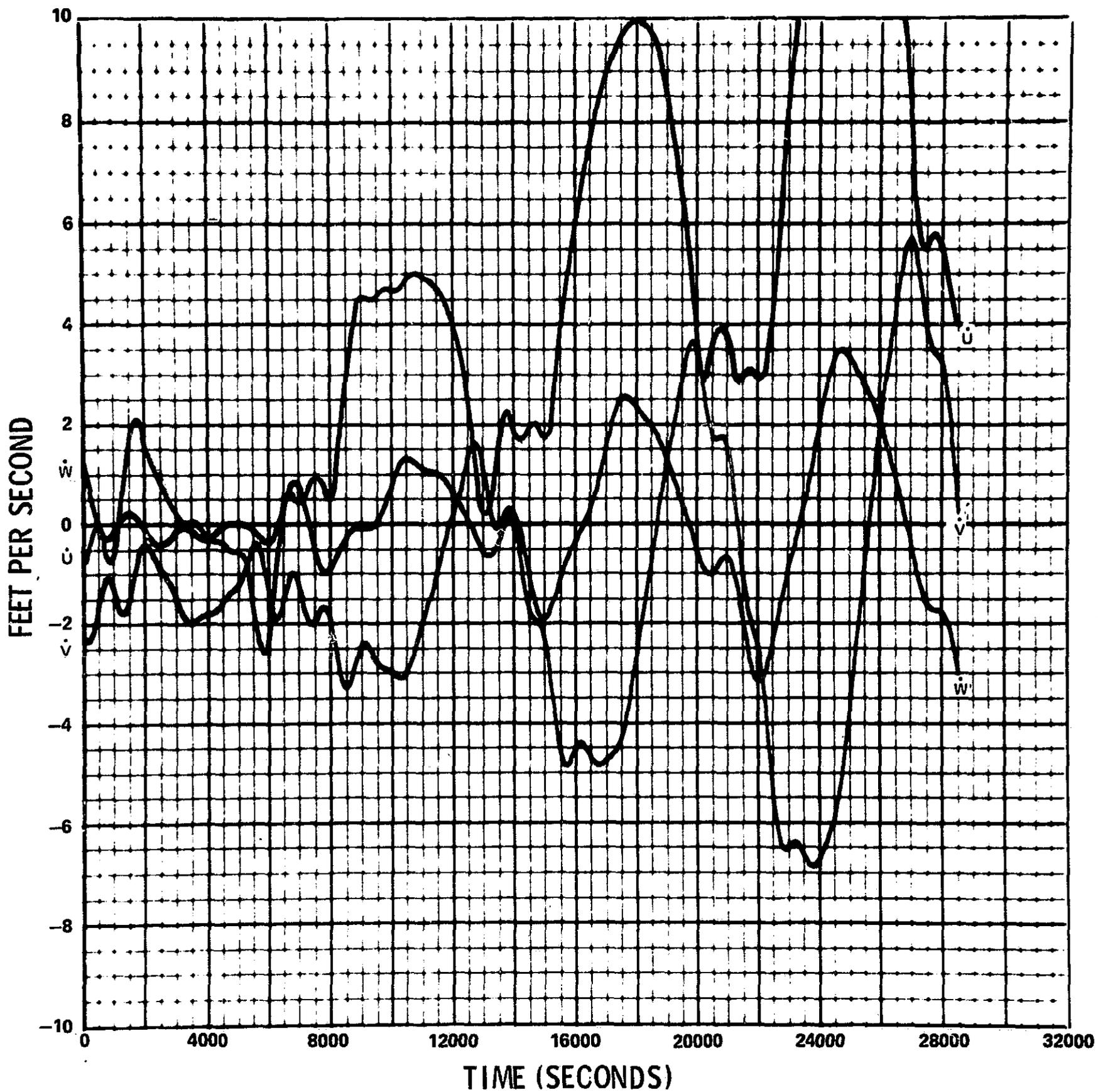
FIGURE 3h
LOW ECCENTRICITY DATA, FITS TO 1 ORBIT
UVW VELOCITY COMPONENT RESIDUALS
ALL ELEMENTS FIT
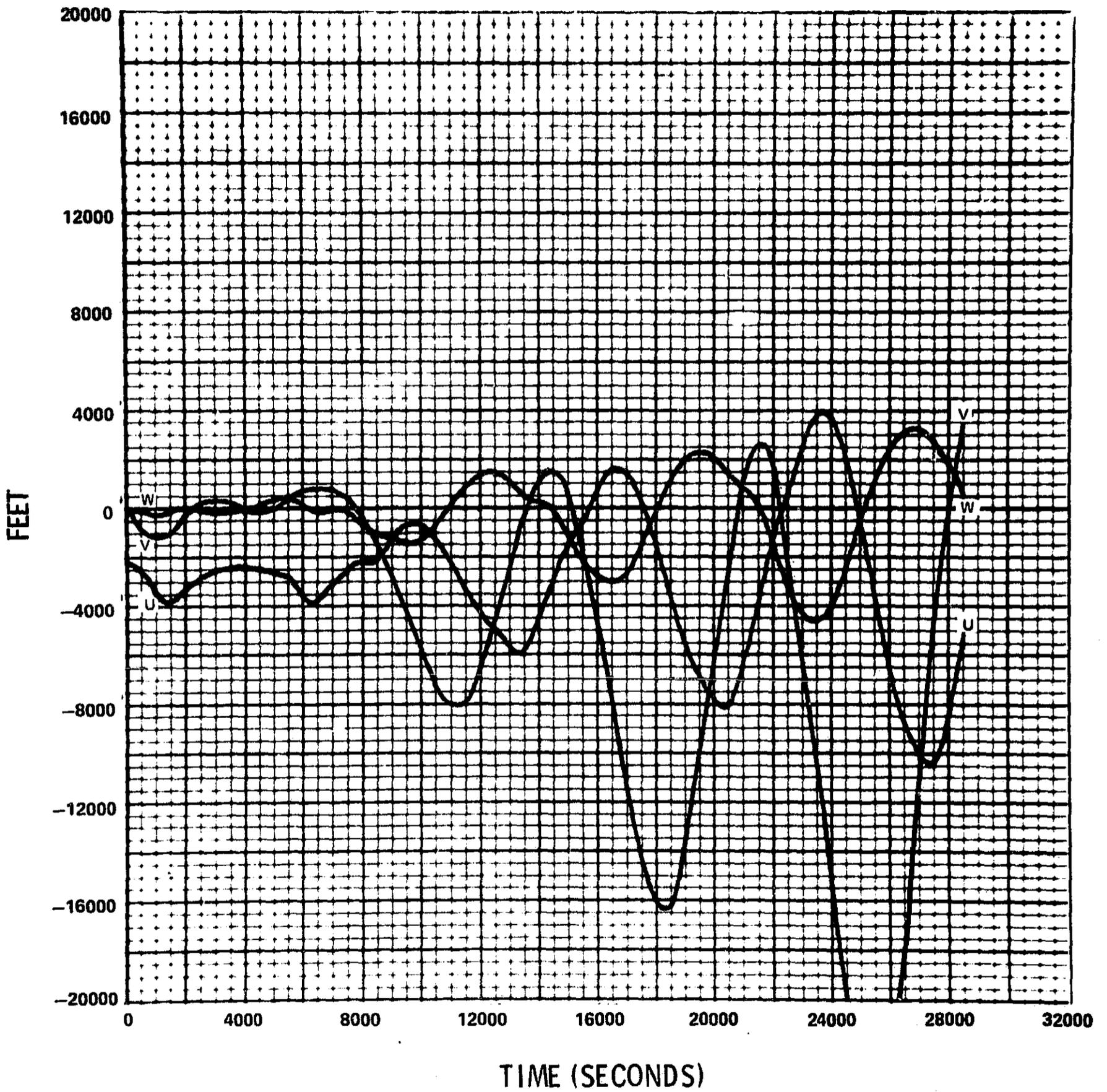
FIGURE 3i
LOW ECCENTRICITY DATA, FITS TO 1 ORBIT
UVW POSITION COMPONENT RESIDUALS
SEMIMAJOR AXIS IMPLIED
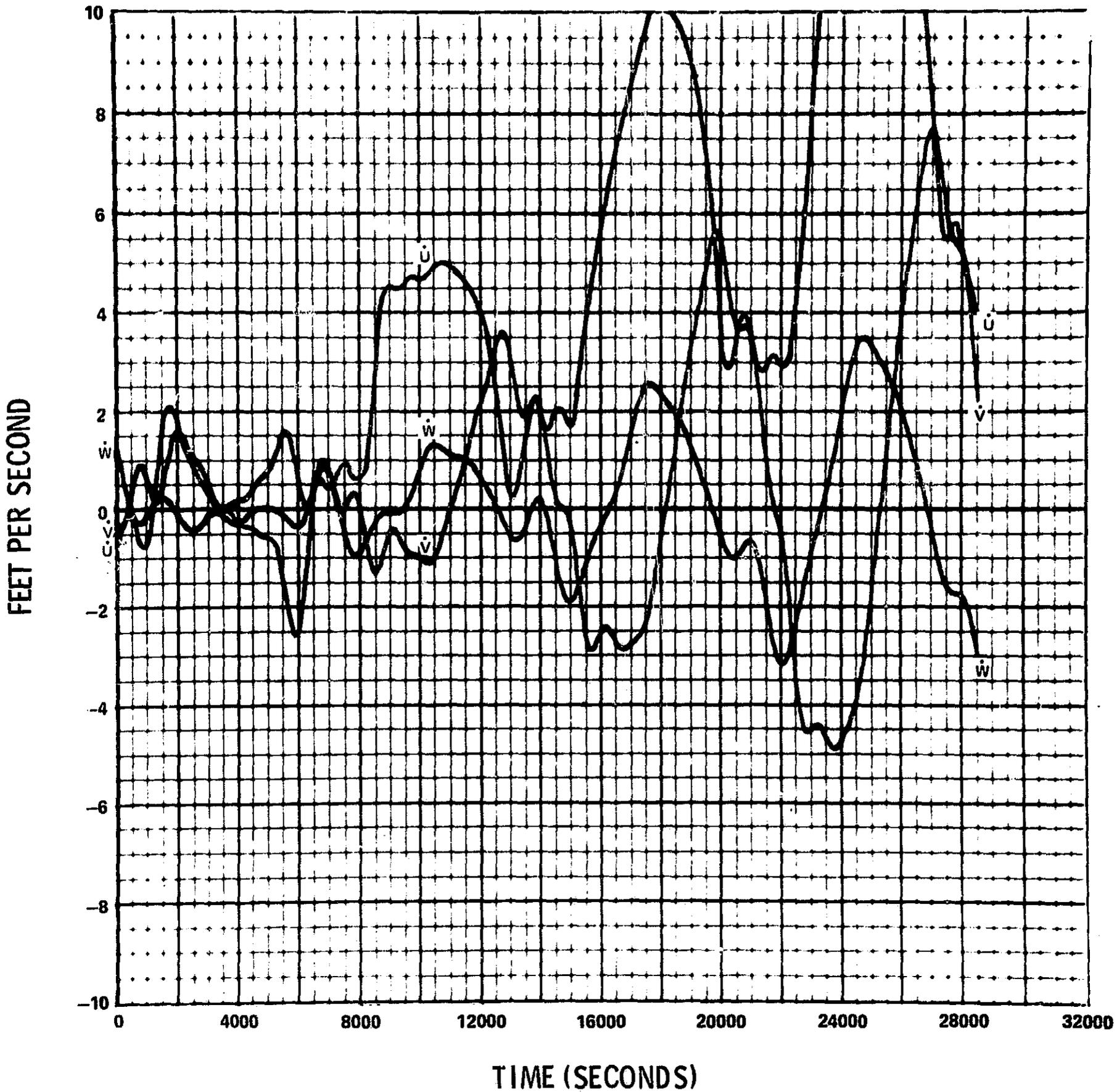
FIGURE 3j
LOW ECCENTRICITY DATA, FITS TO 1 ORBIT
UVW VELOCITY COMPONENT RESIDUALS
SEMIMAJOR AXIS IMPLIED
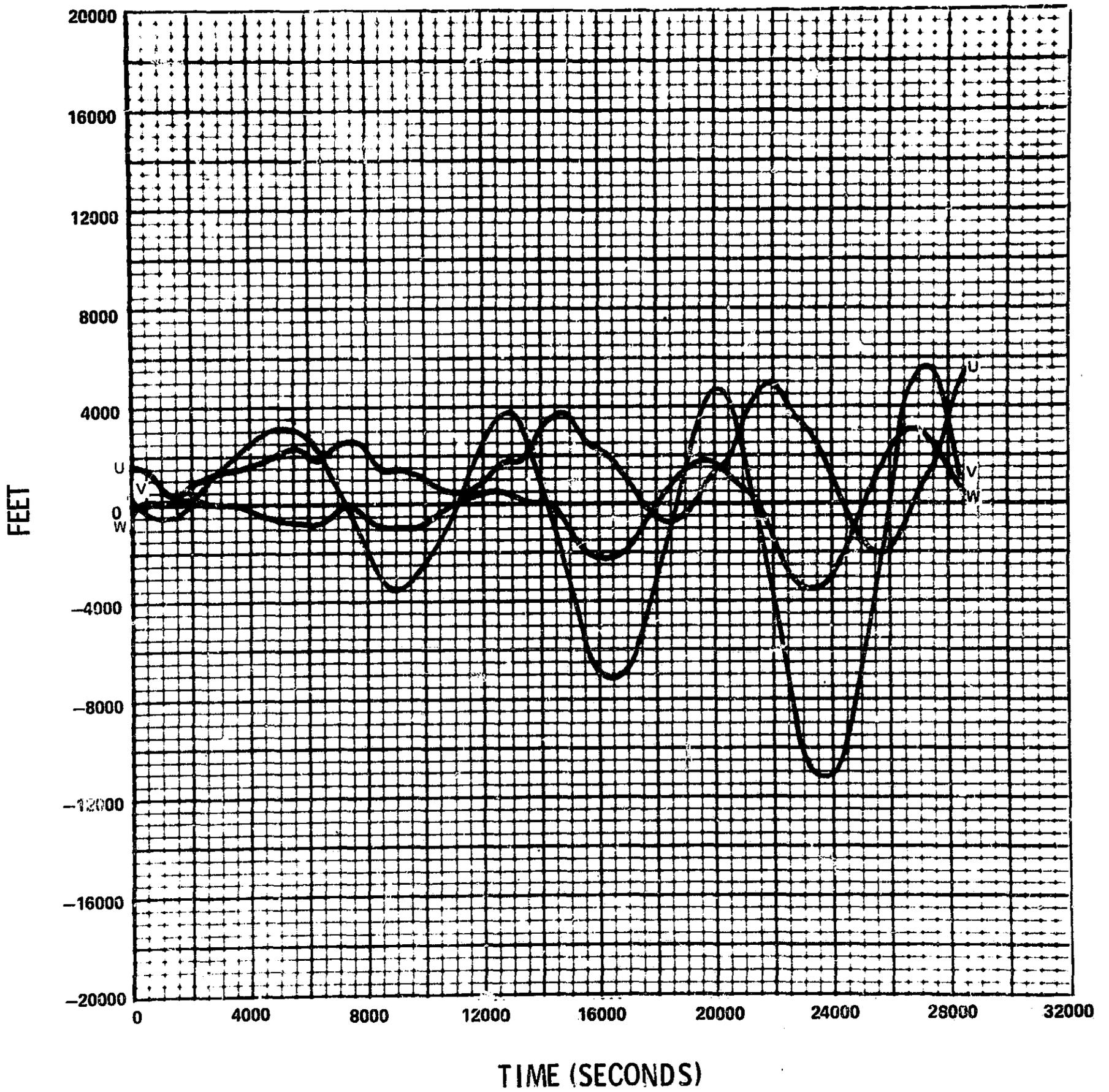
FIGURE 3k
LOW ECCENTRICITY DATA, FITS TO 2 ORBITS
UVW POSITION COMPONENT RESIDUALS
ALL ELEMENTS FIT
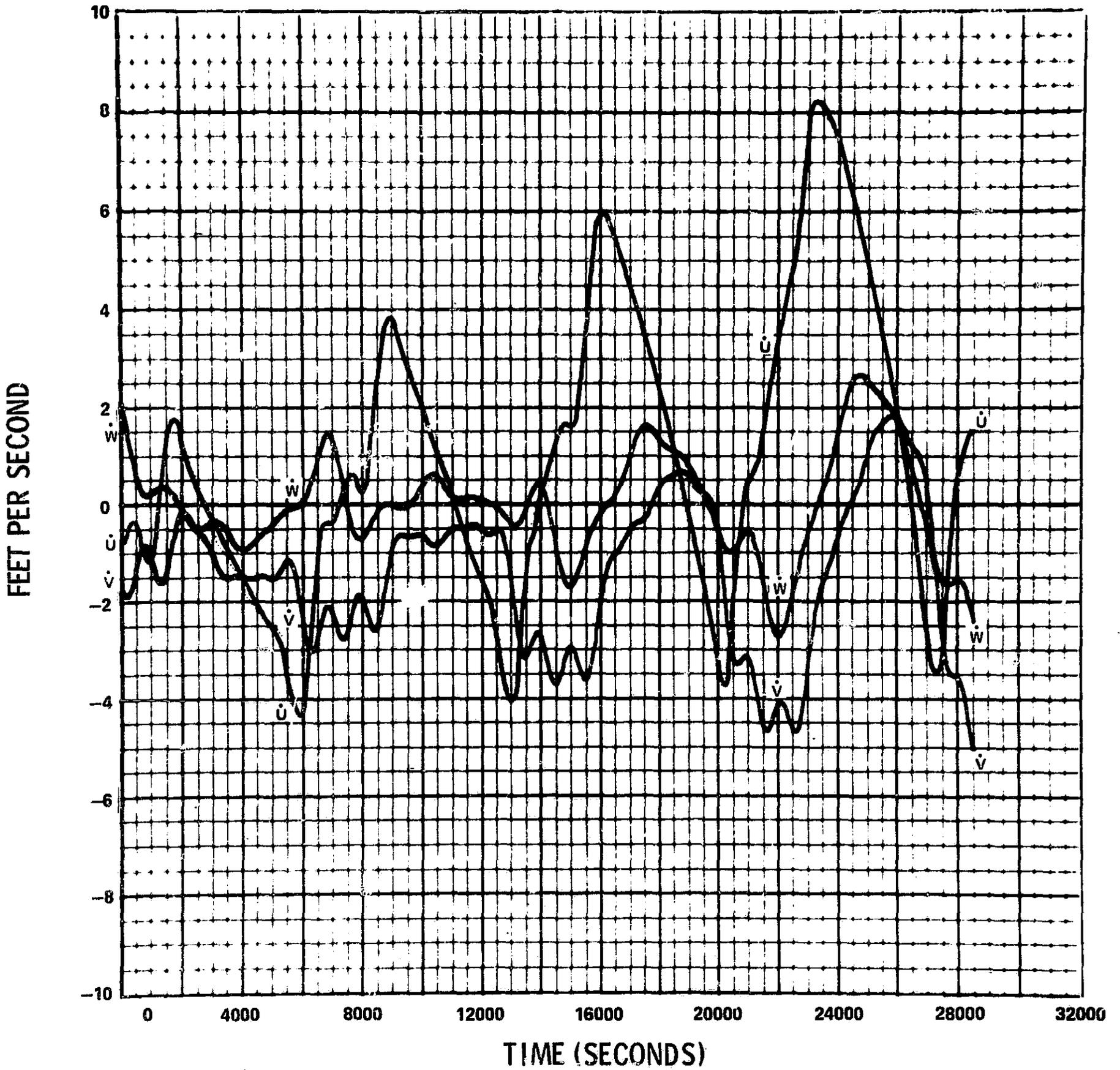
FIGURE 3ℓ
LOW ECCENTRICITY DATA, FITS TO 2 ORBITS
UVW VELOCITY COMPONENT RESIDUALS
ALL ELEMENTS FIT

FIGURE 3m
LOW ECCENTRICITY DATA, FITS TO 2 ORBITS
UVW POSITION COMPONENT RESIDUALS
SEMIMAJOR AXIS IMPLIED

FIGURE 3n
LOW ECCENTRICITY DATA, FITS TO 2 ORBITS
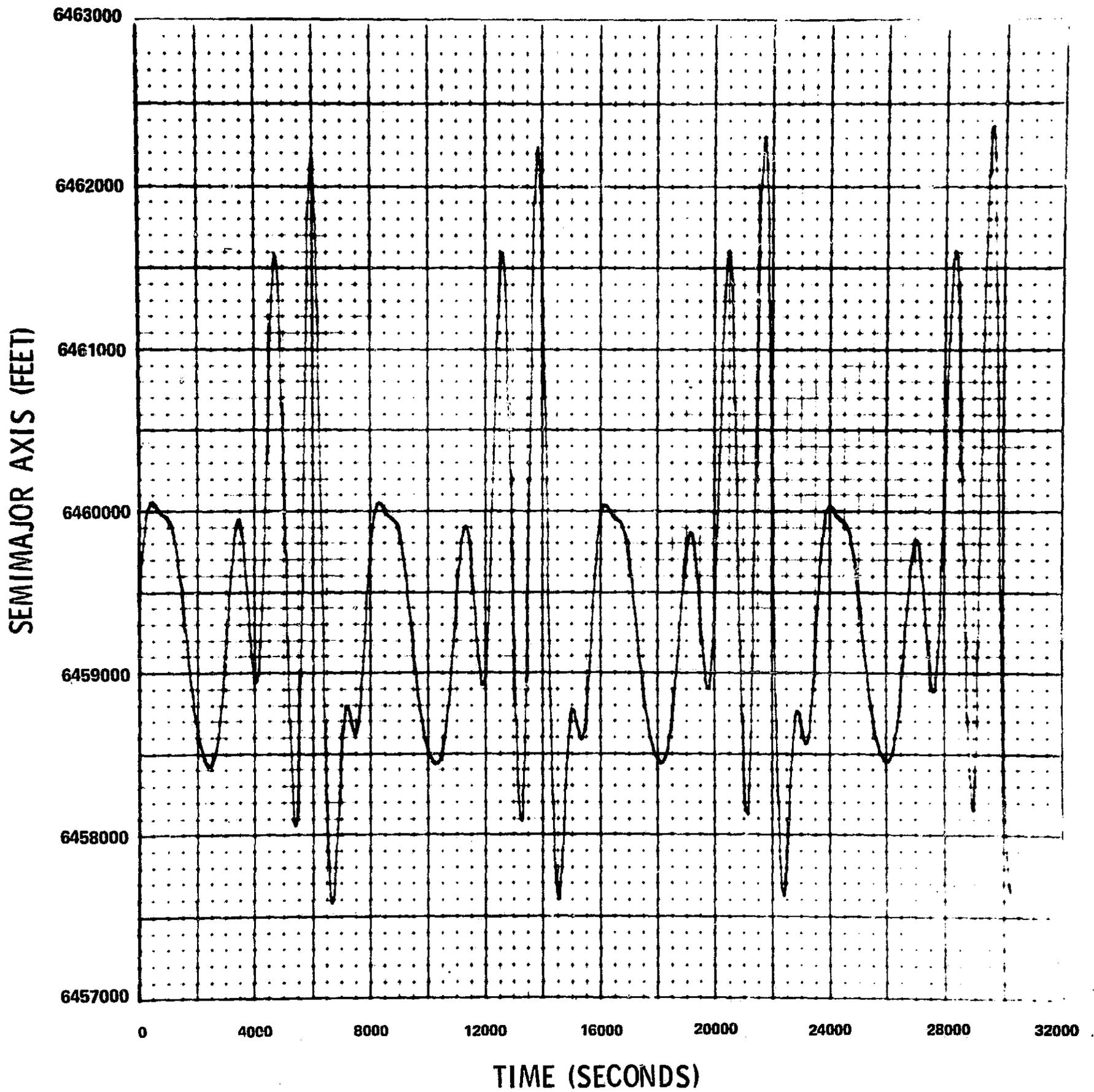UVW VELOCITY COMPONENT RESIDUALS
SEMIMAJOR AXIS IMPLIED
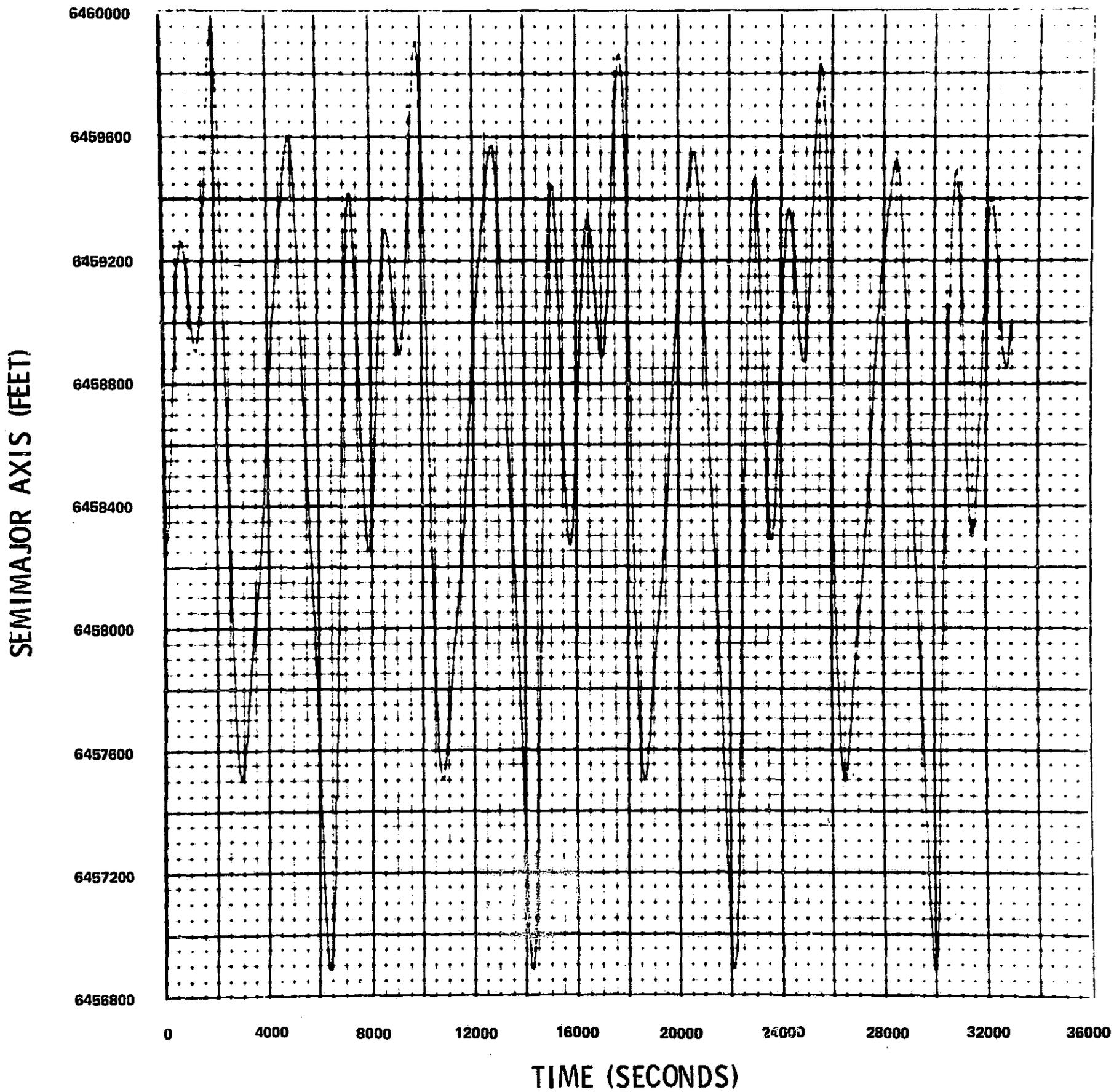
FIGURE 4a
e = .04 DATA
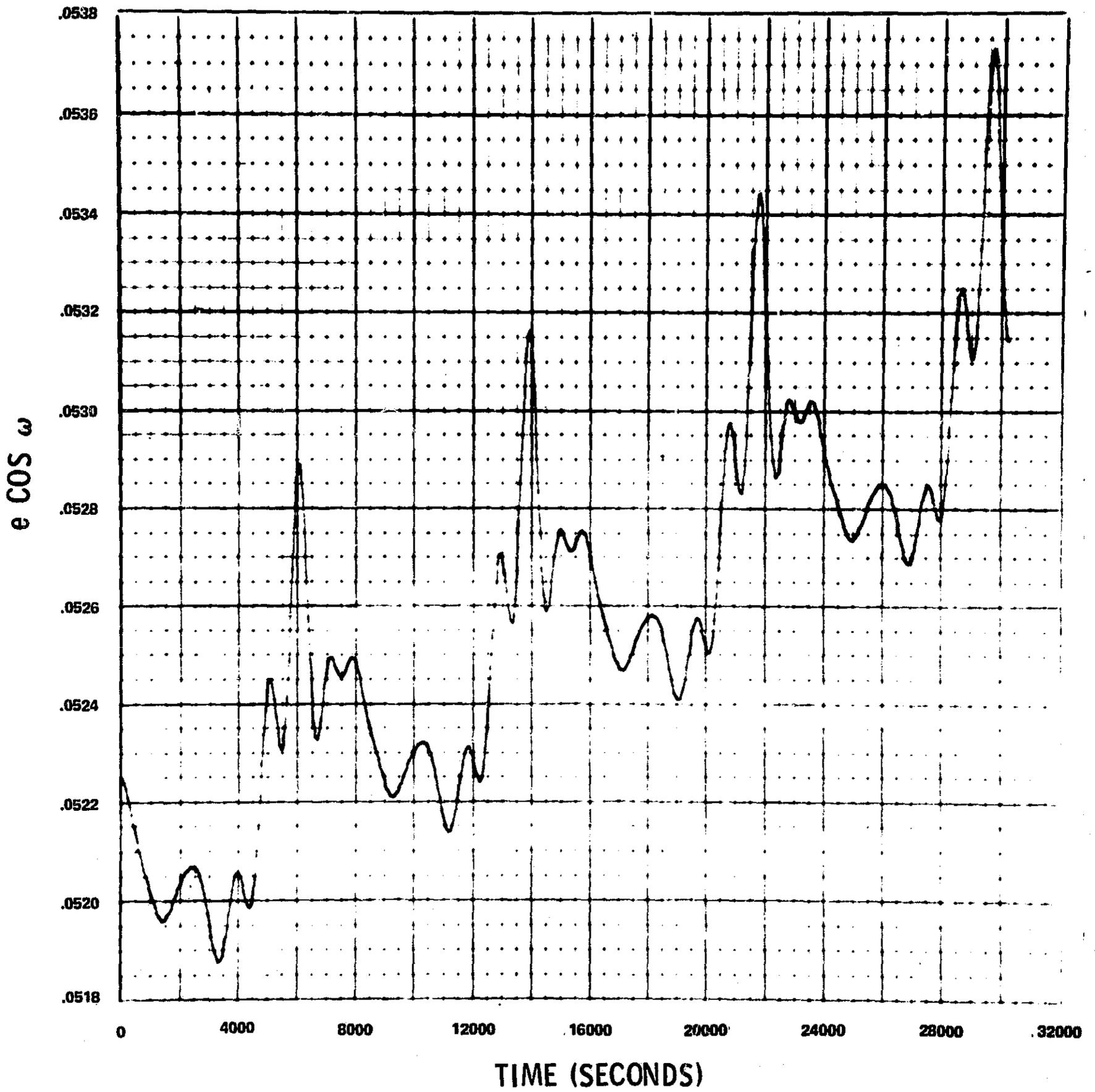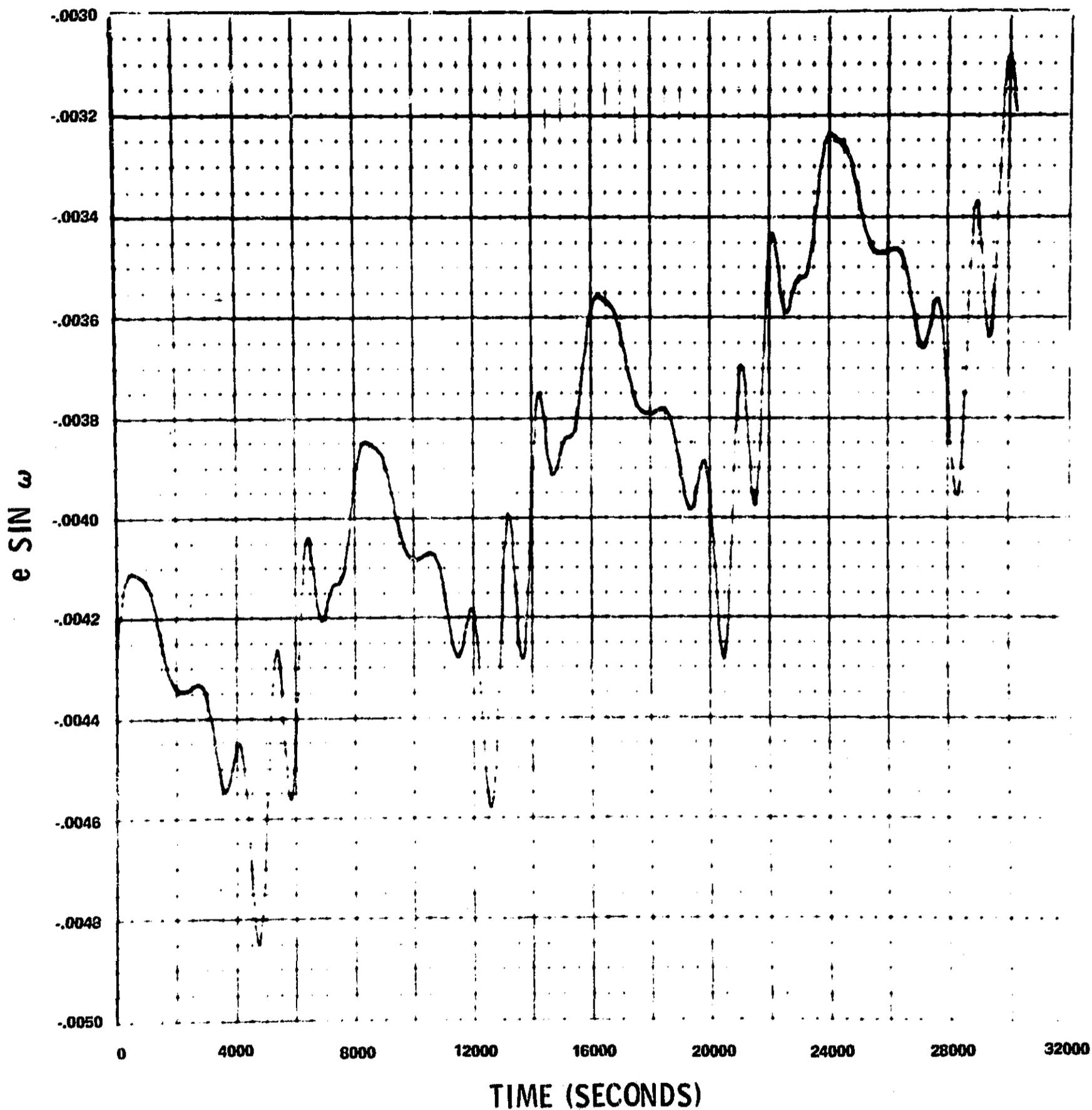SEMIMAJOR AXIS TIME HISTORY
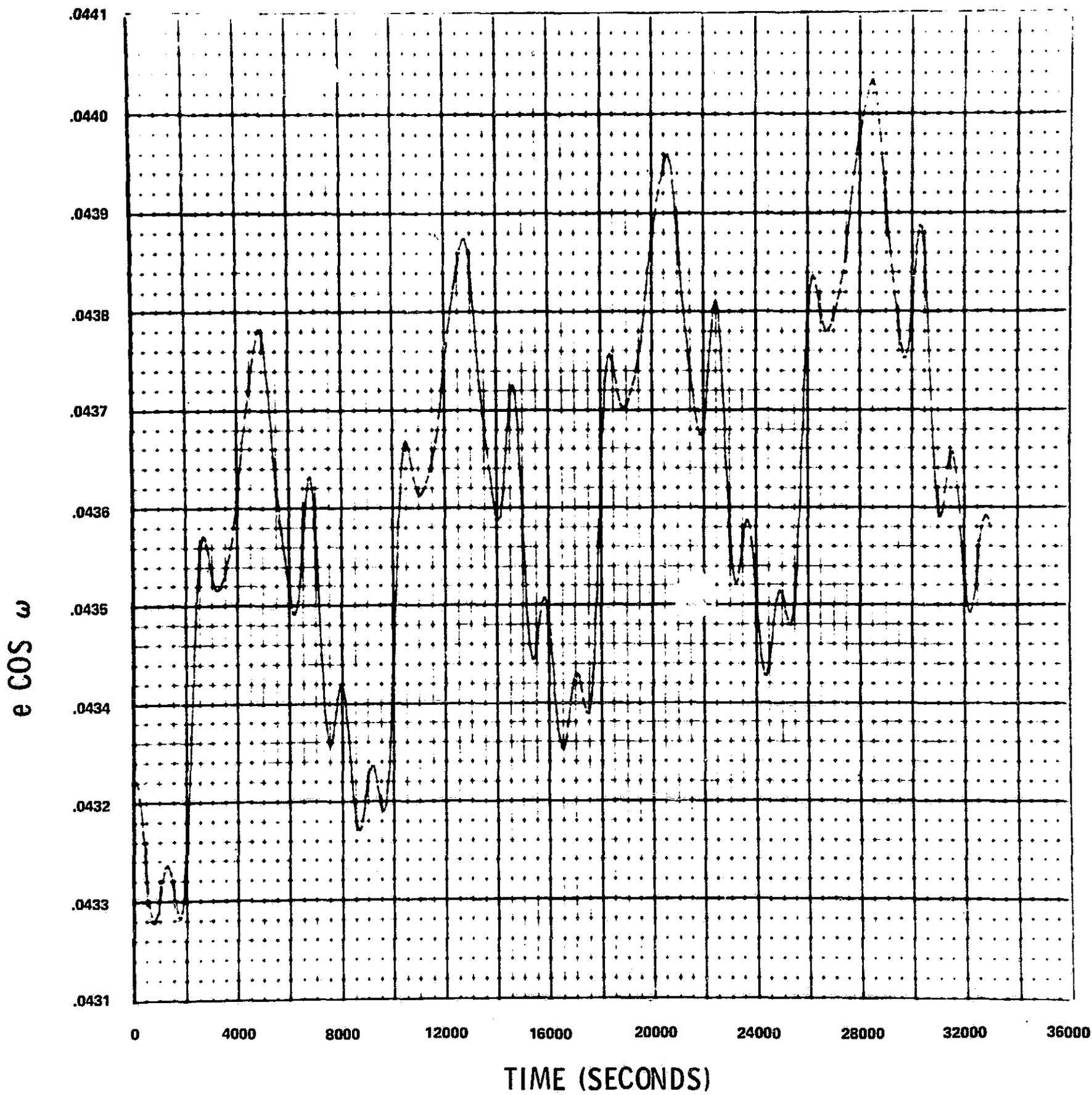
FIGURE 4b
e = .04 DATA
e COS ω TIME HISTORY
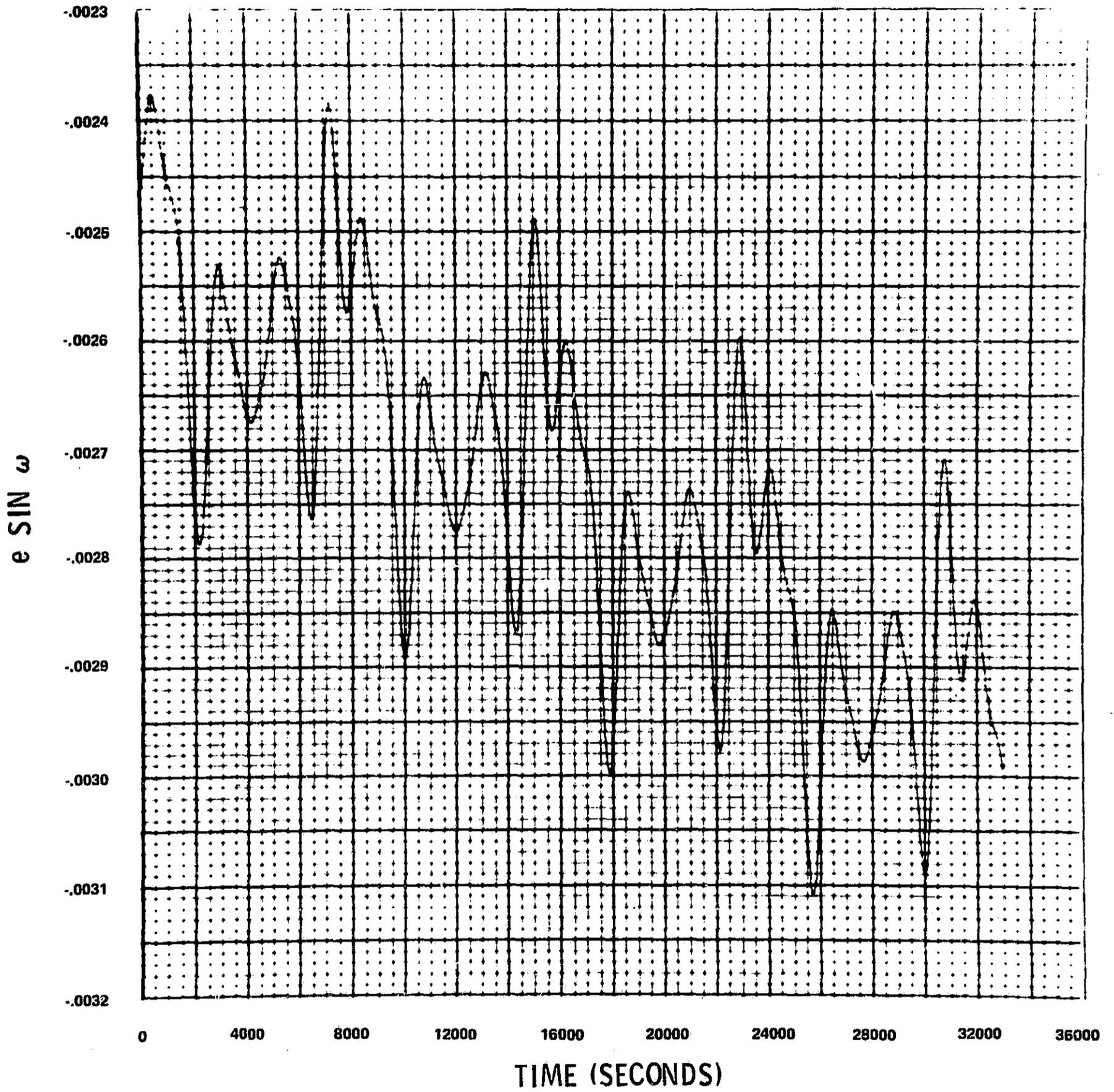
FIGURE 4c
e = .04 DATA
e SIN ω TIME HISTORY
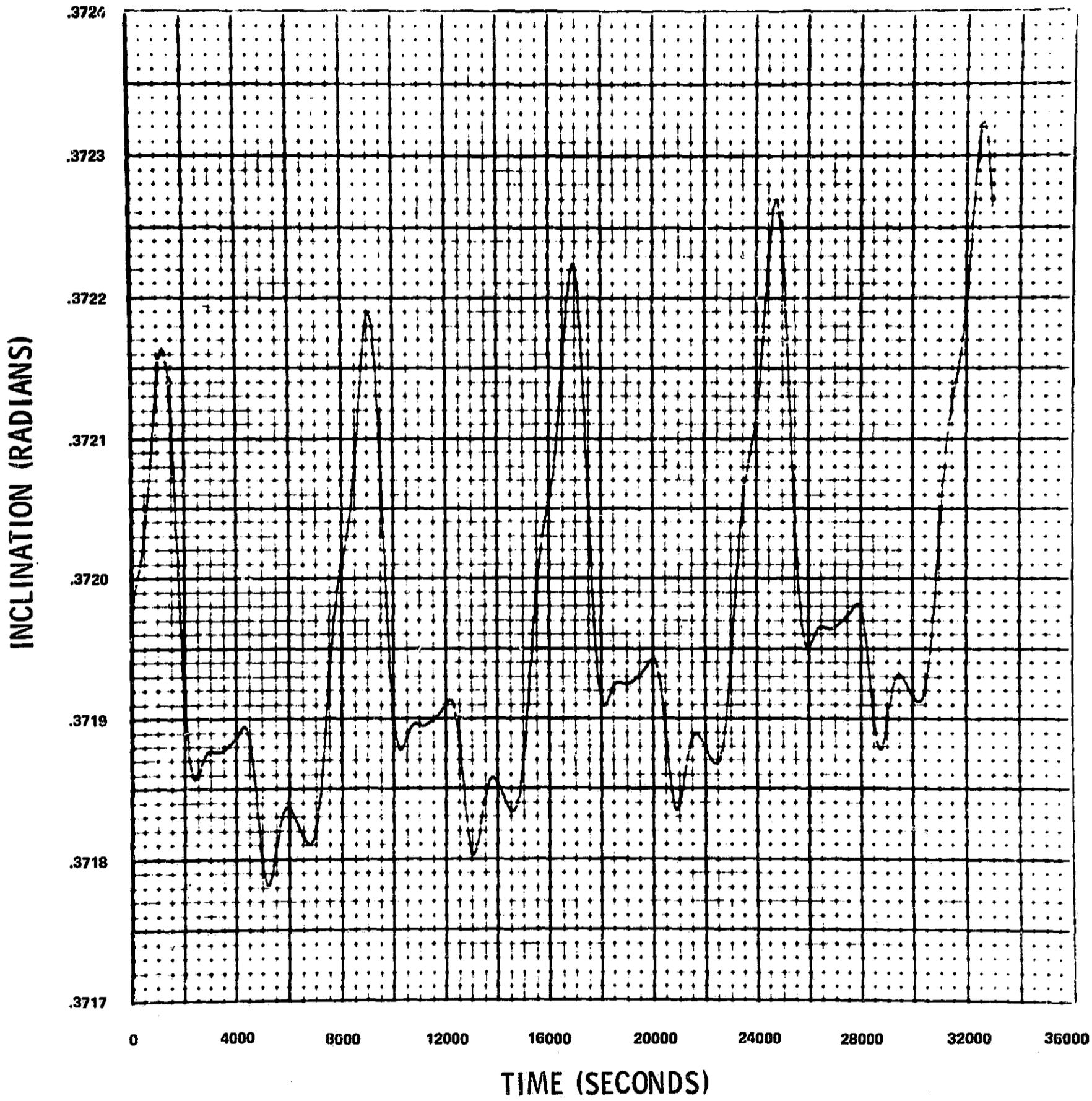
FIGURE 4d
e = .04 DATA
INCLINATION TIME HISTORY
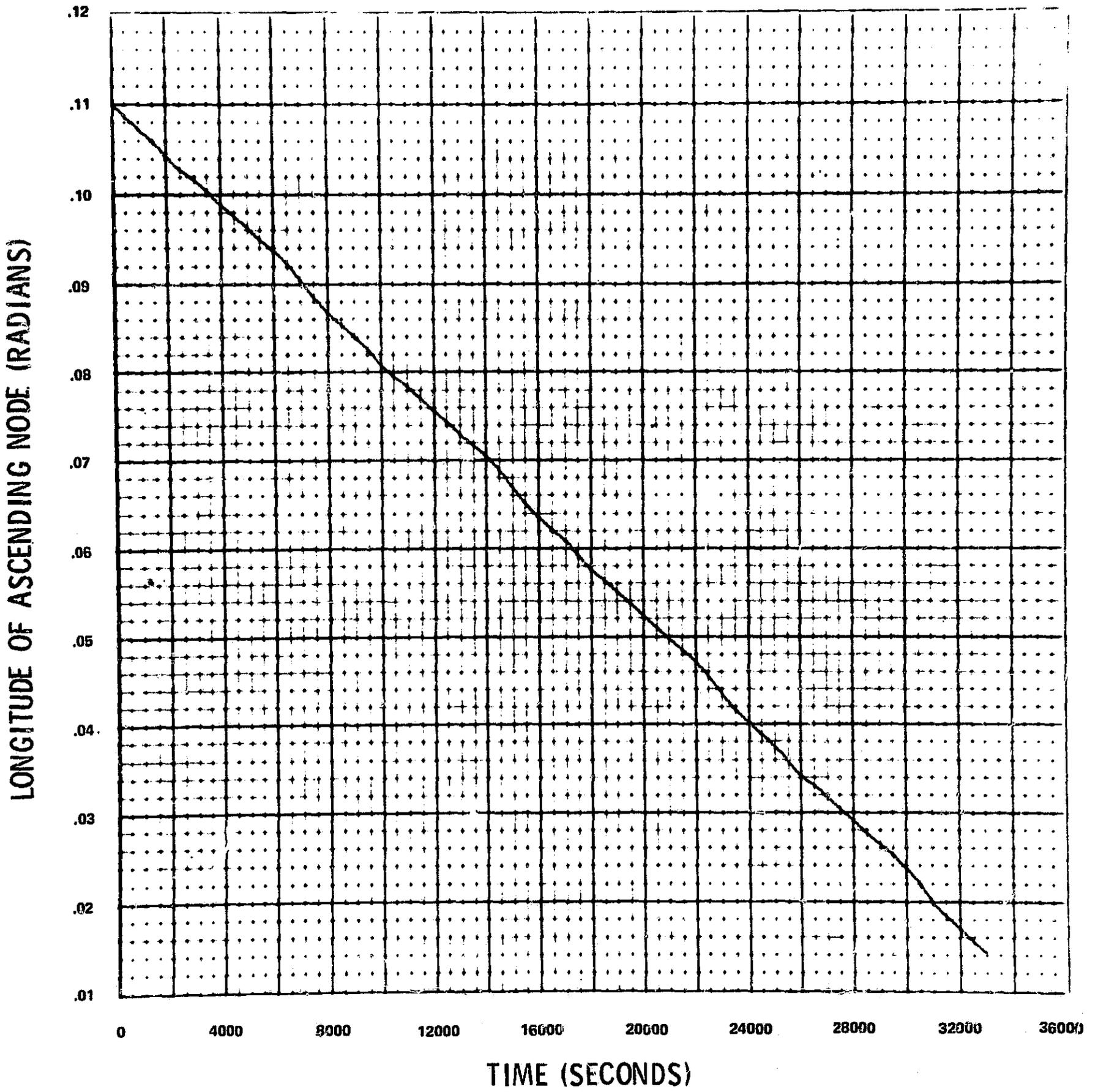
FIGURE 4e
e = .04 DATA
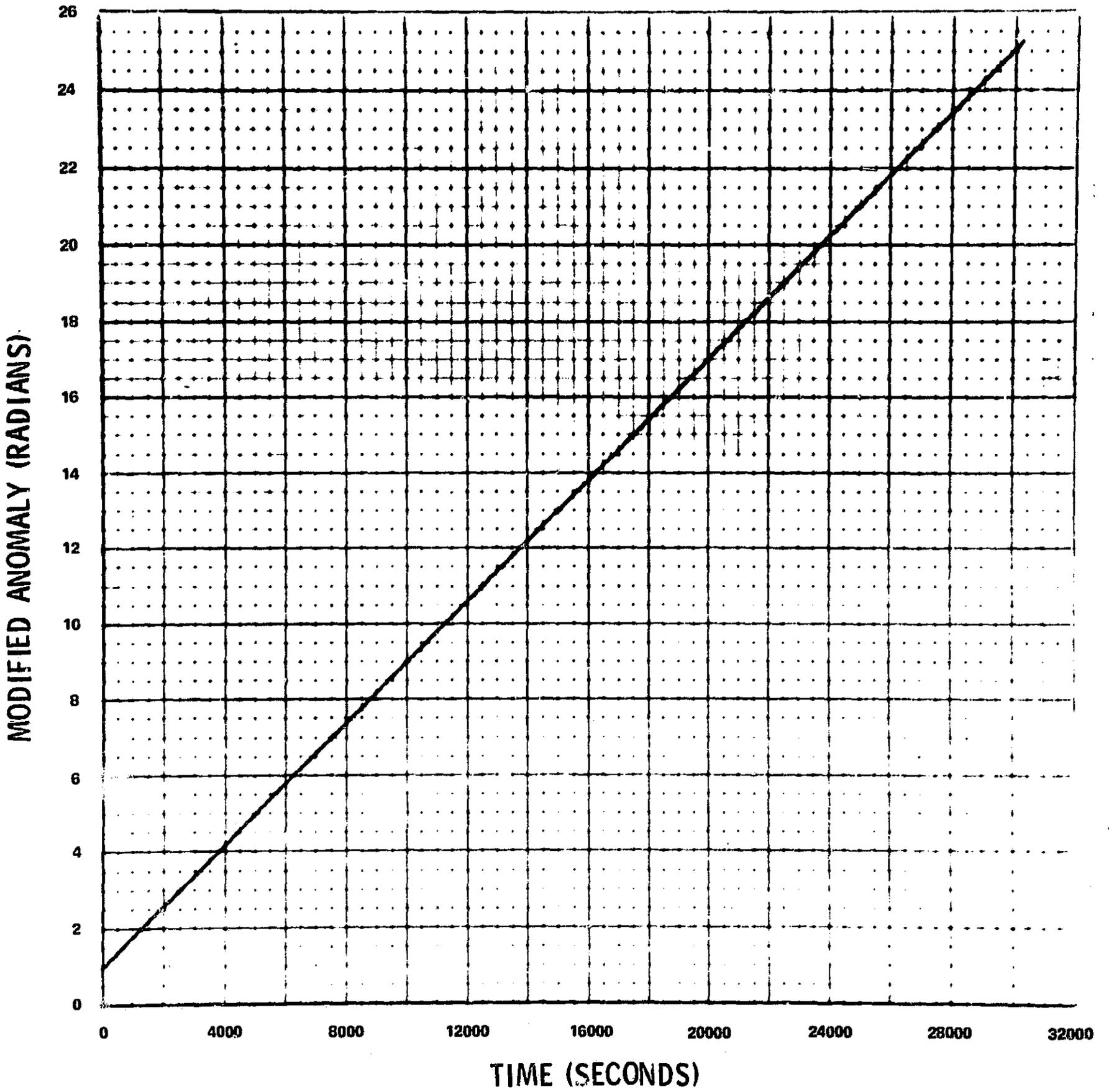**LONGITUDE OF ASCENDING NODE TIME HISTORY**

FIGURE 4f
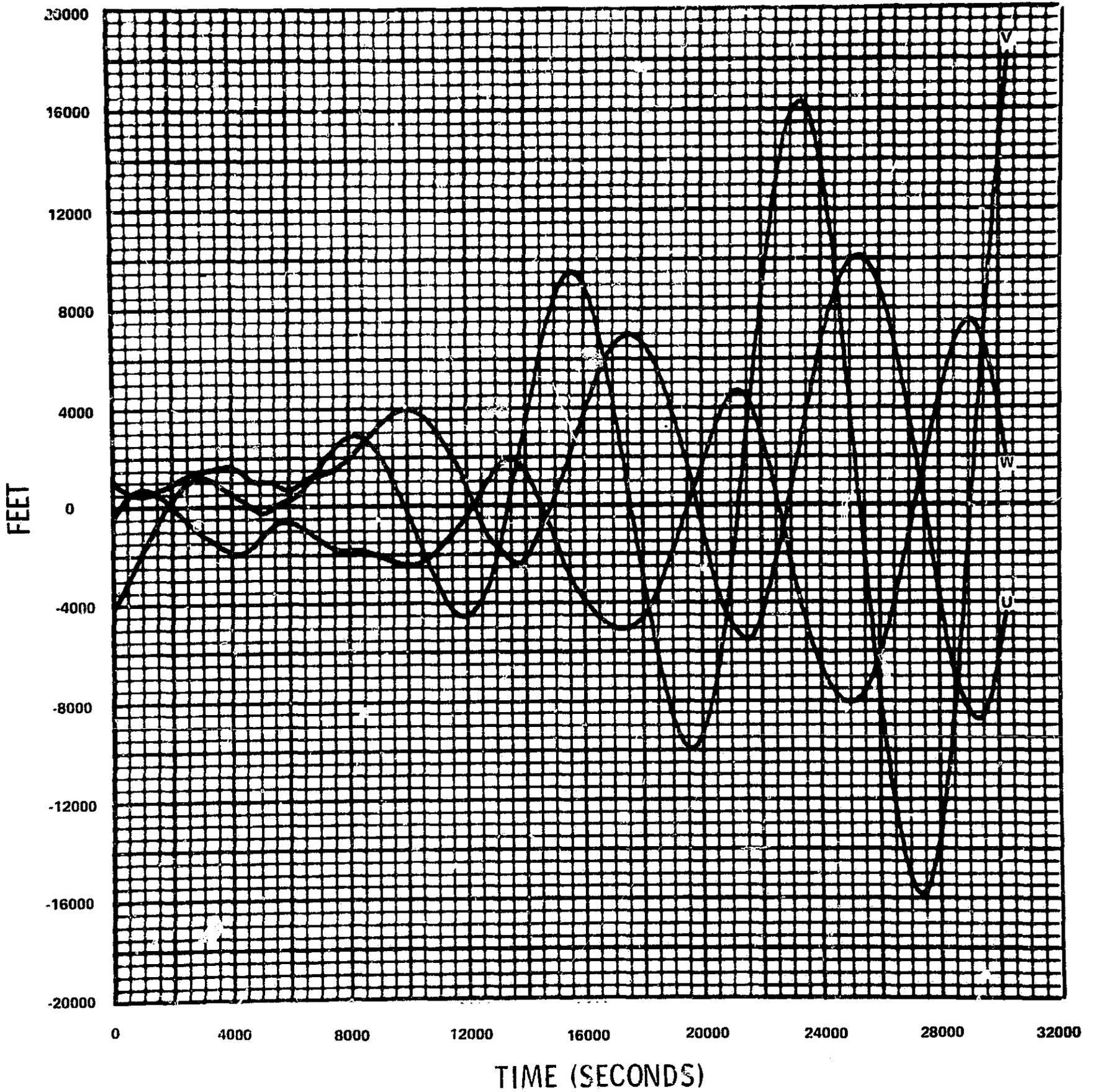e = .04 DATA
MODIFIED ANOMALY TIME HISTORY

FIGURE 4g
e = .04 DATA FITS TO 1 ORBIT
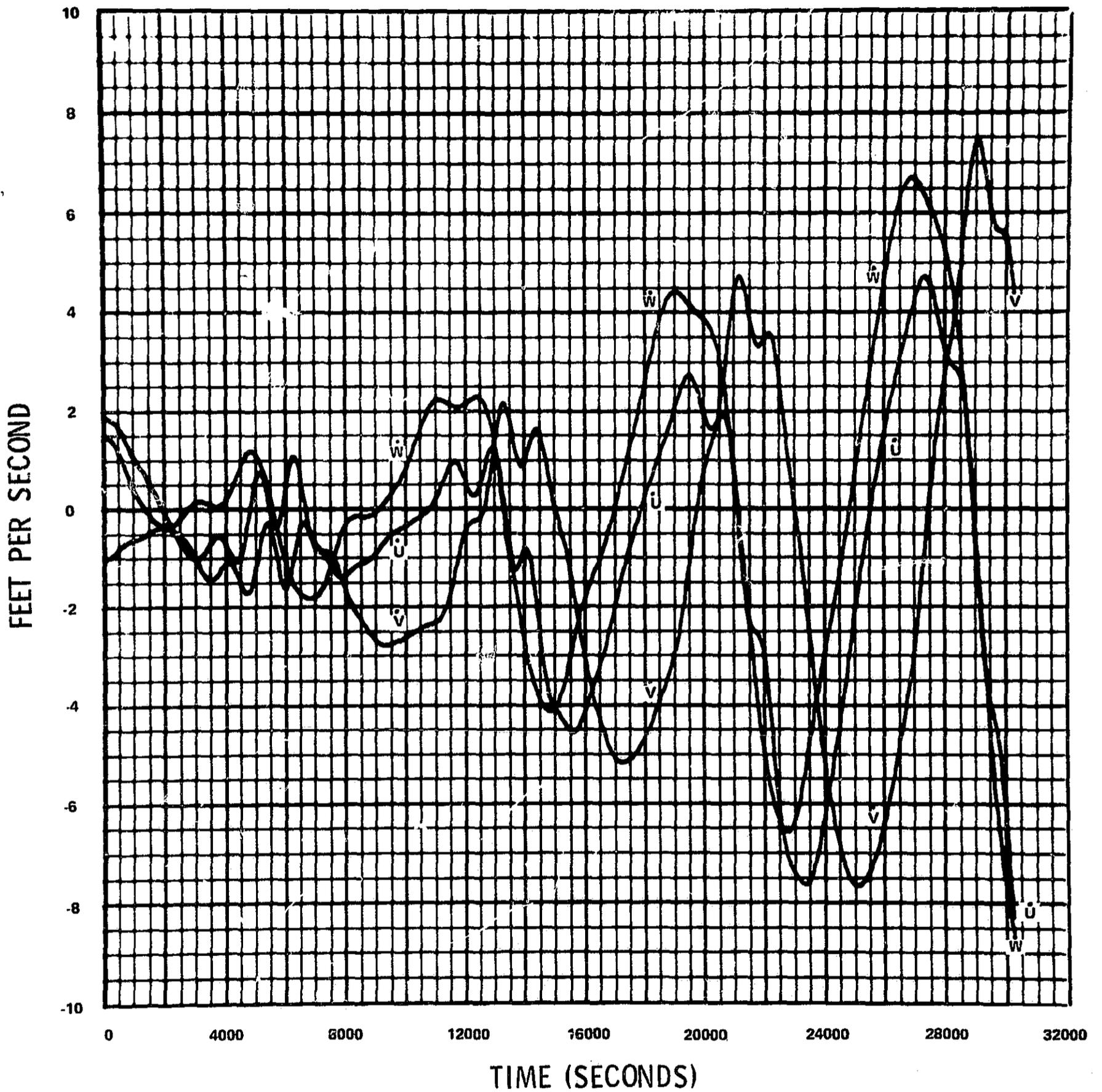UVW POSITION COMPONENT RESIDUALS
ALL ELEMENTS FIT

FIGURE 4h
e = .04 DATA FITS TO 1 ORBIT
UVW VELOCITY COMPONENT RESIDUALS
ALL ELEMENTS FIT

FIGURE 4i
e = .04 DATA FITS TO 1 ORBIT
UVW POSITION COMPONENT RESIDUALS
SEMIMAJOR AXIS IMPLIED

FIGURE 4j
e = .04 DATA FITS TO 1 ORBIT
UVW VELOCITY COMPONENT RESIDUALS
SEMIMAJOR AXIS IMPLIED
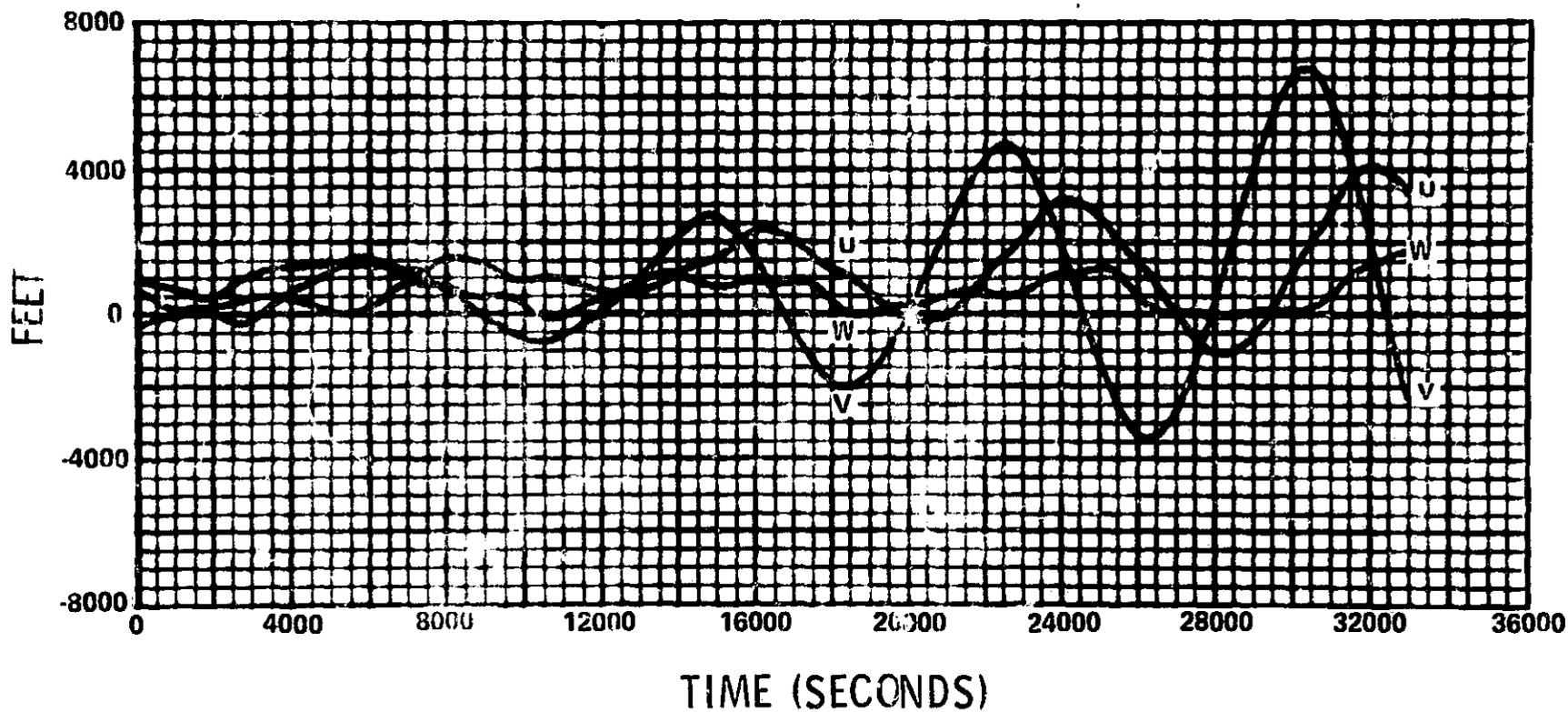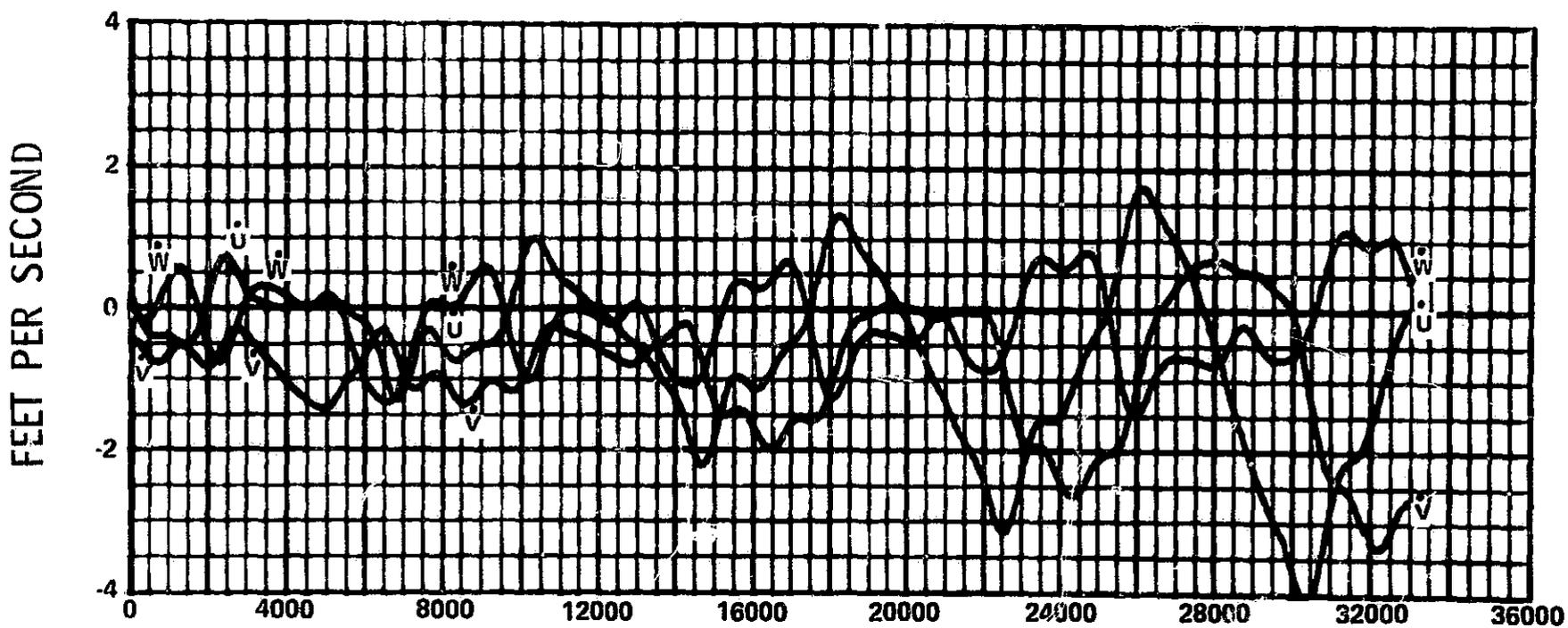
FIGURE 4k
e = .04 DATA FITS TO 2 ORBITS
UVW COMPONENT RESIDUALS
ALL ELEMENTS FIT
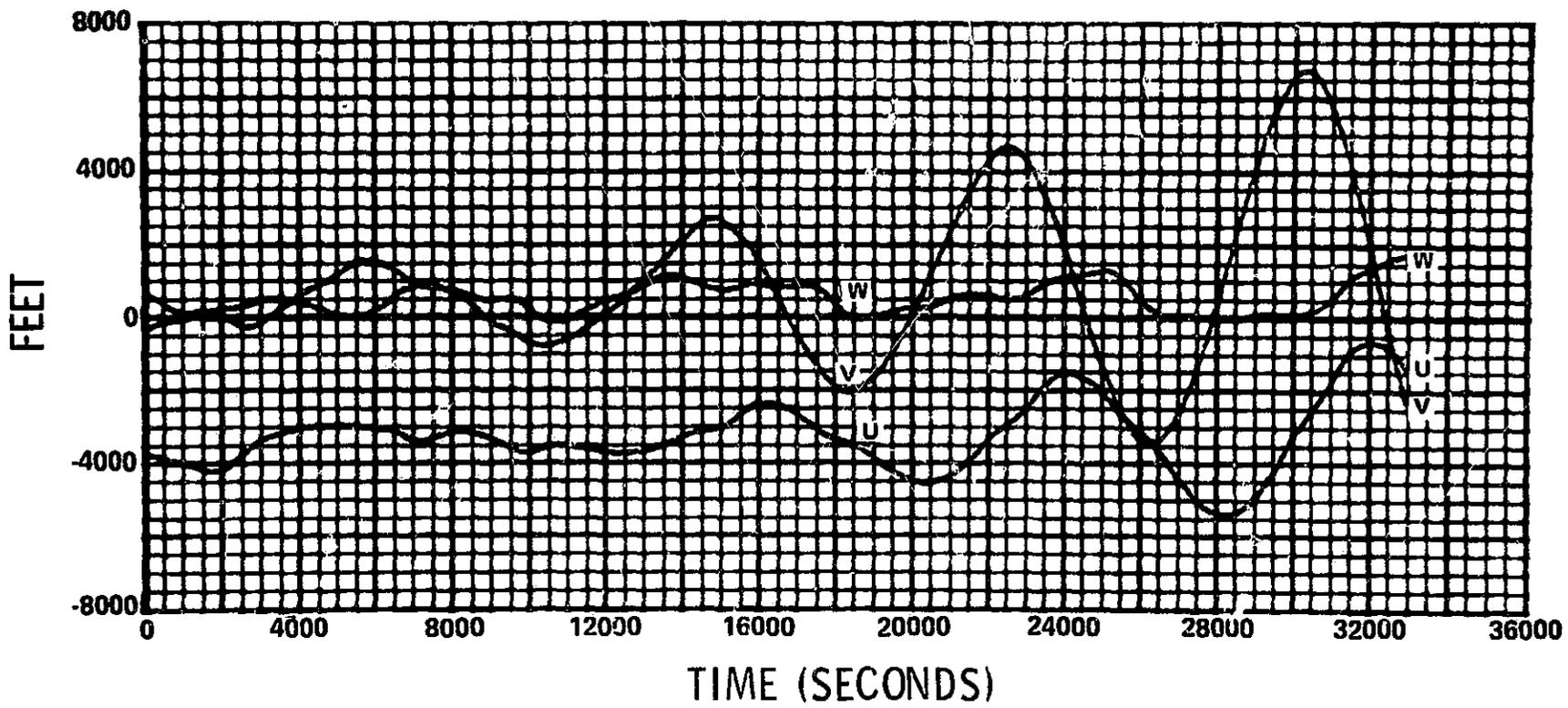
POSITION RESIDUALS
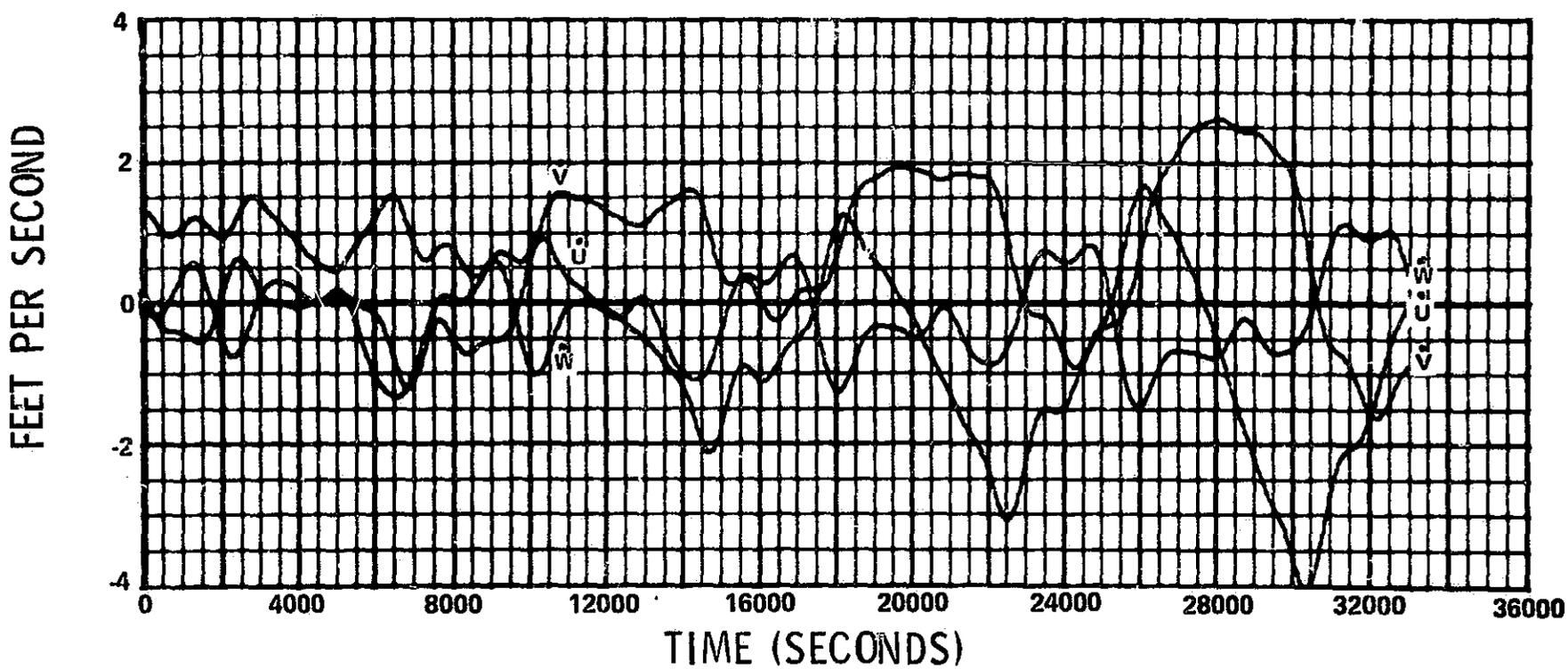
VELOCITY RESIDUALS

FIGURE 4ℓ
e = .04 DATA FITS TO 2 ORBITS
UVW COMPONENT RESIDUALS
SEMIMAJOR AXIS IMPLIED

FIGURE 5a
ARC 305 DATA
SEMIMAJOR AXIS TIME HISTORY

FIGURE 5b
ARC 305 DATA
e COS ω TIME HISTORY

FIGURE 5c
ARC 305 DATA
e SIN ω TIME HISTORY
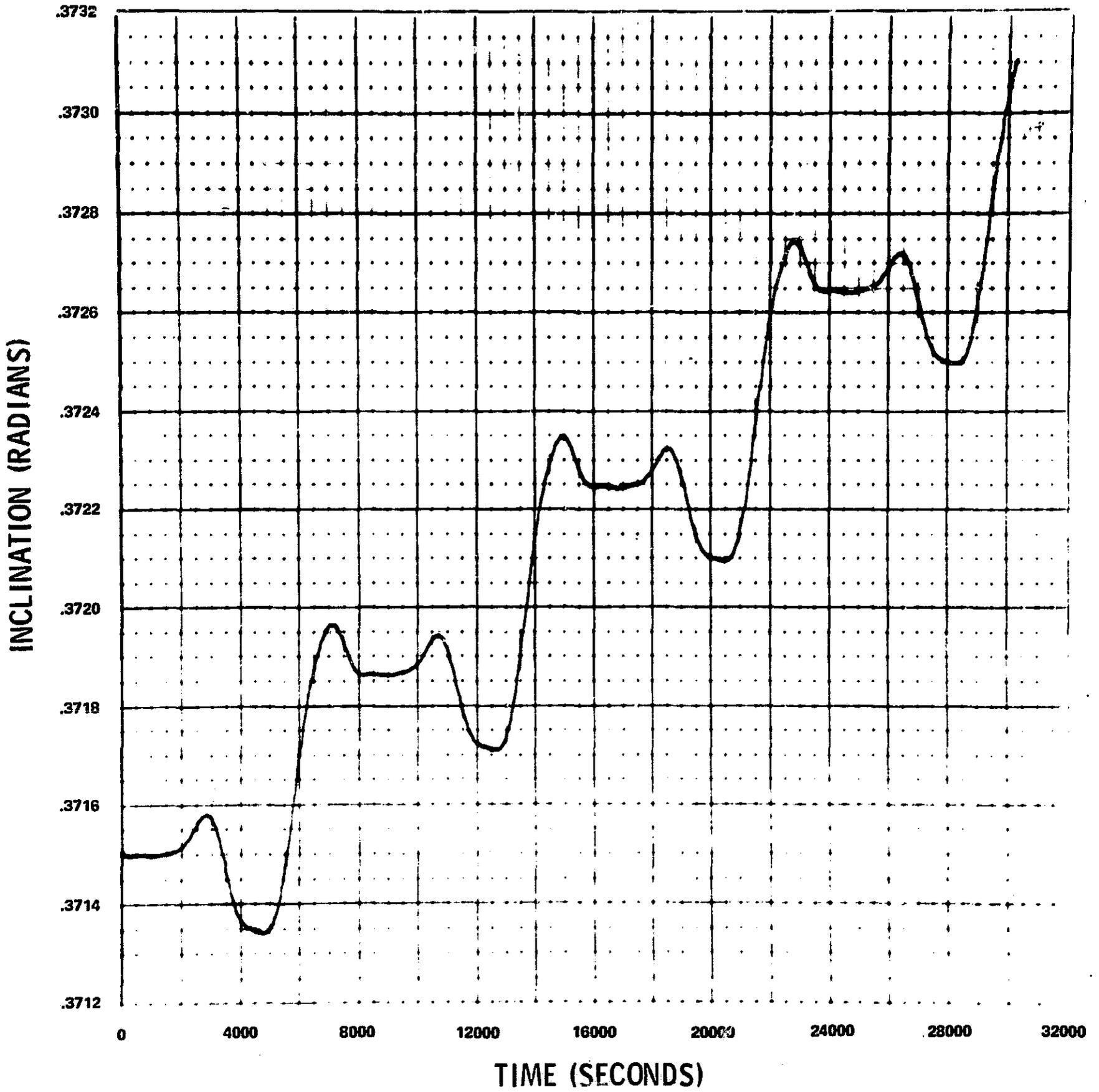
FIGURE 5d
ARC 305 DATA
INCLINATION TIME HISTORY
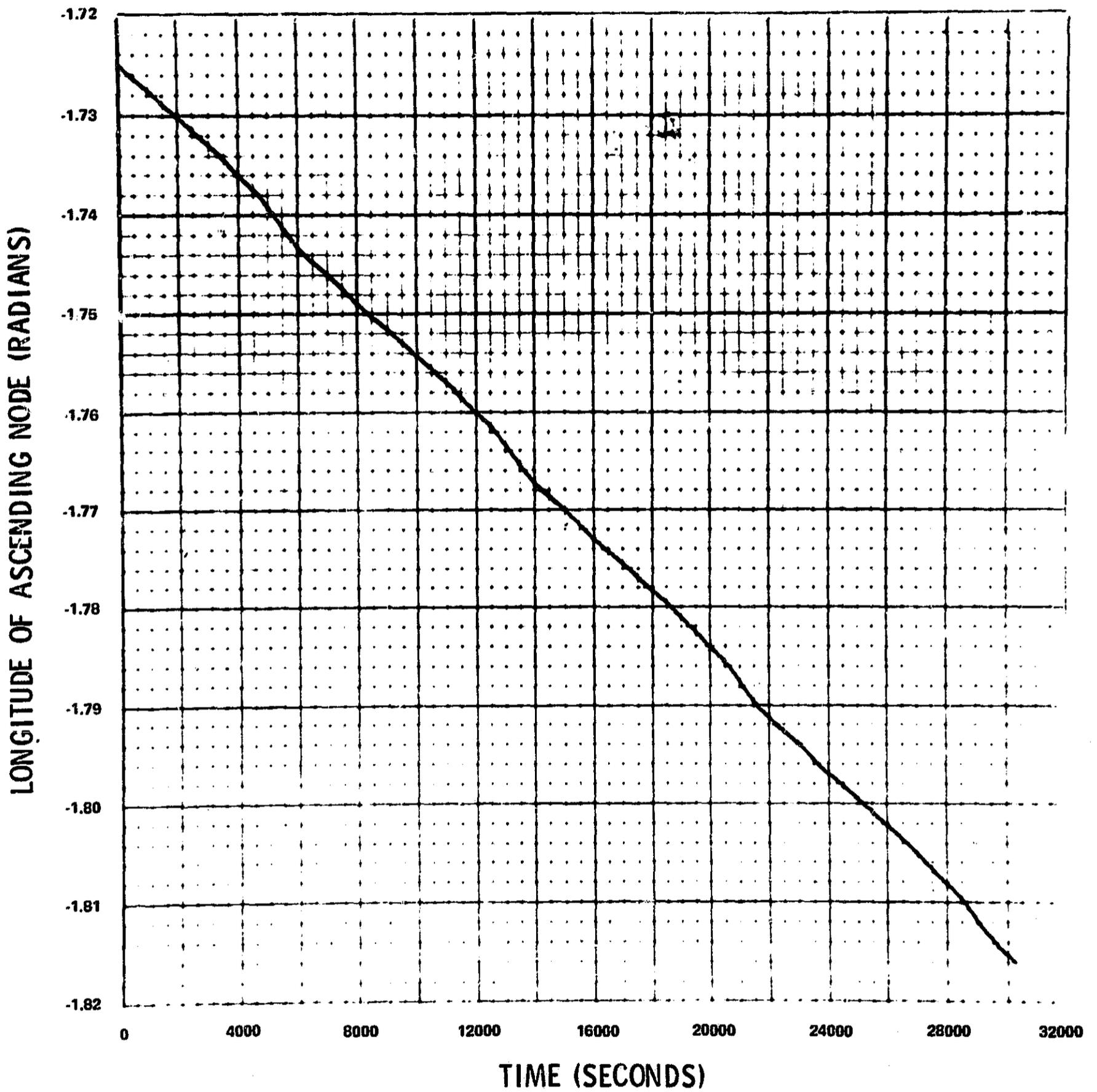
FIGURE 5e
ARC 305 DATA
LONGITUDE OF ASCENDING NODE TIME HISTORY

FIGURE 5f
ARC 305 DATA
MODIFIED ANOMALY TIME HISTORY

FIGURE 5g
ARC 305 DATA FITS TO 1 ORBIT
UVW POSITION COMPONENT RESIDUALS
ALL ELEMENTS FIT

FIGURE 5h
ARC 305 DATA FITS TO 1 ORBIT
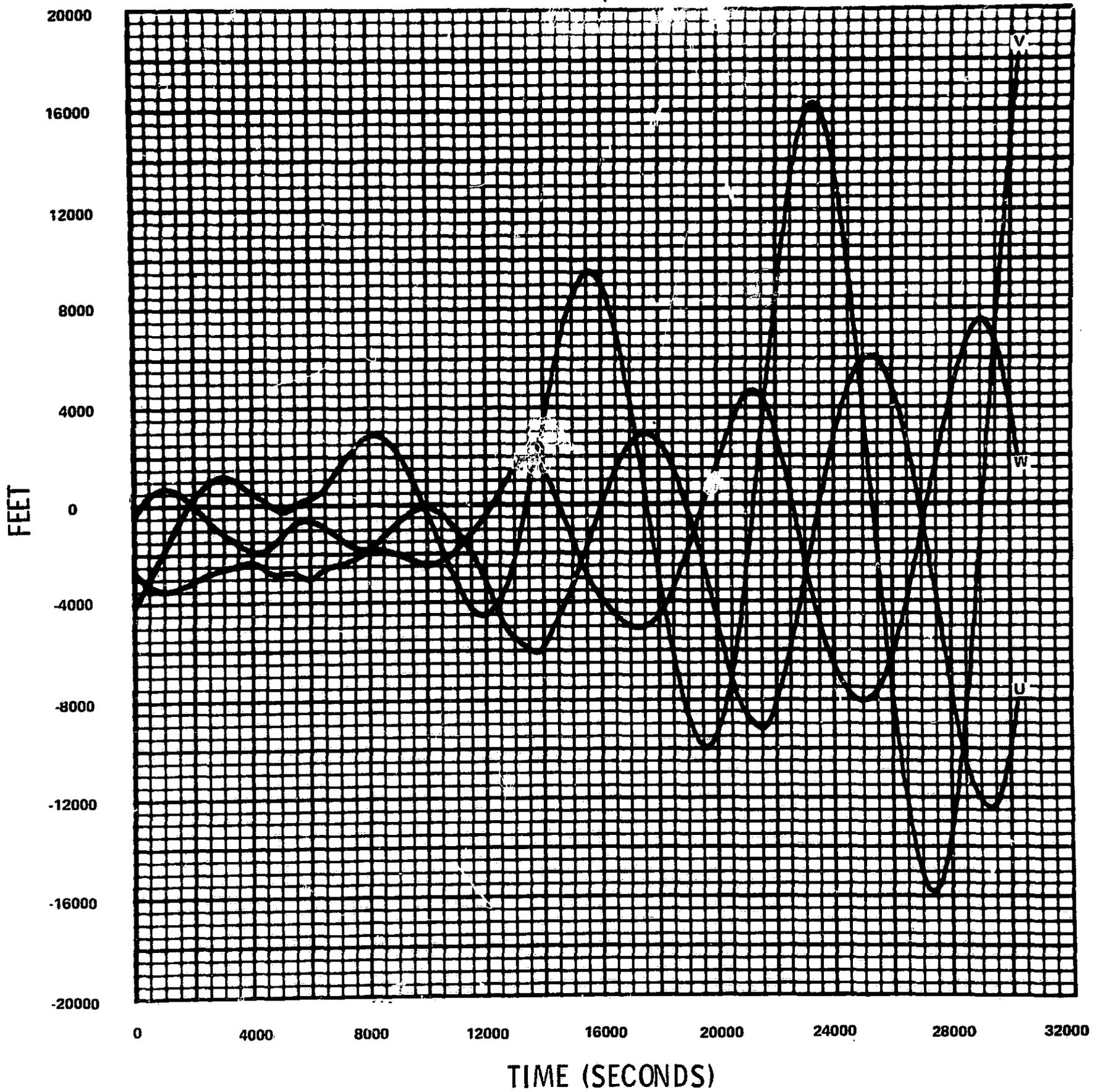UVW VELOCITY COMPONENT RESIDUALS
ALL ELEMENTS FIT

FIGURE 5i
ARC 305 DATA FITS TO 1 ORBIT
UVW POSITION COMPONENT RESIDUALS
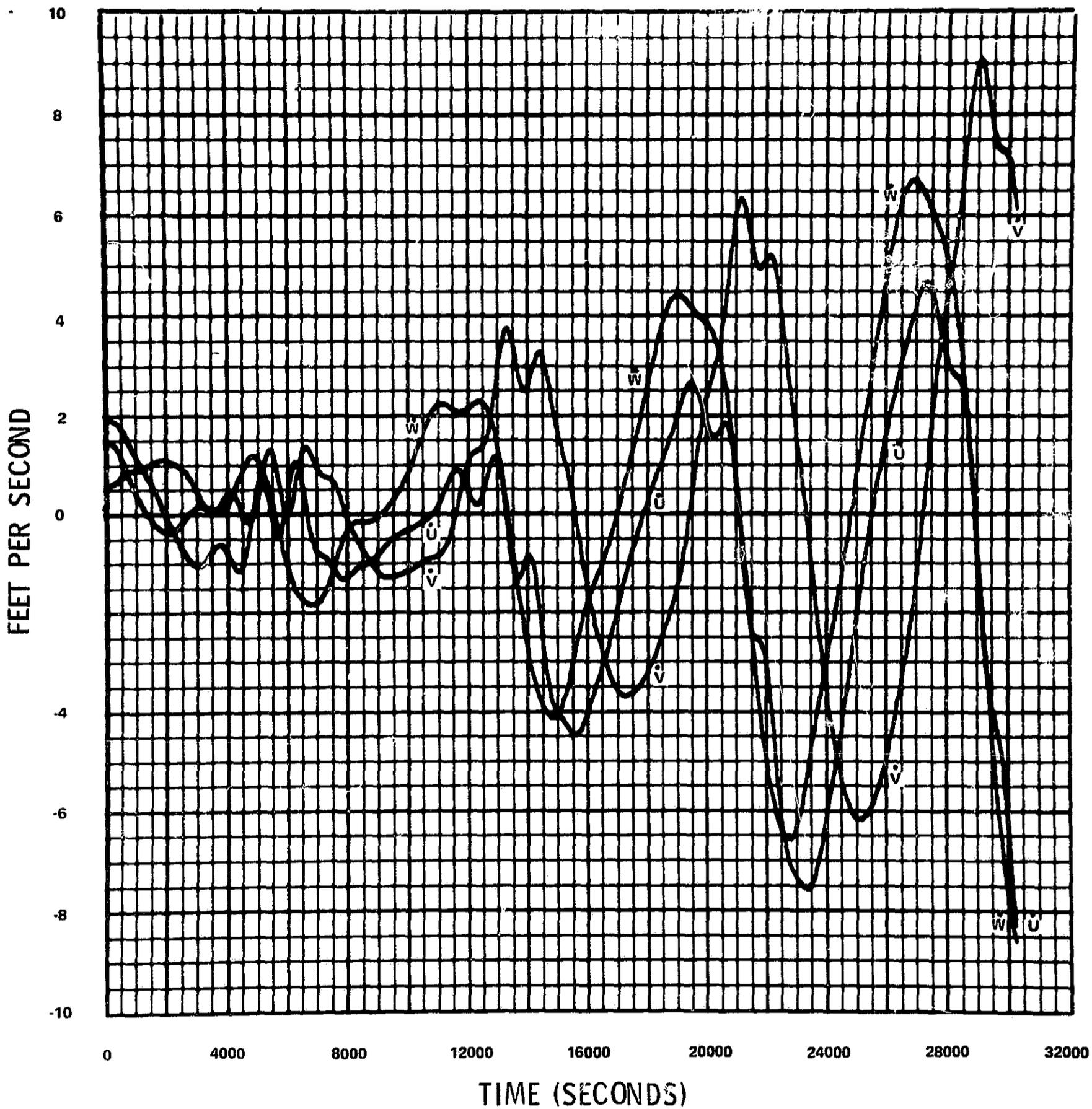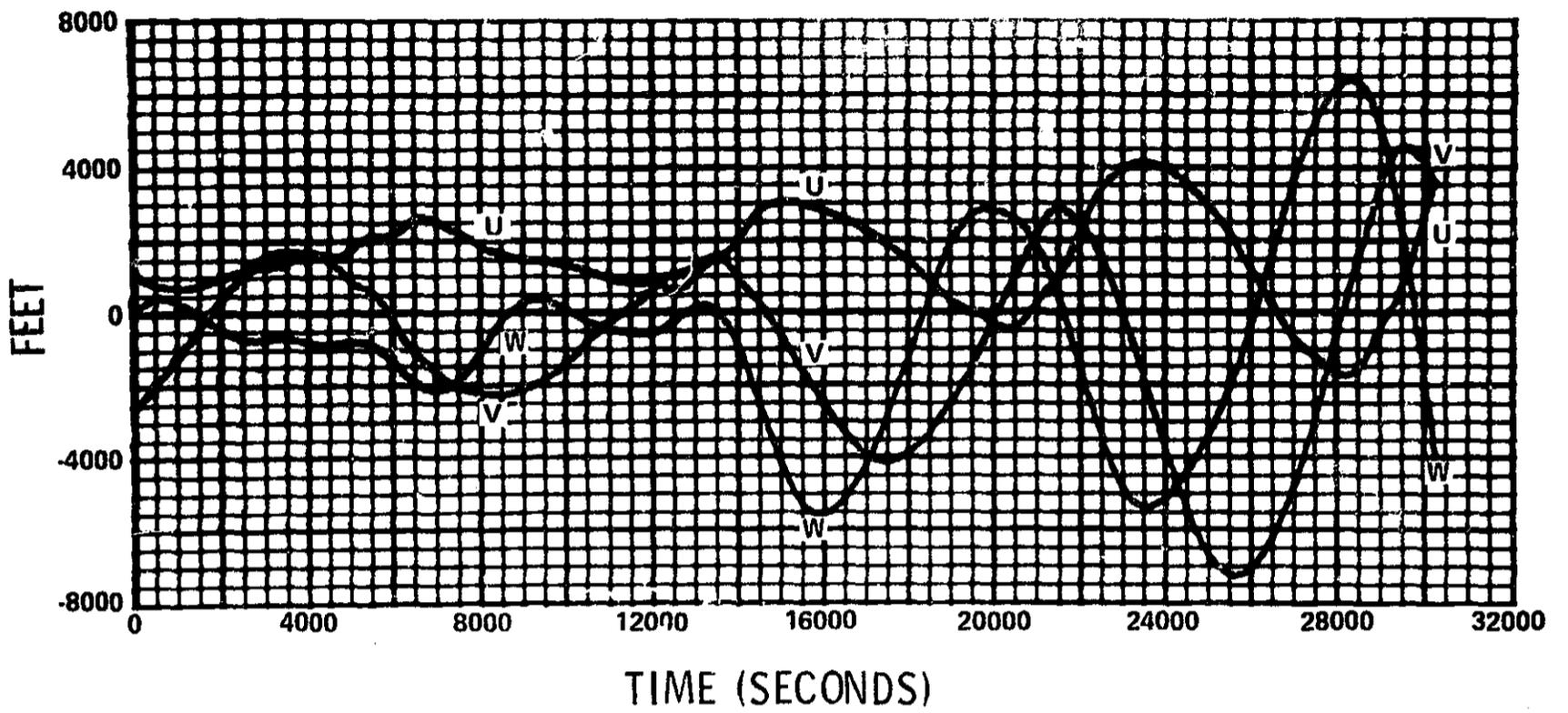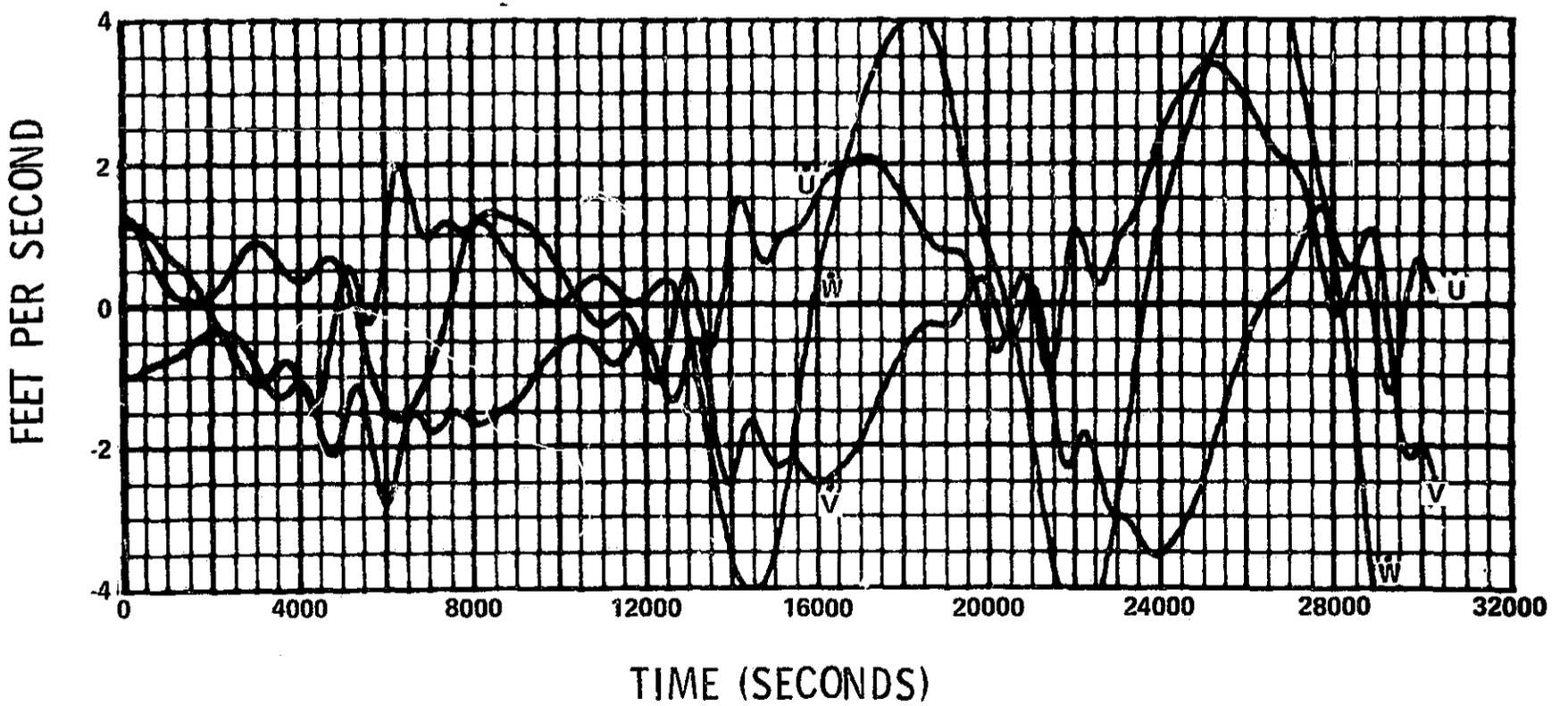SEMIMAJOR AXIS IMPLIED

FIGURE 5j
ARC 305 DATA FITS TO 1 ORBIT
UVW VELOCITY COMPONENT RESIDUALS
SEMIMAJOR AXIS IMPLIED

POSITION RESIDUALS

VELOCITY RESIDUALS

FIGURE 5k
ARC 305 DATA FITS TO 2 ORBITS
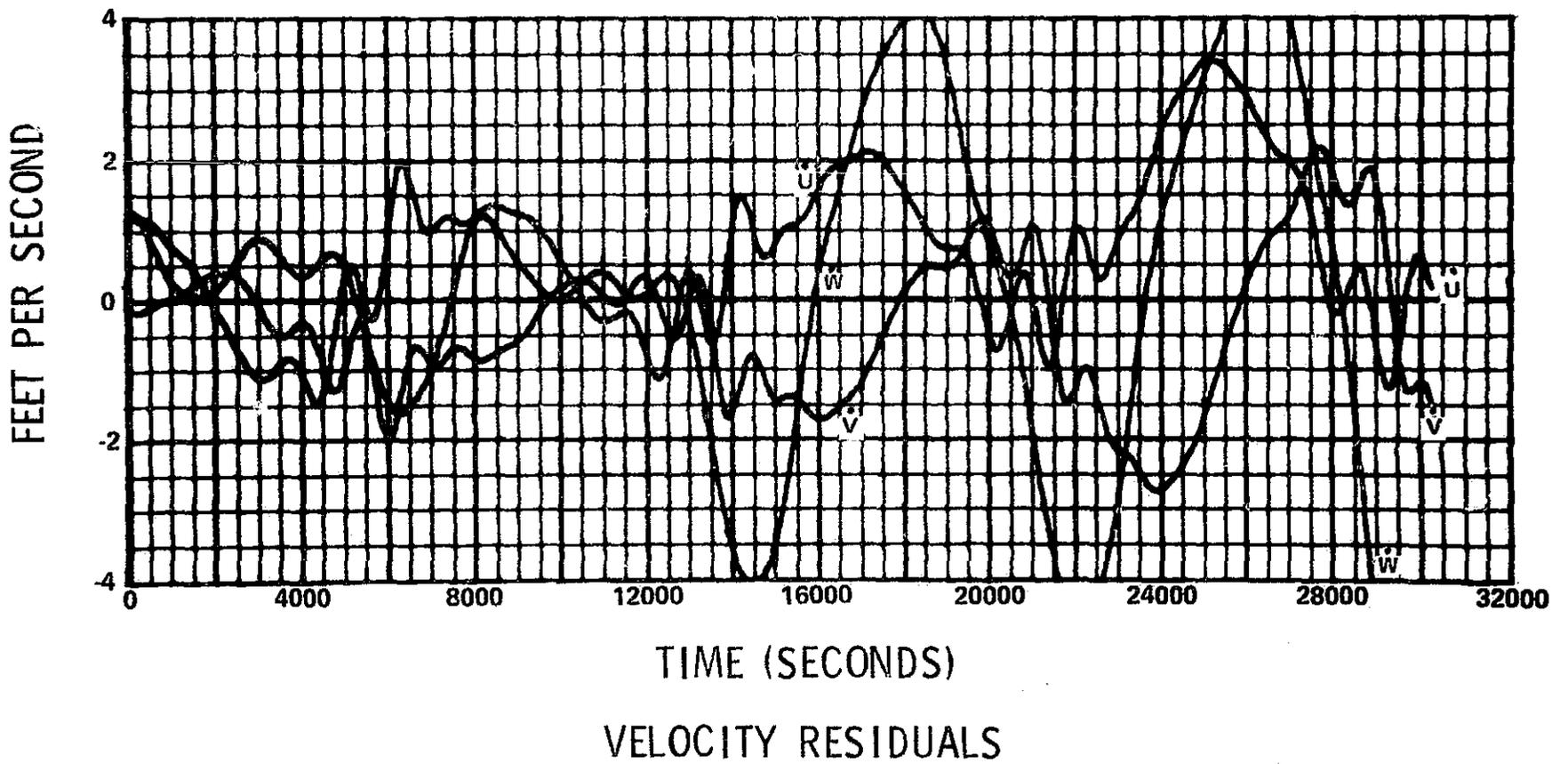UVW COMPONENT RESIDUALS
ALL ELEMENTS FIT

TIME (SECONDS)

POSITION RESIDUALS

TIME (SECONDS)

VELOCITY RESIDUALS

FIGURE 5*l*
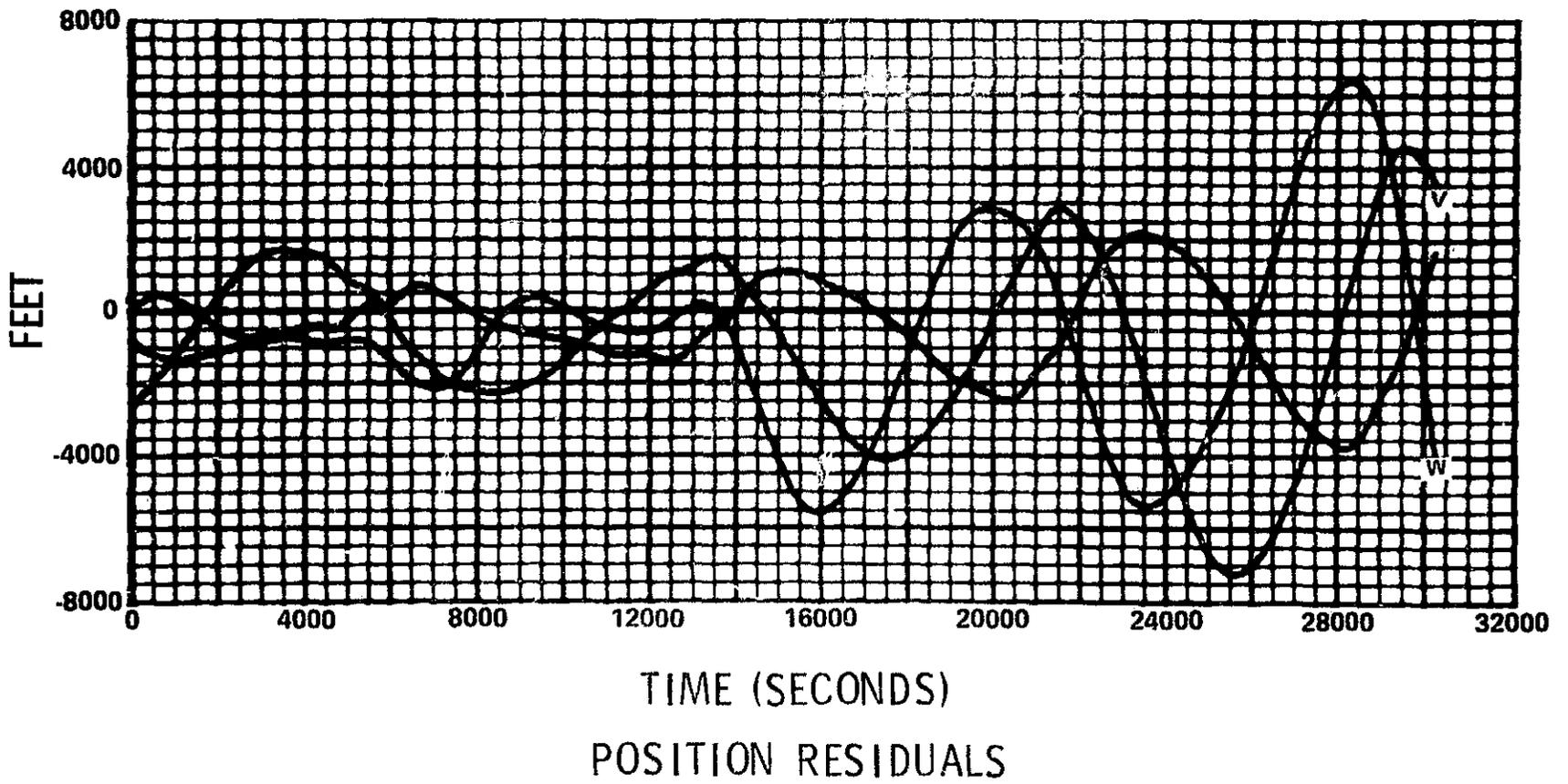ARC 305 DATA FITS TO 2 ORBITS
UVW COMPONENT RESIDUALS
SEMIMAJOR AXIS IMPLIED